"In presenting the dissertation as a partial fulfillment of the requirements for an advanced degree from the Georgia Institute of Technology, I agree that the Library of the Institution shall make it available for inspection and circulation in accordance with its regulations governing materials of this type. I agree that permission to copy from, or to publish from, this dissertation may be granted by the professor under whose direction it was written, or, in his absence, by the dean of the Graduate Division when such copying or publication is solely for scholarly purposes and does not involve potential financial gain. It is understood that any copying from, or publication of, this dissertation which involves potential financial gain will not be allowed without written permission.

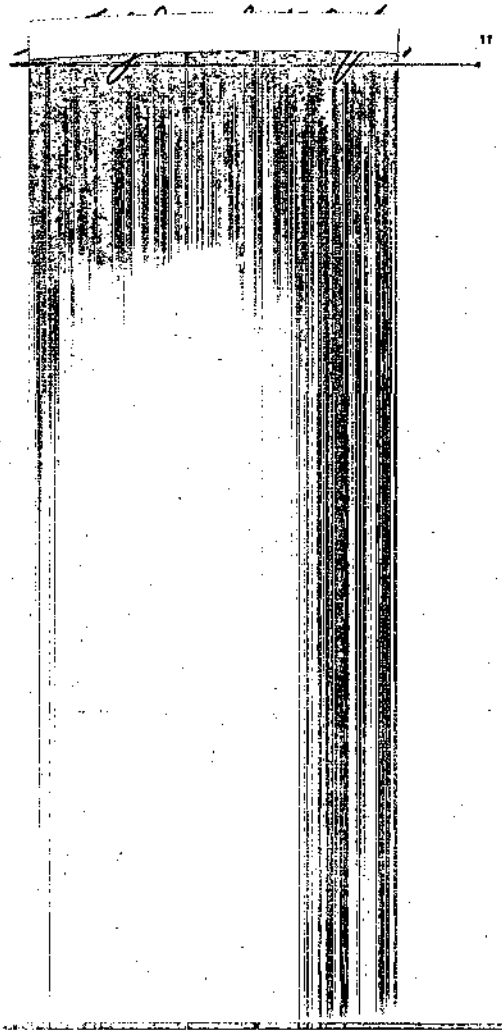

FREE-CONVECTION HEAT TRANSFER FROM THE OUTSIDE OF A VERTICAL ISOTHERMAL CIRCULAR CYLINDER

A THESIS

Presented to

The Faculty of the Graduate Division

by

Carl John Bliem, Jr.

In Partial Fulfillment

of the Requirements for the Degree

Doctor of Philosophy in the

School of Mechanical Engineering

Georgia Institute of Technology

April, 1964

5.8
12-R

FREE-CONVECTION HEAT TRANSFER FROM THE OUTSIDE OF A VERTICAL ISOTHERMAL CIRCULAR CYLINDER

Approved:

Chairman

Date approved by Chairman: 5/22/64

TABLE OF CONTENTS

(Continued)

TABLE OF CONTENTS (Concluded)

ACKNOWLEDGMENTS

The author wishes to express his appreciation to Dr. C. W. Gorton for his efforts and encouragement as thesis advisor and originator of this project. The experimental work in this investigation could not have carried out without the assistance of Messrs. D. W. Crawford and L. V. Cancio, who assisted in the construction of the experimental facility and the taking of the data. The author also wishes to thank Drs. Thomas W. Jackson and Henderson C. Ward for their helpful comments in reviewing the thesis.

The financial support of the National Science Foundation is deeply appreciated. This work could not have been done without it.

The author is very grateful to Dr. Homer S. Weber for his interest and encouragement during the course of his graduate study and also to Dr. J. F. Bailey for his patience and understanding.

Finally, the author wishes to express his gratitude to his wife, DeLane, and his children, Cindy and Caribeth, whose contributions were immeasurable.

LIST OF ILLUSTRATIONS

(Continued)

LIST OF ILLUSTRATIONS (Concluded)

LIST OF TABLES

SUMMARY

The heat transfer from isothermal vertical cylinders in a laminar free-convection flow was investigated analytically and experimentally. The analytical study consisted of taking the boundary-layer differential equations (continuity equation, Navier-Stokes equations, and energy equation after an order-of-magnitude analysis) in cylindrical coordinates and solving this set of equations by a finite-difference scheme proposed by Hellums (33) who used it for the analogous two-dimensional problem of the vertical flat plate. The equations were solved for Prandtl numbers of 0.72, 0.01 and 100.0.

For the case of the Prandtl number of 0.72, the problem has been solved for low values of ξ, where ξ is $2^{3/2}Gr_x^{-1/4}x\ r_o^{-1}$, by Sparrow and Gregg (19) and at high values of ξ by Hama, Recesso and Christiaens (25). Because of some question as to the range of validity of both solutions, the finite-difference approach was used in the present work. In the range of ξ from 0.0 to 1.0, the finite-difference solution is in agreement with Sparrow and Gregg's solution. In the range of ξ from 10.0 to 20.0, the finite-difference solution is in agreement with the results of Hama, Recesso and Christiaens. For larger values of ξ, the finite-difference results are lower than those of Hama, Recesso and Christiaens by approximately ten per cent.

An experimental investigation was carried out by measuring overall heat-transfer coefficients in air (a Prandtl number of approximately 0.72).

The experiments were conducted over a range of ξ from 0.20 to 2.20. The experimental data agrees well with the finite-difference solution and with other experimental data of Carne (16) and Battaglia (29).

The finite-difference equations were also solved for a Prandtl number of 0.01 for a range of ξ from 0.0 to 1.0. A new scheme was devised to treat the data at low ξ values due to a peculiarity in the finite-difference scheme in this range. Empirical equations which fit the finite-difference data in this range are:

$$Nu_{r_o} = \frac{0.1624}{\xi} + 0.4709 - 0.1496\xi$$

$$\overline{Nu}_{r_o} = \frac{0.2165}{\xi} + 0.4709 - 0.1197\xi$$

These equations give results which are within ± 2.0 per cent of the finite-difference values over the entire range. These results also agree well with an approximate solution given by Sparrow and Gregg (19).

At a Prandtl number of 100.0, the finite-difference equations were solved for ξ values ranging from 0.0 to 80.0. These results for the average Nusselt number compared with experimental data obtained by Cox (30) and the finite-difference solution was found to predict Nusselt numbers which were higher than those obtained experimentally. The finite-difference results agree well with the approximate solution of Sparrow and Gregg (19). Equations which fit the finite-difference data for ξ less than 1.414 within ± 4.0 per cent are:

$$Nu_{r_o} = \frac{4.382}{\xi} + 1.250 + 0.232\xi$$

$$\overline{Nu}_{r_o} = \frac{5.843}{\xi} + 1.250 + 0.186\xi$$

LIST OF SYMBOLS

A	surface area, ft^2
α	thermal diffusivity, ft^2/hr
β	coefficient of thermal expansion, $1/^oR$
ε	emissivity
η	flat plate similarity parameter
g	local acceleration of gravity, ft/hr^2
Gr_ℓ	Grashof number based on ℓ, $g\beta(t_s - t_a)\ell^3/\nu^2$
Gr_{r_o}	Grashof number based on r_o, $g\beta(t_s - t_a)r_o^3/\nu^2$
Gr_x	Grashof number based on x, $g\beta(t_s - t_a)x^3/\nu^2$
h	local heat-transfer coefficient, Btu/hr ft^2 ^oR
$\bar{h}$	average heat-transfer coefficient, Btu/hr ft^2 ^oR
J	X index, Figure 2, page 21
k	thermal conductivity, Btu/hr ft ^oR
ℓ	length of cylinder, ft
L	R index, Figure 2, page 21
$\overline{Nu}_\ell$	average Nusselt number based on ℓ for cylinder, $\bar{h}\ell/k$
$\overline{Nu}_{\ell\ fp}$	average Nusselt number based on ℓ for flat plate, $\bar{h}\ell/k$
Nu_{r_o}	local Nusselt number based on r_o for cylinder, hr_o/k
$\overline{Nu}_{r_o}$	average Nusselt number based on r_o for cylinder, $\bar{h}r_o/k$
Nu_x	local Nusselt number based on x for cylinder, hx/k
$Nu_{x\ fp}$	local Nusselt number based on x for flat plate, hx/k
ν	kinematic viscosity, ft^2/hr

LIST OF SYMBOLS (Continued)

P	power to test section, watts
q	rate of heat transfer, Btu/hr
q_{co}	convective heat flux, Btu/hr ft^2
q_{ra}	radiative heat flux, Btu/hr ft^2
q_{to}	total heat flux, Btu/hr ft^2
r	radial distance, ft
r'	non-dimensionalizing constant, ft, equation (25), page 14
r_o	radius of cylinder, ft
R	non-dimensional radial distance, equation (29), page 14
R_∞	non-dimensional radial distance at which infinite boundary conditions are imposed
ΔR	incremental change in R
σ	Prandtl number, ν/α
$\bar{\sigma}$	Stefan-Boltzmann constant = 0.1714×10^{-8} Btu/hr ft^2 $^oR^4$
t	temperature, ^oF
t_a	air temperature, ^oF
t_f	film temperature, ^oF, equation (114), page 57
t_s	surface temperature, ^oF
T	non-dimensional time, equation (30), page 15
T	absolute temperature, ^oR
ΔT	incremental change in T
τ	time, hr
τ'	non-dimensionalizing constant, hr, equation (24), page 14

LIST OF SYMBOLS (Concluded)

θ	non-dimensional temperature, equation (33), page 15
u	velocity in x direction, ft/hr
u'	non-dimensionalizing constant, ft/hr, equation (26), page 14
U	non-dimensional velocity in X direction, equation (31), page 15
v	velocity in r direction, ft/hr
v'	non-dimensionalizing constant, ft/hr, equation (27), page 14
V	non-dimensional velocity in R direction, equation (32), page 15
x	axial distance, ft
x'	non-dimensionalizing constant, ft, equation (23), page 14
X	non-dimensional axial distance, equation (28), page 14
ΔX	incremental change in X
ξ	non-dimensional distance parameter, equation (28), page 14
$\Delta\xi$	incremental change in ξ
Z	$g\beta/\nu^2$, $1/^{\circ}R\ ft^3$

CHAPTER I

INTRODUCTION

There are many applications in which free convection is the principal mode of heat transfer. In any application in which the specific power dissipation is relatively low, free convection may be used to dissipate the energy. Many electronic parts are cooled by free convection. Low power nuclear reactors are also cooled this way.

The present investigation is concerned with the free convection from the outside of a vertical isothermal cylinder immersed in an infinite fluid medium. This problem is one of external flow since the fluid is essentially unbounded. Had the fluid been completely enclosed by the surface, the flow would be said to be internal. Many free convection problems arise with internal flows but these will not be considered here.

Previous Work Related to Present Problem

The free-convection problem associated with the vertical flat plate with a constant surface temperature was solved analytically by Lorenz (1) and Nusselt and Jürgens (2) using differential equations which differ somewhat from the now-accepted boundary-layer equations. Schmidt and Beckmann (3) were the first to apply the boundary-layer differential equations to this problem and with the assistance of Pohlhausen solved the system of equations for a Prandtl number corresponding to that of air. More recently, Ostrach (4) derived the

differential equations in a more rigorous fashion from the Navier-Stokes equations (although ultimately arriving at the same equations as Schmidt and Beckmann) and solved the equations for Prandtl numbers ranging from 0.01 to 1000. Sparrow and Gregg (5) solved the same differential equations for low Prandtl numbers ranging down to 0.003. Squire (6) used an approximate integral method to solve this problem. Free convection from a vertical flat plate has been investigated experimentally by many researchers (e.g., Saunders (7), Weise (8), and Eckert and Soehngen (9)).

Free convection from the lower half of the isothermal horizontal cylinder was solved analytically by Hermann (10) and was investigated experimentally by Jodlbauer (11) and Seftleben (12). External free convection from other geometries has been investigated experimentally. A good review of the experimental work done prior to 1932 is given by King (13).

Under certain conditions, the free-convection boundary layers on a vertical cylinder are essentially the same as those on a flat plate. Merk and Prins (14) demonstrated that a sufficient condition for this to be true is that the thicknesses of both the thermal and hydrodynamic boundary layers are small compared to the radius of curvature of the body in question. In many applications to vertical cylinders, these conditions may not be true.

Among the earliest experimental investigators of vertical cylinders were Griffiths and Davis (15). Unfortunately, in all of the experiments which they ran, in which the effect of curvature would be noticeable,

estimates of the product of the Grashof number based on length and the Prandtl number were greater than 10^9, which would indicate that the flow may not have been laminar near the top of the cylinder. The next important work on cylinders was done by Carne (16) and Elenbaas (17). Carne performed experiments in which he measured the overall heat-transfer coefficient for isothermal cylinders in air. Unfortunately, none of his data was presented in dimensionless form; and, to put it in useful form, an estimate must be made of the air temperature to evaluate the properties of air. A good portion of the work was done under conditions such that the flow was probably no longer laminar near the top of the cylinder as was the case with the work of Griffiths and Davis. When plotted, his data showed considerable scatter and no trends were evident from it. Elenbaas (17) performed an analysis in which he deduced an expression for the average Nusselt number for the vertical isothermal cylinder in steady-state free convection by using the method of Langmuir (18), that the heat transfer in free convection could be treated as a heat conduction problem in an annulus of stagnant fluid around the cylinder. This analysis gave an estimate of the heat-transfer characteristics, but it evaded the real issue by not including the flow characteristics.

More recently, Sparrow and Gregg (19) performed an analytical study of the steady-state laminar free-convection boundary layer outside a vertical isothermal cylinder. Starting with the boundary-layer equations for free convection (analogous to those derived by Ostrach, but for the axi-symmetric geometry) and assuming constant fluid properties except for the effect of temperature on density in the momentum equation,

the dependent variables were assumed to be representable by an infinite power series involving the vertical distance parameter, ξ*. This infinite series was truncated after three terms because of the difficulty in attaining the coefficients of the series, which were functions of the other independent parameter, the radial distance. These coefficients were determined by solving sets of ordinary differential equations numerically. Hama and Christiaens (20) attempted to confirm the analytical results of Sparrow and Gregg for the temperature field with their experimental data. They found that not enough terms of the series were known to fit the experimental data, even near the wall. Nothing can be said definitely about the region of convergence of the solution. S. I. Pai made the comment in his discussion of the paper by Sparrow and Gregg that since the results were expressed in terms of a truncated power series in the variable ξ they would be expected to be valid only for small values of ξ, this means small values of x, the distance from the leading edge. In the order analysis from which the differential equations were derived on the other hand, it was assumed that the flow is a relatively large distance from the leading edge. There is, therefore, some question as to the range of validity of the solution and the differential equations. The authors estimated that if the trends indicated in the series continued, the error at $\xi = 1$ is less than three per cent and would be less for lower values of ξ. Sparrow and Gregg also performed an approximate analysis similar to that of Elenbaas. For

*All symbols are defined in the List of Symbols on page xi.

a Prandtl number of 0.72, their results for the average Nusselt number deviated from the results obtained from the differential equations by less than three per cent in the range of ξ from zero to one.

A somewhat different approach to the same problem was used by LeFevre and Ede (21). They used an integral method similar to the one used by Squire, and reported by Goldstein (6), for the vertical flat plate. In doing this, similar velocity and temperature profiles were assumed at each x station. This assumption is questionable since no similarity transformation for the differential equations and associated boundary conditions has been found for this particular problem (see Yang (22)). (The case of the vertical cylinder with linearly varying surface temperature with zero temperature difference at the leading edge possesses such a transformation and has been solved by Millsaps and Pohlhausen (23), but this cannot be reduced to the isothermal case.)

Hama, Recesso, and Christiaens (20), (24), (25) used a similar approach to that of LeFevre and Ede, but with more realistic velocity and temperature profiles near the wall. In the solution of their problem, however, they neglected the inertia terms in the momentum equation. (LeFevre (26) has shown this to be the case for the vertical isothermal flat plate as the Prandtl number becomes infinite, but at low Prandtl numbers the inertia terms are not negligible.) Again, the form of the temperature and velocity profiles were assumed, but they were not similar. Hama, Recesso, and Christiaens used a method similar to that used by Glauert and Lighthill (27) for the axial flow past a cylinder. Glauert and Lighthill suggested that the most important phase of the

solution was to chose a realistic profile near the wall. The solution of Hama, Recesso, and Christiaens should be most accurate at large distances from the leading edge (large values of ξ), since this is true in the corresponding solution by Glauert and Lighthill. Hama, Recesso, and Christiaens also experimentally determined the temperature profiles on a small diameter tube and a section of wire (large values of ξ) in air, which seem to confirm their theory.

Madden and Piret (28) experimentally measured the heat transfer from horizontal and vertical wires in gases at very low pressures, but this was at extremely high values of ξ. Bataglia (29) measured overall heat-transfer coefficients on the outside of vertical cylinders in air, but the data showed no readily apparent trends. The results of this work ranged from $\xi = 0.25$ to $\xi = 0.60$. Cox (30) measured overall heat-transfer coefficients from a vertical wire in air, water and oil. The value of ξ in air ranged from 25 to 35. Crawford (31) measured a temperature profile and a velocity profile in air at a ξ of approximately 0.5 with a hot-wire anemometer.

Purpose of Present Investigation

The purpose of the present investigation was to obtain analytical free-convection heat-transfer results for the vertical isothermal cylinder by using a finite-difference procedure to solve the appropriate boundary-layer equations. This was done for a Prandtl number of 0.72 (that of air) and also for higher and lower Prandtl numbers. In addition to this, an experimental investigation was carried out to determine the heat-transfer parameters for free convection from a vertical isothermal cylinder in air.

CHAPTER II

FORMULATION OF THE MATHEMATICAL MODEL

The physical situation to be considered is shown in Figure 1, page 8. A cylinder infinite in extent in one direction is placed in an infinite fluid medium. The fluid temperature approaches a constant value at large distances from the cylinder surface. There are four individual cases which may be considered and each can be resolved to the same set of differential equations and boundary conditions by the proper non-dimensionalization. The cases are concerned with whether the cylinder is being heated or cooled and whether the density of the fluid increases or decreases with an increase in temperature. Figure 1 depicts the two cases in which the density decreases with increasing temperature.

In the left hand figure, the case is presented in which the temperature of the wall is greater than that of the ambient fluid and the heat transfer is from the cylinder to the fluid. The fluid near the wall has a higher temperature and lower density than the fluid far from the wall. Thus an upward flow will develop near the wall.

The figure at the right depicts the case when the cylinder wall temperature is less than the ambient fluid temperature. The flow of the fluid will be downward as shown. If the coordinates are taken as shown, the distinction between this and the first case will vanish when the differential equations are non-dimensionalized; and there will be no reason to treat the cases separately. A similar behavior would be shown

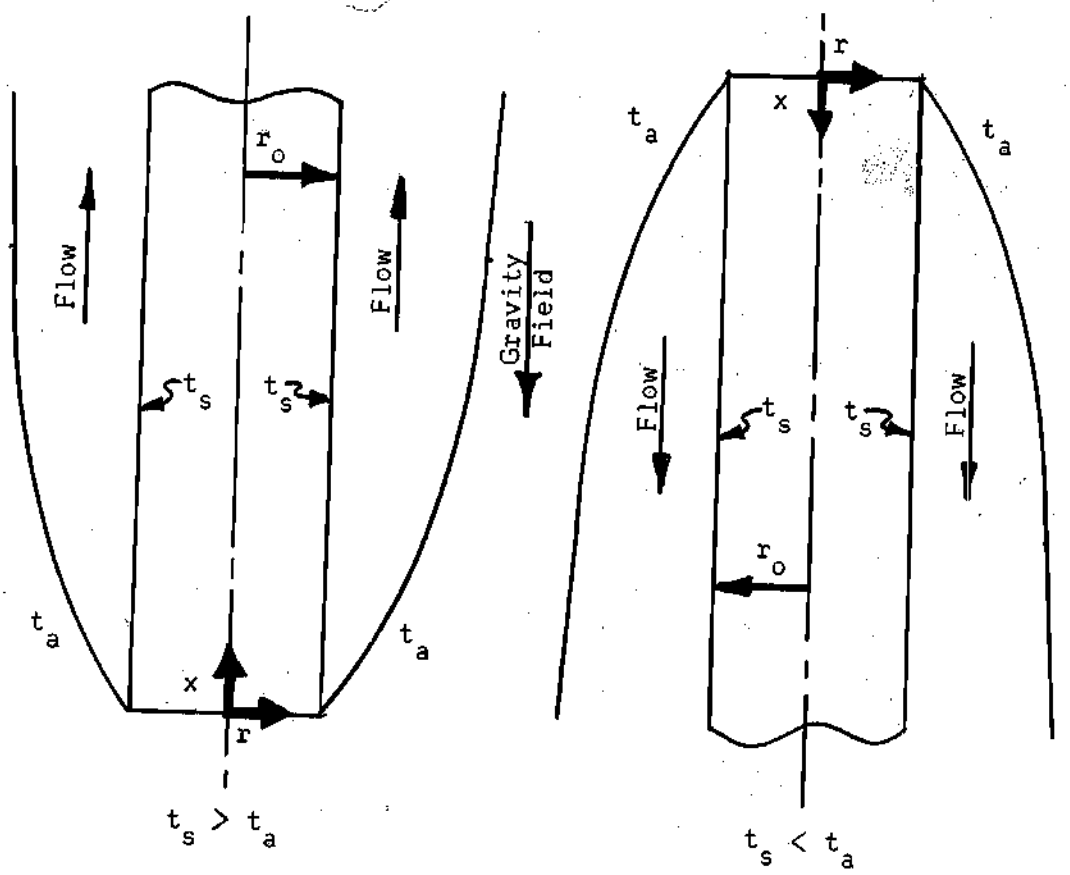

Figure 1. Coordinate System and the Physical Model.

for the opposite variation of density with temperature. Therefore, the analysis will be carried forward for the first case ($t_s > t_a$), but it will be valid for all four cases.

The Basic Equations

The basic differential equations representing this flow are the boundary-layer equations in cylindrical coordinates for the case of an axi-symmetric free-convection flow with μ and k constant. They are identical to those given by Sparrow and Gregg (19) and those used by Ostrach transformed to the cylindrical geometry, but with the addition of the time-dependent terms. The continuity equation is:

$$\frac{\partial(ru)}{\partial x} + \frac{\partial(rv)}{\partial r} = 0 \tag{1}$$

The momentum equation is:

$$\frac{\partial u}{\partial \tau} + u \frac{\partial u}{\partial x} + v \frac{\partial u}{\partial r} = g\beta(t - t_a) + \frac{\nu}{r} \frac{\partial}{\partial r}\left(r \frac{\partial u}{\partial r}\right) \tag{2}$$

The energy equation is:

$$\frac{\partial t}{\partial \tau} + u \frac{\partial t}{\partial x} + v \frac{\partial t}{\partial r} = \frac{\alpha}{r} \frac{\partial}{\partial r}\left(r \frac{\partial t}{\partial r}\right) \tag{3}$$

In these equations, the fluid is considered incompressible except for the effect of temperature on density in the term $g\beta\ (t - t_a)$. Ostrach (4)

has investigated this problem in rectangular coordinates and has concluded that this is a valid simplification provided the product $\beta\ (t_s - t_a)$ is small. For an ideal gas, $\beta = 1/T_a$, where T_a is the absolute temperature. Then, for the ideal gas, the equations are valid if $(t_s - t_a) < T_a$, which is equivalent to putting an upper bound on the magnitude of the temperature difference for a given ambient temperature. It is assumed that the flows considered will meet this requirement.

The equations also assume that ν and α are constant. Since for a gas, these properties are primarily functions of temperature, this again is equivalent to saying that the maximum temperature difference is small. Sparrow and Gregg (32) have investigated the variable fluid property problem for the case of the isothermal vertical flat plate and have recommended that the properties be evaluated at a prescribed mean temperature to obtain answers within engineering accuracy. In accordance with the usual assumptions in free convection, the viscous dissipation terms in the energy equation have been neglected. This is a valid assumption, since the velocities in the free convection are usually relatively small. Also, if the velocities are small, the pressure distribution will not differ significantly from that of static equilibrium.

Ostrach (4) has shown that for the flat plate, the resultant equations are of the boundary-layer form if the Grashof number is fairly large. It would be expected that the same should hold for the axisymmetric geometry. The assumption that the Grashof number is large is valid if the distance from the leading edge is large, since the assumption has previously been made that $\beta\ (t_s - t_a)$ is small. It has been shown

experimentally that the results derived from such a theory for the flat plate are valid for Grashof numbers greater than 10^4. The upper limit of applicability of the solution to these equations is the point where the transition to turbulence begins, which is generally taken to be at the point where the Grashof number is 10^9 for air on a vertical flat plate. It is expected that this criterion is essentially the same for the vertical cylinder.

For the vertical flat plate, Ostrach (4) has shown that a similarity transformation exists which will transform the partial differential equations into ordinary differential equations. Introduction of the stream function reduced the number of equations to two coupled equations.

Yang (22) has investigated many cases in both two-dimensional and axi-symmetric geometries and has found no such transformation for the vertical isothermal cylinder which is compatible with the boundary conditions. The set of partial differential equations (1), (2) and (3) will be solved without reducing the number of independent variables.

Non-dimensionalization of the Basic Equations

Before solving the set of equations (1), (2), (3), the equations will be non-dimensionalized so that the smallest number of parameters will be left in the equations. To do this, a systematic method used by Hellums (33) will be employed. Let:

$$X = \frac{x}{x'} \qquad (4) \qquad\qquad U = \frac{u}{u'} \qquad (7)$$

$$R = \frac{r}{r'} \qquad (5) \qquad\qquad V = \frac{v}{v'} \qquad (8)$$

$$T = \frac{\tau}{\tau'} \qquad (6) \qquad\qquad \theta = \frac{t - t_a}{t_s - t_a} \qquad (9)$$

where x', r', τ', u' and v' are dimensional constants involving the various parameters of the flow. In Chapters II and III, T denotes the non-dimensional time. In Chapter V, T denotes the absolute temperature.

Substituting equations (4) through (9) into equations (1), (2) and (3) gives:

$$\frac{\partial(RU)}{\partial X} + \left[\frac{v'x'}{u'r'}\right] \frac{\partial(RV)}{\partial R} = 0 \qquad (10)$$

$$\frac{\partial U}{\partial T} + \left[\frac{u'\tau'}{x'}\right] U \frac{\partial U}{\partial X} + \left[\frac{v'\tau'}{r'}\right] V \frac{\partial U}{\partial R} = \left[\frac{g\beta(t_s - t_a)\tau'}{u'}\right] \theta \qquad (11)$$

$$+ \left[\frac{\nu\tau'}{r'^2}\right] \frac{1}{R} \frac{\partial}{\partial R}\left(R \frac{\partial U}{\partial R}\right)$$

$$\frac{\partial \theta}{\partial T} + \left[\frac{u'\tau'}{x'}\right] U \frac{\partial \theta}{\partial X} + \left[\frac{v'\tau'}{r'}\right] V \frac{\partial \theta}{\partial R} = \left[\frac{\alpha\tau'}{r'^2}\right] \frac{1}{R} \frac{\partial}{\partial R}\left(R \frac{\partial \theta}{\partial R}\right) \qquad (12)$$

In order that no parameters be left in the equations, all of the bracketed terms would have to be constants. Tentatively, they are assigned the following set of values:

$$\frac{v'x'}{u'r'} = 1/4 \qquad (13)$$

$$\frac{u'\tau'}{x'} = 4 \qquad (14)$$

$$\frac{v'\tau'}{r'} = 1 \qquad (15)$$

$$\frac{g\beta(t_s - t_a)\tau'}{u'} = 1 \qquad (16)$$

$$\frac{\nu\tau'}{r'^2} = 1 \qquad (17)$$

$$\frac{\alpha\tau'}{r'^2} = 1 \qquad (18)$$

Equation (13) is (14) divided by (15) and is therefore not independent. Also, equations (17) and (18) cannot be satisfied simultaneously unless $\nu = \alpha$. If (17) is satisfied, then (18) becomes:

$$\frac{\alpha\tau'}{r'^2} = \frac{\alpha}{\nu} = \frac{1}{\sigma}$$

where σ is the Prandtl number.

The set of differential equations (10), (11) and (12) then becomes:

$$4\frac{\partial(RU)}{\partial X} + \frac{\partial(RV)}{\partial R} = 0 \tag{19}$$

$$\frac{\partial U}{\partial T} + 4U\frac{\partial U}{\partial X} + V\frac{\partial U}{\partial R} = \theta + \frac{1}{R}\frac{\partial}{\partial R}\left(R\frac{\partial U}{\partial R}\right) \tag{20}$$

$$\frac{\partial \theta}{\partial T} + 4U\frac{\partial \theta}{\partial X} + V\frac{\partial \theta}{\partial R} = \frac{1}{\sigma R}\frac{\partial}{\partial R}\left(R\frac{\partial \theta}{\partial R}\right) \tag{21}$$

Thus, the only parameter left in the equations is the Prandtl number, σ, which is a property of the fluid.

Equations (19), (20) and (21) are valid only if the set of equations (14) through (17) is satisfied. This set consists of four equations in five unknowns. The choice of one of the unknowns is then arbitrary. To facilitate the comparison with the theory of Sparrow and Gregg (19), x' is chosen so that X bears the following relation to ξ:

$$X = \xi^4 = \left(\frac{2^6 \nu^2}{g\beta(t_s - t_a)r_o^4}\right) x \tag{22}$$

Then,

$$x' = \frac{g\beta(t_s - t_a)r_o^4}{2^6 \nu^2} \tag{23}$$

Equations (14) through (17) are then solved along with (23) and the following are obtained for u', v', r', and τ':

$$\tau' = \frac{r_o^2}{4\nu} \tag{24}$$

$$r' = \frac{r_o}{2} \tag{25}$$

$$u' = \frac{g\beta(t_s - t_a)r_o^2}{2^2 \nu^2} \tag{26}$$

$$v' = \frac{2\nu}{r_o} \tag{27}$$

The non-dimensional variables defined in equations (4) through (9) become:

$$X = \xi^4 = \frac{2^6}{Gr_{r_o}} \frac{x}{r_o} \tag{28}$$

$$R = 2\frac{r}{r_o} \tag{29}$$

$$T = 4\frac{\nu\tau}{r_o^2} \tag{30}$$

$$U = \frac{4}{Gr_{r_o}}\frac{r_o u}{\nu} \tag{31}$$

$$V = \frac{1}{2}\frac{r_o v}{\nu} \tag{32}$$

$$\theta = \frac{t - t_a}{t_s - t_a} \tag{33}$$

Associated Boundary and Initial Conditions

The boundary conditions associated with the differential equations for a vertical isothermal cylinder are:

$$\text{At } r = r_o, \qquad t = t_s \tag{34}$$

$$u = 0 \tag{35}$$

$$v = 0 \tag{36}$$

$$\text{At } r = \infty, \qquad t = t_a \tag{37}$$

$$u = 0 \tag{38}$$

$$\text{At } x = 0, \qquad t = t_a \tag{39}$$

$$u = 0 \tag{40}$$

The above are the normal boundary conditions associated with the differential equations in the free-convection problem.

If the unsteady equations are to be solved and a complete transient solution obtained, initial conditions must be specified giving the values of u, v and t at some time. An example of typical initial conditions would be those associated with the problem of the fluid initially at rest at the temperature of the ambient, and the cylinder surface given a step function increase in temperature from t_a to t_s. The initial conditions would then be:

$$\text{When } \tau = 0\text{; at } r = r_o,\ t = t_s\text{; elsewhere, } t = t_a \tag{41}$$

$$u = 0\text{ , everywhere} \tag{42}$$

$$v = 0\text{ , everywhere} \tag{43}$$

The boundary and initial conditions in terms of the set of dimensionless variables are:

$$\text{At } R = 2, \qquad \theta = 1 \tag{44}$$

$$U = 0 \tag{45}$$

$$V = 0 \tag{46}$$

$$\text{At } R = \infty, \qquad \theta = 0 \tag{47}$$

$$V = 0 \tag{48}$$

At $X = 0$, $\theta = 0$ (49)

$V = 0$ (50)

and at $T = 0$, except at $R = 2$, $\theta = 0$ (51)

$U = 0$ (52)

$V = 0$ (53)

In the next chapter, a method of solution of equations (19), (20) and (21) subject to the boundary conditions (44) through (50) and certain initial conditions will be discussed.

CHAPTER III

METHOD OF SOLUTION OF THE MATHEMATICAL PROBLEM

Although in this work, the main interest lies in the steady-state solution to the differential equations (19), (20) and (21) along with their boundary conditions given by equations (44) through (50), a scheme was employed in which the unsteady equations were used to generate the steady-state solution as a limiting case. This method was proposed by Hellums (33). He applied the method with success to the free-convection problems associated with the vertical isothermal flat plate and inside a horizontal cylinder.

Basically, the method involves the use of the finite-difference approximation, in which the differential equations are replaced by a set of difference equations, which may be solved algebraically at each point in a space grid. In this connection, there are two different approaches which may be taken: the steady-state method and the unsteady method.

The Steady-state Method Versus the Unsteady Method

In the steady-state method, the unsteady terms are dropped from the equations leaving only the independent variables X and R and the dependent variables U, V and θ. If the X and R dimensions are divided, respectively, into N-1 and M-1 increments, there will be MN grid points. At each of these points, the three difference equations must be satisfied. This will

mean that 3MN algebraic equations must be solved. For the problem considered here most of these equations are non-linear. The methods for solving non-linear algebraic equations are not very highly developed at the present time. Associated with some of these schemes, however, there is no stability problem as is inherently associated with the unsteady approach, but Hellums (33) concluded that there were other advantages which made the unsteady approach preferable. Douglas and Peaceman (34) indicated that even for the heat-conduction problem, in which the equations are linear, the unsteady approach is often preferable.

The unsteady method, on the other hand, is concerned with the full set of equations. The independent variables are X, R, and T and the dependent variables U, V, and θ. The equations are explicit in time, that is, the value of one of the dependent variables at a given time depends only on values of the dependent variables at a previous time. This means that the value of any dependent quantity may be completely determined if all of the values are known at the previous time, and values may be solved for, one at a time, as opposed to solving a set of simultaneous equations as encountered in the steady-state approach. The stability problem is the only disadvantage of this method. In general, this problem can be circumvented by choosing an appropriately small time step. If the time step becomes too large, the solution obtained from this method will oscillate or diverge. However, the unsteady method is chosen as preferable for the present problem.

In the subsequent sections, the space grid and notation, the finite-difference approximation, and the stability analysis for the proposed problem will be investigated.

Notation of the Space Grid and the Difference Problem

To facilitate the understanding of the actual computer program used to solve the system of equations, a notation will be presented which corresponds to that used in the program given in Appendix A. Before discussing the notation, the physical space grid is defined.

The space grid is shown in Figure 2, page 21. The point J = 1, L = 1 corresponds to the leading edge of the cylinder where $x = 0$, $r = r_o$, or in non-dimensional coordinates $X = 0$, $R = 2$. With this grid, $X = (J - 1)\Delta X$ and $R = 2 + (L - 1)\Delta R$, where ΔX and ΔR are the incremental changes in X and R.

The space position at which the dependent variable is evaluated is noted by giving the J and L values as subscripts. To make this notation more completely resemble the computer program, the subscripts are put in parentheses after the quantity. For example: U(J,L) is the value of U at $X = (J - 1)\Delta X$ and $R = R_o + (L - 1)\Delta R$. U(J - 1, L + 1) is the value of U at $X = (J - 2)\Delta X$ and $R = R_o + (L)\Delta R$.

In the finite-difference solution two times are needed: T and $T + \Delta T$. The unprimed dependent variable is evaluated at time T; the primed variable at $T + \Delta T$. For example U(J,L) is U evaluated at time T. U'(J,L) is U evaluated at $T + \Delta T$.

In the finite-difference approximations, the derivatives in the differential equations are replaced by difference ratios, and the resultant algebraic equations are then solved. For instance, the term $\frac{\partial U}{\partial X}$ may be approximated by the following expressions:

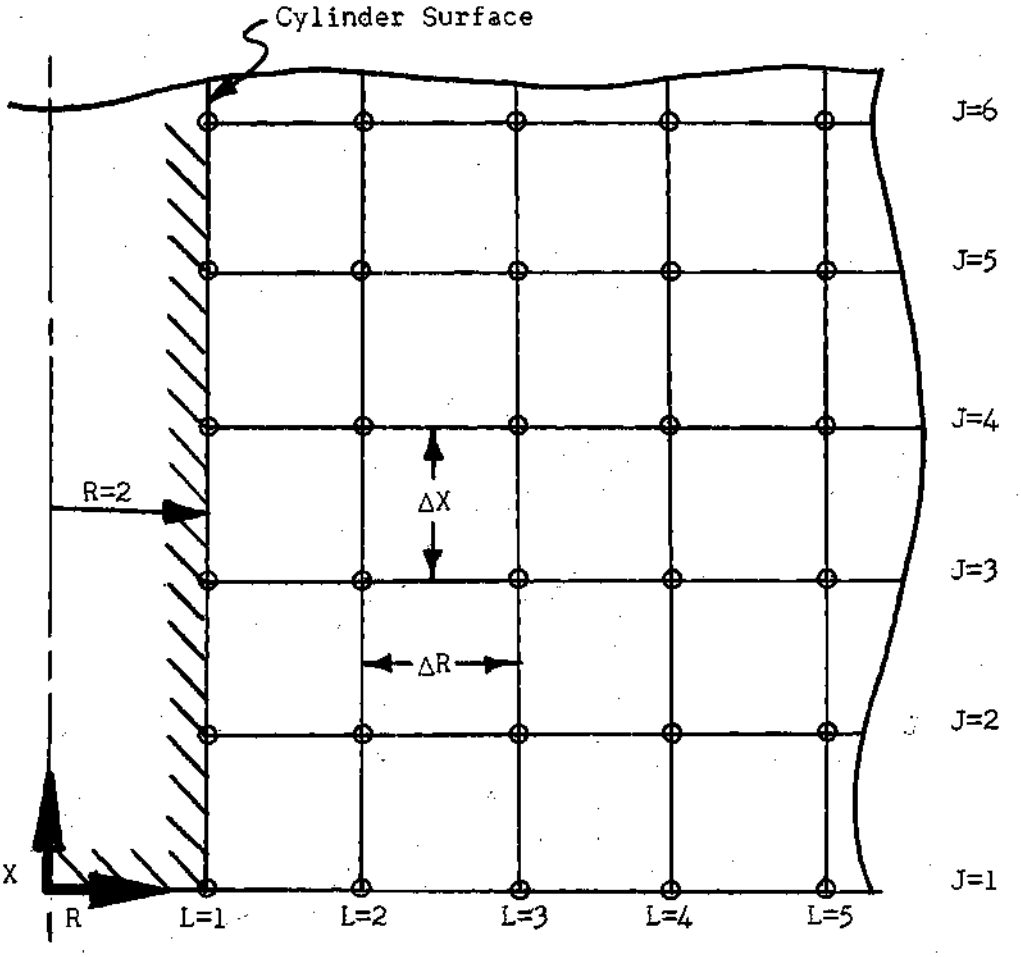

Figure 2. Space Grid for the Finite-Difference Solution.

$$\frac{\partial U(J,L)}{\partial X} \approx \frac{U(J+1,L) - U(J,L)}{\Delta X}$$

$$\approx \frac{U(J,L) - U(J-1,L)}{\Delta X}$$

$$\approx \frac{U(J+1,L) - U(J-1,L)}{2(\Delta X)}$$

In the limit as ΔX approaches zero, all of these will approach the value of the derivative. An estimate of the error in the approximation can be determined by considering a Taylor series expansion of the function U. In the first two approximations, the error is of the order of magnitude of ΔX; in the third, it is of the order of $(\Delta X)^2$. Therefore, for small values of ΔX, the third approximation would be the best one. However, it is found that the stability requirements will dictate the type of difference approximation to use.

Stability Criterion and the Difference Scheme

The approach used in this chapter is based on the work of Hellums (33) who draws his basic method from Richtmyre (35). Stability of a system of difference equations is, in essence, putting a limit on the extent to which any part of the initial data can be amplified in the numerical procedure. In the case to be considered, if the following inequality holds, the system will be said to be stable:

$$\text{Max}_{(J,L)}|U'(J,L)| \leq (\text{Max}_{(J,L)}|U(J,L)|)(1 + M_1\Delta T) + M_2\Delta' T \qquad (54)$$

where $M_1 \geq 0$, $M_2 \geq 0$

and $\text{Max}_{(J,L)}|U(J,L)|$ is the largest absolute value of U at time T. This is essentially the definition given by Richtmyre (35). Hellums showed that (54) implies that for a fixed T as ΔT approaches zero, the solution is bounded independent of the way in which ΔT approaches zero. It may be shown for many linear systems that stability is a sufficient condition for the solution of the difference equations as the increments approach zero to converge to the solution of the differential equations. This has not been shown for this particular system of equations, but it has been generally true for many such non-linear systems. Ultimately, the solution may be checked against experimental data and other analytical solutions to determine its validity. The definition of stability given here is different from that given by many authors. Others define stability in terms of the damping out of errors introduced in the equations. It may be shown that the two definitions of stability are quite similar in nature.

The case to be considered here is actually somewhat simpler than equation (54) indicates. For the momentum equation, $M_1 = 0$ and for the energy equation $M_1 = M_2 = 0$.

To investigate the stability of a particular difference equation, the following procedure is used:

1) Arrange the differential equation so that the time derivative is set equal to the remaining terms.
2) Replace the time derivative with a forward difference ratio in time.
3) Replace all space derivatives in such a way that the coefficient

of the function evaluated at the point in question is negative (by using the appropriate forward or backward difference).

4) Solve for the value of the dependent function at the new time.

5) Inspect the resulting equation to determine the necessary inequalities in order that conditions for stability as defined in equation (54) are satisfied.

Rearranging equations (20) and (21) in accordance with step (1) gives:

$$\frac{\partial U}{\partial T} = -4U\frac{\partial U}{\partial X} - V\frac{\partial U}{\partial R} + \frac{1}{R}\frac{\partial}{\partial R}\left(R\frac{\partial U}{\partial R}\right) + \theta \qquad (55)$$

$$\frac{\partial \theta}{\partial T} = -4U\frac{\partial \theta}{\partial X} - V\frac{\partial \theta}{\partial R} + \frac{1}{\sigma R}\frac{\partial}{\partial R}\left(R\frac{\partial \theta}{\partial R}\right) \qquad (56)$$

Equation (19) does not involve a time derivative and is therefore stable in time. From the nature of the problem and from the solution of the vertical flat plate; it is expected that U is always greater than or equal to zero, while V is always less than or equal to zero in the solution with the prescribed boundary conditions and suitable initial conditions. This was confirmed <u>a posteriori</u>. If this had not been true, four sets of equations would have had to be used depending on the signs of U and V. Noting the above, steps (2) and (3) may be completed noting further that a representation of the last derivative may be given as follows:

$$\frac{1}{R}\frac{\partial}{\partial R}\left(R\frac{\partial U}{\partial R}\right) \approx \left(\frac{1}{R\Delta R}\right)\left[\frac{(R+\frac{\Delta R}{2})(U(J,L+1)-U(J,L))}{\Delta R}\right. \tag{57}$$

$$\left. -\frac{(R-\frac{\Delta R}{2})(U(J,L)-U(J,L-1))}{\Delta R}\right]$$

$$= \frac{1}{(\Delta R)^2}\left[U(J,L+1)-2U(J,L)+U(J,L-1)\right]$$

$$+\frac{1}{2R\Delta R}\left[U(J,L+1)-U(J,L-1)\right]$$

This approximation satisfies the criterion that the coefficient of $U(J,L)$ be negative.

Under the difference approximation, equations (55) and (56) become:

$$\frac{U'(J,L)-U(J,L)}{\Delta T} = -4U(J,L)\left[\frac{U(J,L)-U(J-1,L)}{\Delta X}\right] \tag{58}$$

$$-V(J,L)\left[\frac{U(J,L+1)-U(J,L)}{\Delta R}\right]$$

$$+\frac{1}{(\Delta R)^2}\left[U(J,L+1)-2U(J,L)+U(J,L-1)\right]$$

$$+\frac{1}{2R\Delta R}\left[U(J,L+1)-U(J,L-1)\right]+\theta'(J,L)$$

$$\frac{\theta'(J,L)-\theta(J,L)}{\Delta T} = -4U(J,L)\left[\frac{\theta(J,L)-\theta(J-1,L)}{\Delta X}\right] \tag{59}$$

$$-V(J,L)\left[\frac{\theta(J,L+1)-\theta(J,L)}{\Delta R}\right]$$

$$+ \frac{1}{\sigma(\Delta R)^2}\left[\theta(J,L+1) - 2\theta(J,L) + \theta(J,L-1)\right]$$

$$+ \frac{1}{2\sigma R\Delta R}\left[\theta(J,L+1) - \theta(J,L-1)\right]$$

Replacing the derivatives in equation (19) by backward differences at time T+ΔT gives:

$$\frac{4[RU'(J,L) - RU'(J-1,L)]}{\Delta X} + \frac{[RV'(J,L) - (R-\Delta R)V'(J,L-1)]}{\Delta R} = 0 \qquad (60)$$

Solving (58) for U'(J,L), (59) for θ'(J,L) and (60) for V'(J,L) gives:

$$U'(J,L) = \left(1 - \frac{4\Delta T}{\Delta X}U(J,L) + \frac{\Delta T}{\Delta R}V(J,L) - \frac{2\Delta T}{(\Delta R)^2}\right)U(J,L) \qquad (61)$$

$$+ \left(\frac{4\Delta T}{\Delta X}U(J,L)\right)U(J-1,L) + \left(\frac{\Delta T}{(\Delta R)^2} + \frac{\Delta T}{2r\Delta R}\right.$$

$$\left. - \frac{\Delta T}{\Delta R}V(J,L)\right)U(J,L+1) + \left(\frac{\Delta T}{(\Delta R)^2} - \frac{\Delta T}{2R\Delta R}\right)U(J,L-1)$$

$$+ \Delta T\,\theta'(J,L)$$

$$\theta'(J,L) = \left(1 - \frac{4\Delta T}{\Delta X}U(J,L) + \frac{\Delta T}{\Delta R}V(J,L) - \frac{2\Delta T}{\sigma(\Delta R)^2}\right)\theta(J,L) \qquad (62)$$

$$+ \left(\frac{4\Delta T}{\Delta X}U(J,L)\right)\theta(J-1,L) + \left(\frac{\Delta T}{\sigma(\Delta R)^2} + \frac{\Delta T}{2\sigma R\Delta R}\right.$$

$$\left. - \frac{\Delta T}{\Delta R}V(J,L)\right)\theta(J,L+1) + \left(\frac{\Delta T}{\sigma(\Delta R)^2} - \frac{\Delta T}{2\sigma R\Delta R}\right)\theta(J,L-1)$$

$$V'(J,L) = \frac{R - \Delta R}{R} V'(J,L-1) - \frac{4\Delta R}{\Delta X}\left(U'(J,L) - U'(J-1,L)\right) \tag{63}$$

If

$$A(J,L) = \frac{4\Delta T}{\Delta X} U(J,L) \tag{64}$$

$$B(J,L) = -\frac{\Delta T}{\Delta R} V(J,L) \tag{65}$$

$$C = \frac{\Delta T}{(\Delta R)^2} \tag{66}$$

$$D(L) = \frac{\Delta T}{2R\Delta R} \tag{67}$$

$$G(L) = \frac{R - \Delta R}{R} \tag{68}$$

$$H = \frac{4\Delta R}{\Delta X} \tag{69}$$

Then, equations (61), (62) and (63) become:

$$\theta'(J,L) = \left(1 - A(J,L) - B(J,L) - \frac{2C}{\sigma}\right)\theta(J,L) + A(J,L)\theta(J-1,L) \tag{70}$$
$$+ \left(\frac{C}{\sigma} + \frac{D(L)}{\sigma} + B(J,L)\right)\theta(J,L+1) + \left(\frac{C}{\sigma} - \frac{D(L)}{\sigma}\right)\theta(J,L-1)$$

$$U'(J,L) = (1 - A(J,L) - B(J,L) - 2C)U(J,L) + A(J,L)U(J-1,L) \tag{71}$$
$$+ (C + D(L) + B(J,L))U(J,L+1)$$
$$+ (C - D(L))U(J,L-1) + \Delta T\theta'(J,L)$$

$$V'(J,L) = G(L)V'(J,L-1) - H(U'(J,L) - U'(J-1,L)) \qquad (72)$$

The above set of equations then represents a scheme for finding θ, U, and V at the point J,L in terms of θ, U, and V at the previous time. Starting with initial conditions on θ, U, and V, the values of θ, U, and V may be calculated at time ΔT and then the procedure repeated for as many time steps as desired. It has not yet been shown that the set of equations (70), (71) and (72) is stable. This will be done next.

Conditions for Stability

Equations (70), (71) and (72) show the conditions necessary to satisfy the stability requirement as stated in equation (54). In equation (70) for all J and L; A(J,L), B(J,L), C, D(L), and G(L) are all positive since U(J,L) is always a positive number and V(J,L) is always negative. Therefore, the sum of the coefficients of all of the θ's is unity, and each will be positive if the following inequalities are satisfied:

$$1 - A(J,L) - B(J,L) - 2\frac{C}{\sigma} \geq 0 \qquad (73)$$

$$\frac{C}{\sigma} - \frac{D(L)}{\sigma} \geq 0 \qquad (74)$$

Since all of the coefficients of θ are positive and add up to one, they are all between zero and one. Equation (70) may then be thought of as saying that the value of θ at any point is between the highest and the lowest values at the points around the point in question

at the previous time. Or, in more precise terms:

$$\text{Max}(J,L)|\theta'(J,L)| \leq \text{Max}(J,L)|\theta(J,L)| \tag{75}$$

Therefore, $M_1 = M_2 = 0$ if the inequalities (73) and (74) are satisfied, and the energy equation is stable.

In equation (74), substituting for C and D(L) gives:

$$\frac{\Delta T}{\sigma(\Delta R)^2} \geq \frac{\Delta T}{\sigma R \Delta R} \tag{76}$$

or, therefore

$$R \geq \Delta R \tag{77}$$

since ΔT, σ, ΔR and R are all positive quantities. The first R considered in the space grid for iteration purposes is $R_o + \Delta R$, so

$$R_o + \Delta R \geq \Delta R \tag{78}$$

is always satisfied since $R_o = 2$. Equation (73) will be seen to be the condition for stability for Prandtl numbers less than one.

In equation (71), the sum of all of the coefficients of the U's is one. Each coefficient will be positive if:

$$1 - A(J,L) - B(J,L) - 2C \geq 0 \tag{79}$$

$$C - D(L) \geq 0 \tag{80}$$

If the inequalities hold, then:

$$\text{Max}(J,L)|U'(J,L)| \leq \text{Max}(J,L)|U(J,L)| + \theta'(J,L)\Delta T \qquad (81)$$

Since it has already been shown that $\theta(J,L)$ is bounded and positive, equation (81) is seen to satisfy the stability criterion of equation (54). From the initial and boundary conditions, θ is initially between 0 and 1; and, therefore, if the inequality for the energy equation holds, is always between 0 and 1. Therefore, considering equation (71):

$$0 \leq M_2 \leq 1 \quad \text{and} \quad M_1 = 0$$

Equation (80) will always be satisfied since it is the same as equation (74) multiplied by a constant.

There is no stability argument necessary for equation (72) since the value of $V(J,L)$ is dependent only on values of U and V at time T.

To summarize the conditions for stability as shown previously in this chapter, equations (73) and (79) must be satisfied. Rearranging the equations gives:

$$A(J,L)^{\cdot\cdot} + B(J,L) + \frac{2C}{\sigma} \leq 1 \qquad (82)$$

$$A(J,L) + B(J,L) + 2C \leq 1 \qquad (83)$$

Considering as an example the case where $\sigma = 0.72$, (82) is the condition to be considered since if it is satisfied, (83) will also be satisfied. Substituting into equation (82), the expressions for A, B, and C gives

$$\frac{4\Delta T}{\Delta X} U(J,L) - \frac{\Delta T}{\Delta R} V(J,L) + \frac{2\Delta T}{\sigma(\Delta R)^2} \leq 1 \tag{84}$$

This may be written as a restriction on ΔT as follows:

$$\Delta T \leq \frac{1}{\frac{4U(J,L)}{\Delta X} - \frac{V(J,L)}{\Delta R} + \frac{2}{\sigma(\Delta R)^2}} \tag{85}$$

Therefore, for a given ΔX and ΔR; ΔT may be chosen small enough to satisfy the inequality (85). The value of ΔT will depend on the maximum values of U(J,L) and V(J,L), but it may be chosen sufficiently small to satisfy equation (85) and, thereby, insure stability of the system.

Actual Method of Computer Solution

The choice of the space grid is extremely important in obtaining a solution. On the one hand, if the spacing in the R direction is too coarse, the slope of the temperature profile at the wall cannot be accurately determined; and, therefore, the heat-transfer coefficient will be inaccurate. On the other hand, if it is too fine, the time step is diminished because of stability consideration and the length of computer time required to reach steady state becomes too long to be feasible.

With the spacing in the X direction as noted by Hellums (33), only after one gets a number of grid points away from the leading edge does the finite-difference solution begin to approach the solution of the differtial equation. This would imply a small X increment; and, consequently, a great amount of computer time for steady state to be achieved. Alternatively, the parameter of real interest is ξ which is equal to $X^{1/4}$. Therefore, to obtain a large range of ξ, the range in X must be very much larger.

Another problem that is intimately related to the finite-difference approximation is the determination of a point at some finite value of R to impose the boundary conditions of $R = \infty$. Since a finite number of steps in the R direction are taken, some point sufficiently far from the cylinder surface must be chosen to impose the conditions that $U = 0$, $\theta = 0$ which in the differential equations are imposed at $R = \infty$.

A trial run with $\sigma = 0.72$, $\xi = 0.025$, $\Delta\xi = 0.025$, $\Delta R = .0025$ and the infinite boundary conditions placed respectively at 50, 60, 70, 80, 90, and 100 grid spaces from the wall was made. The results of this are summarized in Table 1, page 33. In each case, the approach to steady-state to the desired accuracy took the same number of iterations through the entire grid, but, of course, a longer computer time was required when there were more grid points. The computed Nusselt numbers differed only three parts in one million for any of the runs and were the same (to machine accuracy) for the 70, 80, 90, and 100 point runs. The value of θ near the point at which the infinity condition was imposed changed to a greater degree. At the fortieth grid point from the wall, with only 50 points, the value of θ was 5.6 per cent lower than that for the 100 point run. The value of θ at the fortieth grid point for all runs with more than 50 grid points differed less than 3.5 parts in 10,000. It was

Table 1. Selection of R_∞ for a Prandtl Number of 0.72

$\xi = 0.025$ $\Delta R = 0.0025$

R_∞	η	Number of Iterations	Nu_{r_o}	H(2,2)	H(2,40)
2.125	5.0	170	61.827600	0.92273286	.66546274
2.150	6.0	170	61.827520	0.92273287	.70613573
2.175	7.0	170	61.827680	0.92273273	.70637586
2.200	8.0	170	61.827680	0.92273273	.70637600
2.225	9.0	170	61.827680	0.92273273	.70637600
2.250	10.0	170	61.827680	0.92273273	.70637600

therefore decided for a Prandtl number of 0.72 to use as an infinite point the spacing corresponding to 60 grid points in the R direction to insure accuracy in the Nusselt number and to give accurate temperature profiles away from the cylinder.

The use of 60 grid points is related to the flat plate problem in which η goes from 0.0 to 6.0. An "equivalent" η may be defined for the cylinder by $\eta = \frac{R - 2}{\xi}$. On a flat plate at $\eta = 6$, Ostrach's solution gives $\theta = 0.0012$ and $U = 0.0015\xi^2$ or $U = 0.00544U_{max}$. Thus the conditions $\theta = 0$, $U = 0$ are approximately met by Ostrach's solution for the flat plate at this point and the corresponding θ and U should be closer to zero at the same distance from the surface on the cylinder.

The infinite radial boundary conditions are set at the point where $\eta = 6$. Therefore, at each ξ station, R_∞ is taken as the next grid point past the point where:

$$R_\infty = 2.0 + 6.0\xi \tag{86}$$

For other Prandtl numbers, a similar procedure is followed. R_∞ is determined by considering the flat plate solution and choosing an η for which θ and U are approximately zero. For a Prandtl number of 100 this is taken as 4.0 to obtain sufficient accuracy in the temperature profiles. For a Prandtl number of 0.01, η is approximately 22.

Equations (70), (71) and (72) may be solved for any space grid subject to the restriction on ΔT given by (85). Initially, it was decided to solve the equations for a 21 by 21 space grid with a step

change in the cylinder wall temperature. This went from $\xi = 0$ to $\xi = 1$ in equal increments of $\Delta\xi$, and from $R = 2$ to $R = 6$ in equal increments of ΔR. It was planned to start with initial conditions as represented by equations (51), (52) and (53). Using the computer, storage limited the solution to a 21 by 21 space grid. After trying this, it was found that the increment in the R direction was not fine enough to give sufficient accuracy in the derivatives at the wall. Several other configurations were tried using fewer ξ positions and more R positions.

The final attempt, which was successful, used equal X increments and no more than 50 R positions. Starting at the boundary where $X = 0$ and proceeding in equal X increments, the equations may be solved for the various values of X independent of subsequent values of X because the equations are parabolic in nature. Therefore, the computer program solved the velocity and temperature profiles at a particular value of X in terms of the value at the previous X station. At the new X, boundary conditions were placed at $R = 2$ and $R = R_\infty$ as defined previously. Then, equations (70), (71) and (72) were used to find new values of U, V, and θ. This continued until the values of the variables changed less than a prescribed amount in ten iterations. Because of time considerations, it was decided to use a better initial approximation of the steady-state velocity and temperature profiles. Therefore, after the first X position, the values of θ at the previous X position, were used as initial guesses for θ at the new X position. A new set of U's were computed at each X station such that $U_{New} = U_{Old} \left(\frac{X_{New}}{X_{Old}}\right)^{1/2}$. (For the flat plate $U/X^{1/2}$ is the similar velocity and therefore gives the

same curve for each X position.) Of course, in doing this the unsteady portion of the solution is physically meaningless and only the steady-state solution was obtained from the computer.

In the actual solutions for $\sigma = 0.72$, starting at the boundary 40 equal steps with $\Delta X = 0.00001$ were taken. Then, ΔX was increased to 0.00004 for 40 steps to a value of $X = 0.0020$. Then, ΔX was increased to 0.00040 for five steps to $X = 0.0040$. From that point on, ΔX was increased every nine steps by a factor of 10. This continued until $X = 400{,}000$. ΔR was initially taken as 0.1 and doubled when the number of R positions between $R = 2$ and R_∞ were greater than 50. A detailed description of the program and method of solution is given in Appendix A, page 92.

Heat-Transfer Parameters from Temperature Profiles

The local heat-transfer coefficient, h, is defined as

$$h = \frac{q/A}{t_s - t_a} \tag{86}$$

q/A may be calculated from the temperature profiles since all of the heat at the surface of the cylinder is transferred by conduction to the fluid so that

$$q/A = -k \left(\frac{\partial t}{\partial r}\right)_{r = r_o} \tag{87}$$

Thus

$$h = \frac{-k \left(\frac{\partial t}{\partial r}\right)_{r = r_o}}{t_s - t_a} \tag{88}$$

Or in terms of the dimensionless variables

$$h = -\frac{2k}{r_o} \left(\frac{\partial \theta}{\partial R}\right)_{R = 2} \tag{89}$$

Thus, the local Nusselt number based on r_o, Nu_{r_o}, is

$$Nu_{r_o} = -2 \left(\frac{\partial \theta}{\partial R}\right)_{R = 2} \tag{90}$$

Initially, the first difference ratio was used to approximate the derivative at the wall. At higher values of X and, therefore, larger values of ΔR, the effect of curvature could not be neglected; and, the following scheme was devised to evaluate the heat flow. Since the velocity at the first grid point is relatively small, the heat may be considered to be conducted through a cylindrical element whose inner radius is R = 2 and outer radius is R = 2 + ΔR. This assumes that the heat convected into the element is equal to that convected out. The heat transferred through a cylindrical shell is given by

$$q/A = \frac{k(t_1 - t_2)}{r_1 \ln(r_2/r_1)} \tag{91}$$

where the subscript 1 refers to the inner surface and 2 to the outer surface.

Then, from the definition of the heat-transfer coefficient, h is:

$$h = \frac{k}{r_1} \frac{(t_1 - t_2)}{\ell n(r_2/r_1)(t_s - t_a)} \tag{92}$$

if surface 1 is the cylinder wall, $t_1 = t_s$ and $r_1 = r_o$. Putting the equations in non-dimensional form gives

$$h = \frac{k}{r_o} \left[\frac{1 - \theta(J,2)}{\ell n(1 + \Delta R/2)}\right], \tag{93}$$

or putting it in terms of the Nusselt number, Nu_{r_o}

$$Nu_{r_o} = \frac{1 - \theta(J,2)}{\ell n(1 + \Delta R/2)} \tag{94}$$

Note that for small ΔR, this reduces to

$$Nu_{r_o} = 2\left[\frac{1 - \theta(J,2)}{\Delta R}\right] \tag{95}$$

which is the result obtained by simply replacing $\left(\frac{\partial \theta}{\partial R}\right)_{R = 2}$ by its finite difference ratio.

Conventionally, the Nusselt number based on x is used. Now

$$Nu_x = \frac{x}{r_o} Nu_{r_o} \tag{96}$$

But since,

$$\xi = \frac{2^{3/2}}{Gr_x^{1/4}} \frac{x}{r_o} \tag{97}$$

then,

$$Nu_x = \left(\frac{Gr_x}{4}\right)^{1/4} \frac{\xi Nu_{r_o}}{2} \tag{98}$$

For the flat plate, Ostrach (4) obtained the following for a Prandtl number of 0.72

$$Nu_{x\ fp} = 0.5046 \left(\frac{Gr_x}{4}\right)^{1/4} \tag{99}$$

Therefore, the ratio of the Nusselt number for a cylinder to that for a flat plate is:

$$\frac{Nu_x}{Nu_{x\ fp}} = \frac{\xi Nu_{r_o}}{1.0092} \tag{100}$$

For the present problem, the overall heat-transfer coefficient is defined as

$$\bar{h} = \frac{1}{\ell}\int_0^{\ell} h \, dx \tag{101}$$

The average Nusselt number based on r_o, Nu_{r_o}, is:

$$\overline{Nu}_{r_o} = \frac{1}{\ell}\int_0^{\ell} Nu_{r_o} \, dx \tag{102}$$

Transforming into non-dimensional quantities gives,

$$\overline{Nu}_{r_o} = \frac{1}{L}\int_0^{L} Nu_{r_o} \, dx \quad \text{where} \quad L = X(\ell) = \frac{2^6 \ell}{Gr_{r_o}} \tag{103}$$

This integration was carried out numerically using the trapezoidal rule.

From this, the other parameters may be obtained as follows:

$$\overline{Nu}_{\ell} = \frac{\ell}{r_o}\,\overline{Nu}_{r_o} \tag{104}$$

or

$$\overline{Nu}_{\ell} = \left(\frac{Gr}{4}\ell\right)^{1/4} \frac{\xi \overline{Nu}_{r_o}}{2} \tag{105}$$

Ostrach (4) has determined that for the flat plate with $\sigma = 0.72$:

$$\overline{Nu}_{\ell\ fp} = \frac{4}{3}(0.5046)\left(\frac{Gr_\ell}{4}\right)^{1/4} \tag{106}$$

Thus,

$$\frac{\overline{Nu}_\ell}{\overline{Nu}_{\ell\ fp}} = \frac{\xi_\ell \overline{Nu}_{r_o}}{1.3456} \tag{107}$$

Similar calculations may be made for other Prandtl numbers.

CHAPTER IV

EXPERIMENTAL APPARATUS

Cylinders of various heights and diameters were held rigidly on a support of equal diameter, with their axes vertical and heated by means of an electrical current passed through resistance elements inside the cylinders. A guard heater was placed on top of each to eliminate conduction out the top of the last section. The power input to the heater was measured with an A. C. wattmeter. Thermocouples were placed in the cylinder walls as well as in the ambient air around the test section. From the above data, the overall heat-transfer coefficient could be calculated along with the fluid properties of the air.

Test Enclosure

All of the tests were conducted with the test cylinder in an enclosure which was four feet by four feet by eight feet high. Figure 3, page 43, shows the test enclosure with a test cylinder in it. It was completely enclosed at top and bottom to eliminate drafts and other flows. Initially, it had been designed to have a baffled opening at the top and bottom to let in outside air to keep the ambient air temperature from rising during a given run. It was found that the baffles did not eliminate drafts in the enclosure so the openings were closed. The power dissipated by the cylinders was small enough that no noticeable rise in ambient air temperature for the duration of a single run was noted. The

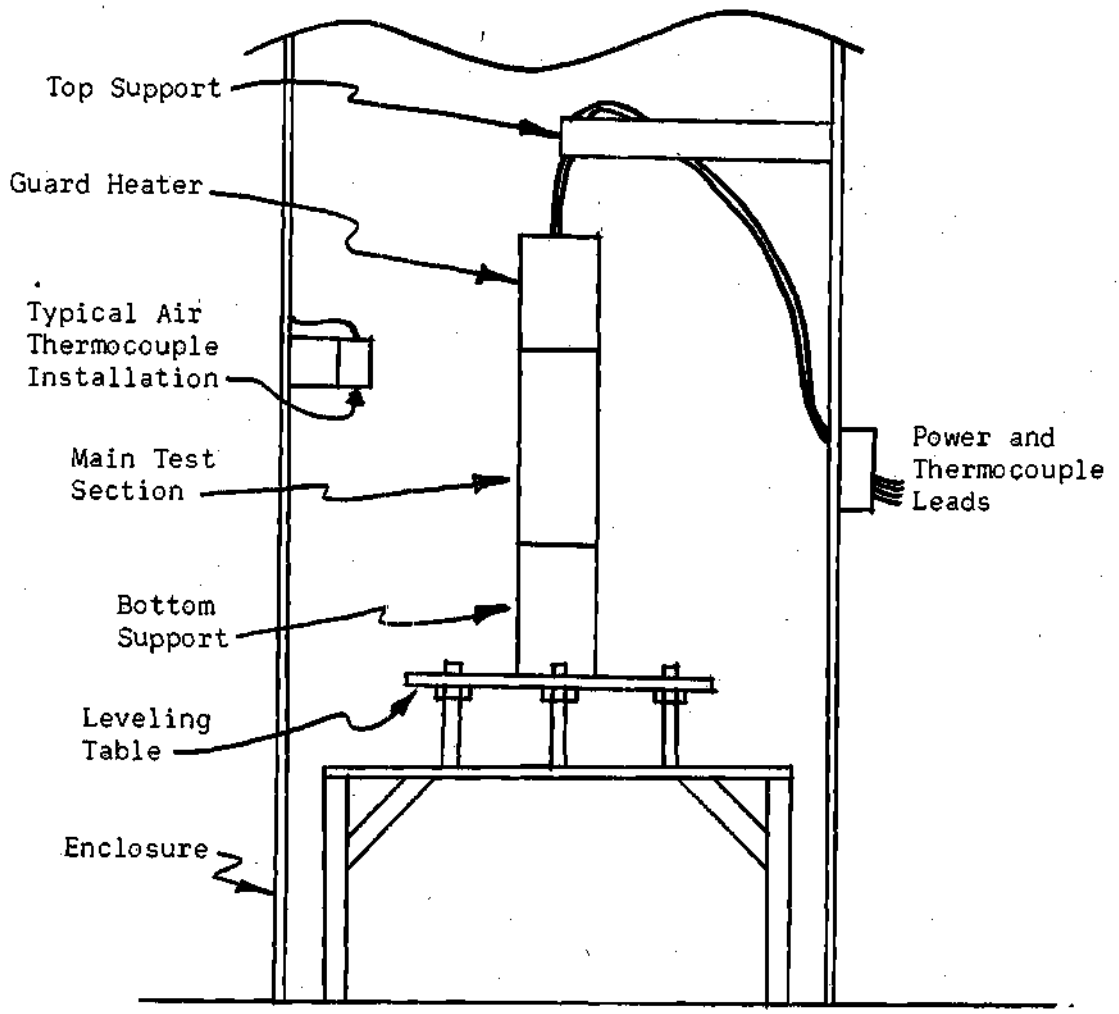

Figure 3. Test Enclosure.

walls of the test cell were covered with aluminum foil to reduce radiation heat transfer between the test section and the enclosure walls.

A table was bolted to the floor inside the test enclosure. On the table was a plate supported by nuts on three studs bolted to the table so that the plate could be leveled and locked in place.

The wooden support was screwed to the leveling plate and the test and guard heater sections were placed on top of this support. Leads from inside the cylinders were brought out the top of the guard heater and through a support attached to the enclosure. For all test sections of one inch diameter or greater, this was sufficient to insure that the sample remained vertical. For the one-half inch diameter test pieces, an additional restraint at the top supporting piece had to be used. The one-half inch diameter test pieces were threaded at the top and screwed into a wooden brace, which was rigidly attached to the support. In addition, the one-half inch diameter pieces were held at the leading edge section in the same manner as the larger sections. Thermocouples were mounted on each wall of the enclosure to determine the wall temperature. Shielded thermocouples gave the air temperature at various points inside the enclosure.

Test Sections

The first test section built was 6.625 inches in diameter (6 inch extra-strong copper pipe, 0.432 inch wall thickness) and 18 inches high plated with one-half mill of bright nickel. Its purpose was to check the instrumentation and procedure by obtaining flat plate results. An electric heater was made by winding 20 gauge Nichrome wire around a five

inch diameter pipe covered with a thin layer of asbestos. The top and bottom of the test section had insulated covers and the entire assembly sat directly on a wooden cylinder of the same diameter as the copper pipe. It was found that within a reasonable experimental error, the data confirmed the equation given by McAdams (36) for vertical flat plates which is given below:

$$\overline{Nu}_{\ell} = 0.590(Gr_{\ell} \cdot \sigma)^{1/4} \qquad (108)$$

McAdams' equation was chosen over the analytical results of Ostrach (4) for two basic reasons. First, McAdams' equation is an experimental correlation, while Ostrach's equations are analytical; and it was thought that the experimental work should be compared with an experimental correlation. Second, Ostrach's work assumed constant fluid properties, while McAdams accounts for this by evaluating all properties at the arithmetic mean temperature. It was decided that all experimental work would be compared with the equation of McAdams while all analytical work would be compared with Ostrach's results.

As a result of using this large cylinder, certain modifications were made on the subsequent cylinders used to determine the effects of curvature. The bottom support was a wooden cylinder as shown in Figure 4, page 46. The wooden support was screwed to the leveling plate. A cylinder of aluminum foil the diameter of the cylinder was used to aid in obtaining a step rise in temperature at the leading edge of the test section. Because of air gap between the wood and the aluminum foil, the

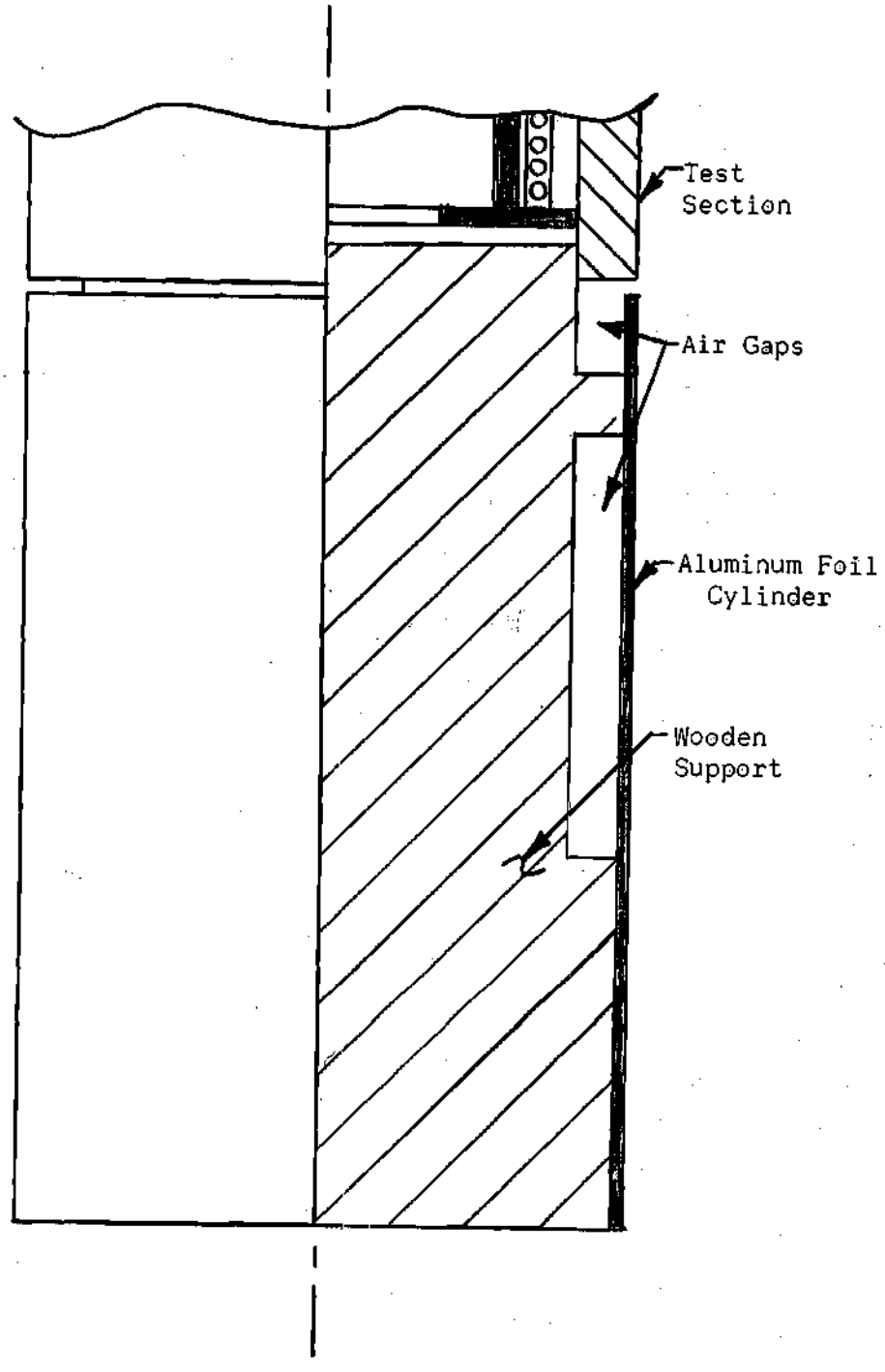

Figure 4. Test Support.

foil remained essentially at ambient temperature. When the six inch diameter cylinder was built and set directly on a wooden support, the temperature of the wood rose above the ambient temperature, thus causing the flow to begin below the leading edge of the test section. This was eliminated by the above-described arrangement. The test section proper was fitted onto the wooden piece as shown in the figure.

The test section itself was made from standard thick-walled copper pipe (0.540, 1.050 and 1.900 inches in outside diameter). The outer surface of the test section was plated with one-half mill of bright nickel plate. This gave a surface which had a low emissivity (approximately 0.05), and one which did not oxidize on heating the cylinder. The one inch and two inch diameter sections were made in pieces three or six inches long which could be fitted into each other to make cylinders up to 18 inches high. (The one-half inch diameter test section was made in one piece and cut off to give smaller lengths.) Each of these small pieces was a unit in itself with its own heater and thermocouples mounted on it. A typical test section of this diameter is shown in Figure 5, page 48. Thermocouples were placed in the walls of the test sections by drilling small holes through the walls, inserting the thermocouple from the inside, and filling each hole with a commercial mixture of steel filings and plastic binder known as "Liquid Steel." The thermocouple leads were brought out the center of the pipe. By putting the thermocouple leads near the heater for some length, conduction down the leads of the thermocouples was minimized. Thermocouples were placed at least every two inches along the vertical length of the test section at

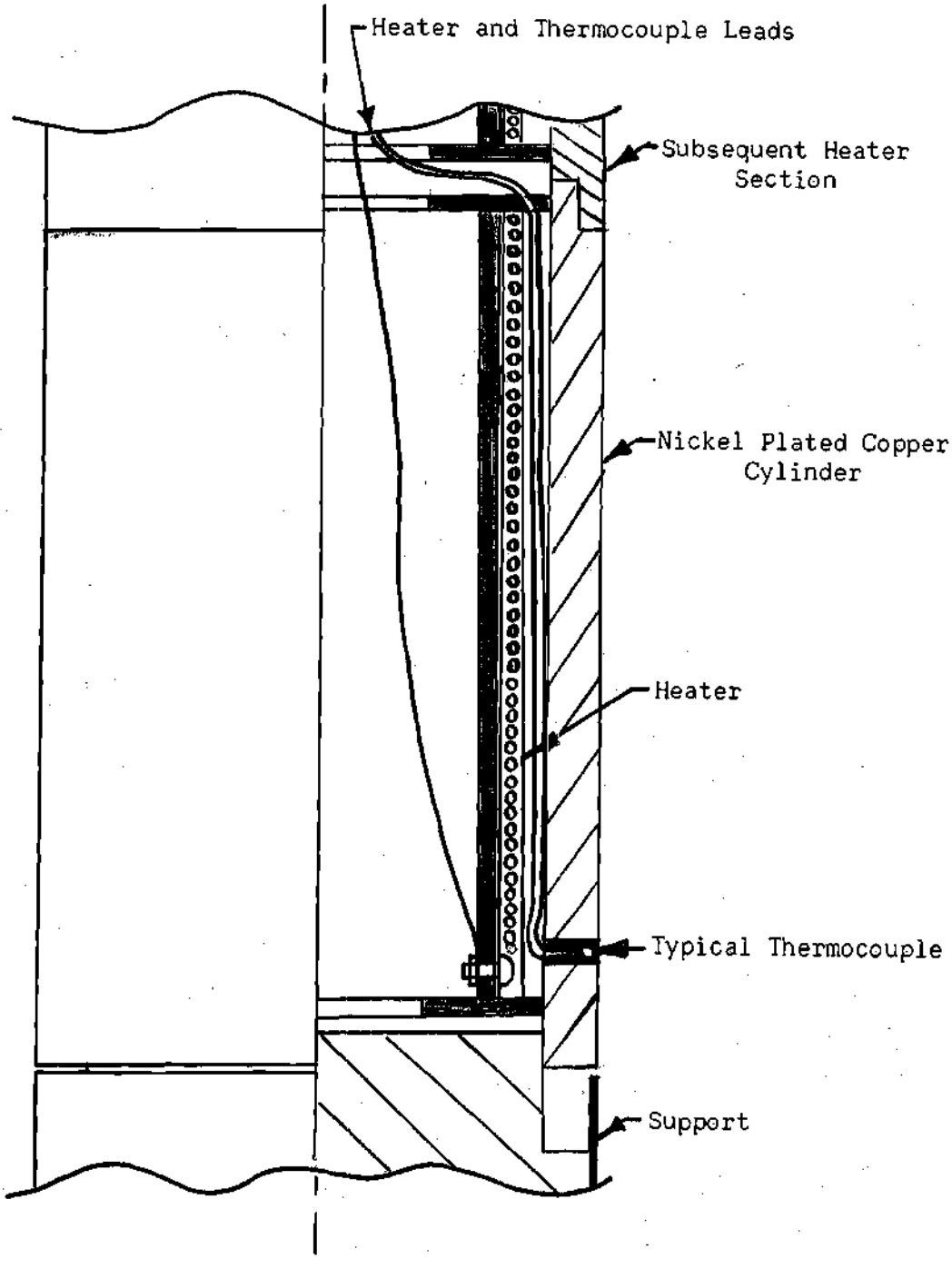

Figure 5. Portion of Test Section.

three equally-spaced angular positions with one an inch from the leading edge at the bottom and one within one-half inch of the guard heater section at the top.

The heaters in the test section were electrical resistance elements wound especially for the cylinders. In the case of all but the one-half inch diameter cylinders, the heaters were wound on copper tubing of a smaller size than the inside diameter of the pipe. This tubing had been split into two sections, and glued back together with a piece of insulation between them so that the two sides were electrically insulated from one another and could be used as leads for the heaters. A layer of asbestos about 1/32 inch thick was wrapped around the heater and cemented on with Sauerreisen #63 cement. The heater was made by wrapping 34 gauge Nichrome wire around the asbestos. The wire used was enamel-coated. The enamel probably burned off when the wire was heated, but it kept the wire from shorting until the whole assembly could be coated with Sauerreisen #63 electrical heater cement which held the wires rigidly in place and kept them from touching one another. An insulator washer, whose outer diameter was approximately the inner diameter of the copper pipe, was cemented to each end of the heater which held the heaters in the copper pipes. Notches were cut in the washers to allow the thermocouple leads from that particular section to be brought into the center of the heater for the next run. The heater leads were made by attaching wires to the two sides of the split copper pipe. All of the heater and thermocouple leads were brought out the center of the heater sections.

Because of the small inside diameter of the one-half inch sections,

the heaters were wound on solid rods with fiberglass sleeving used to insulate the heaters from the rod and the cylinder itself. The rod itself was used for one of the heater leads and the heater was wound so as to bring the other lead out the top of the section.

On top of the test section was another section of similar construction and three inches high. It was separated from the main test section by a piece of asbestos about one-half inch thick as shown in Figure 6, page 51. The heater in this section was controlled separately and acted as a guard heater to eliminate conduction out the top of the test section. Conduction from the top of the six-inch diameter cylinder had been found to be appreciable. Thermocouples were mounted one-half inch from the bottom of the guard heater and one-half inch from the top of the test section. The power to the guard heater was controlled so as to keep these thermocouples reading essentially the same temperature. All of the leads were brought out the center of the guard heater and the remaining space was filled with vermiculite.

Power Supply and Instrumentation

The power was supplied to the heaters as shown by the schematic diagram in Figure 7, page 52. A Sorensen A. C. Regulator No. 2501 was used to maintain a voltage of 115 volts ± 0.5 per cent. To control the actual voltages to the heaters, two separate Superior Type 21 powerstats were used, one to regulate the voltage to the main heater, the other to regulate the voltage to the guard heater. This permitted the voltage of each heater to be varied from 0 to 115 volts independently of the other. The power dissipated in the test section heater was measured with a Weston

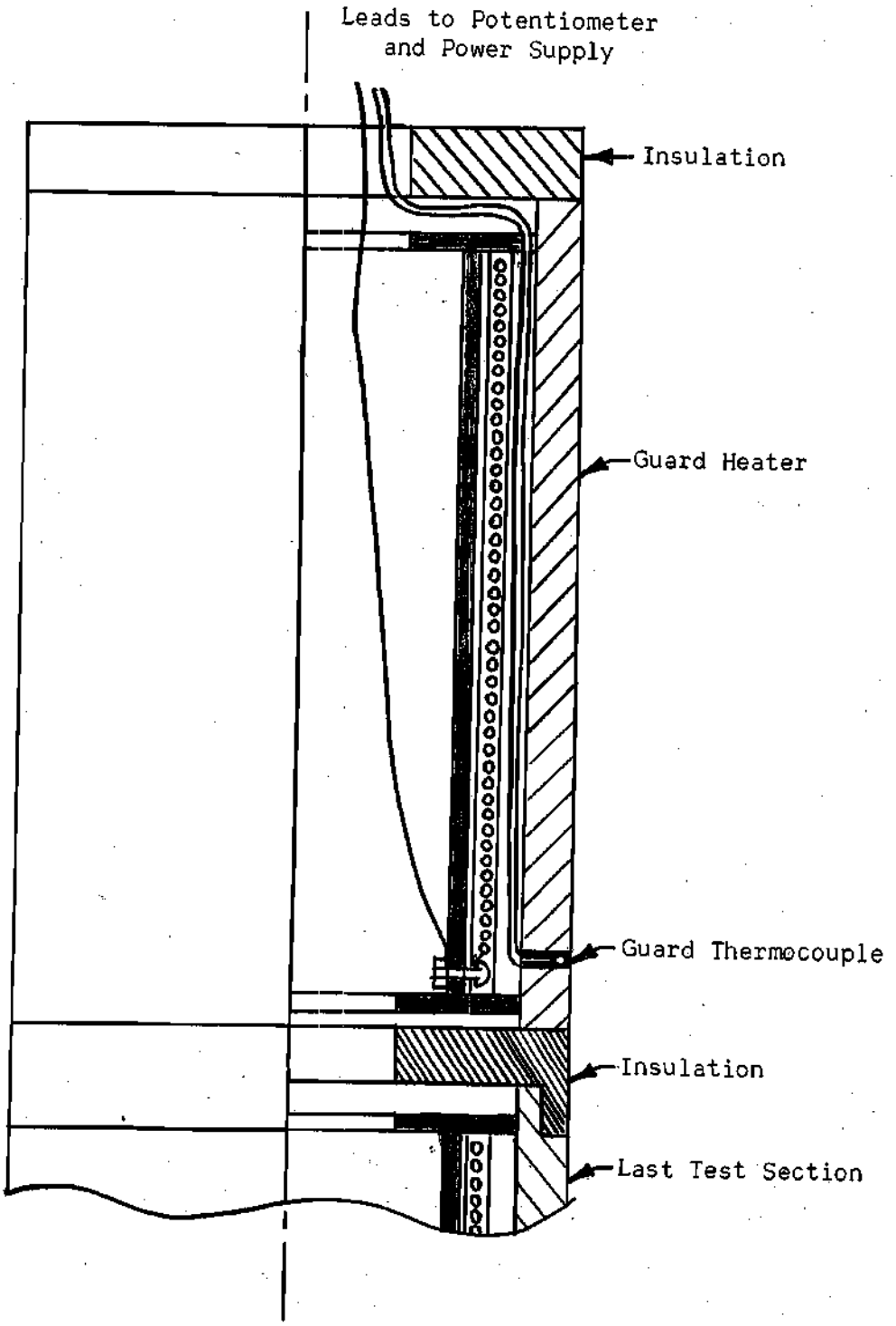

Figure 6. Guard Heater.

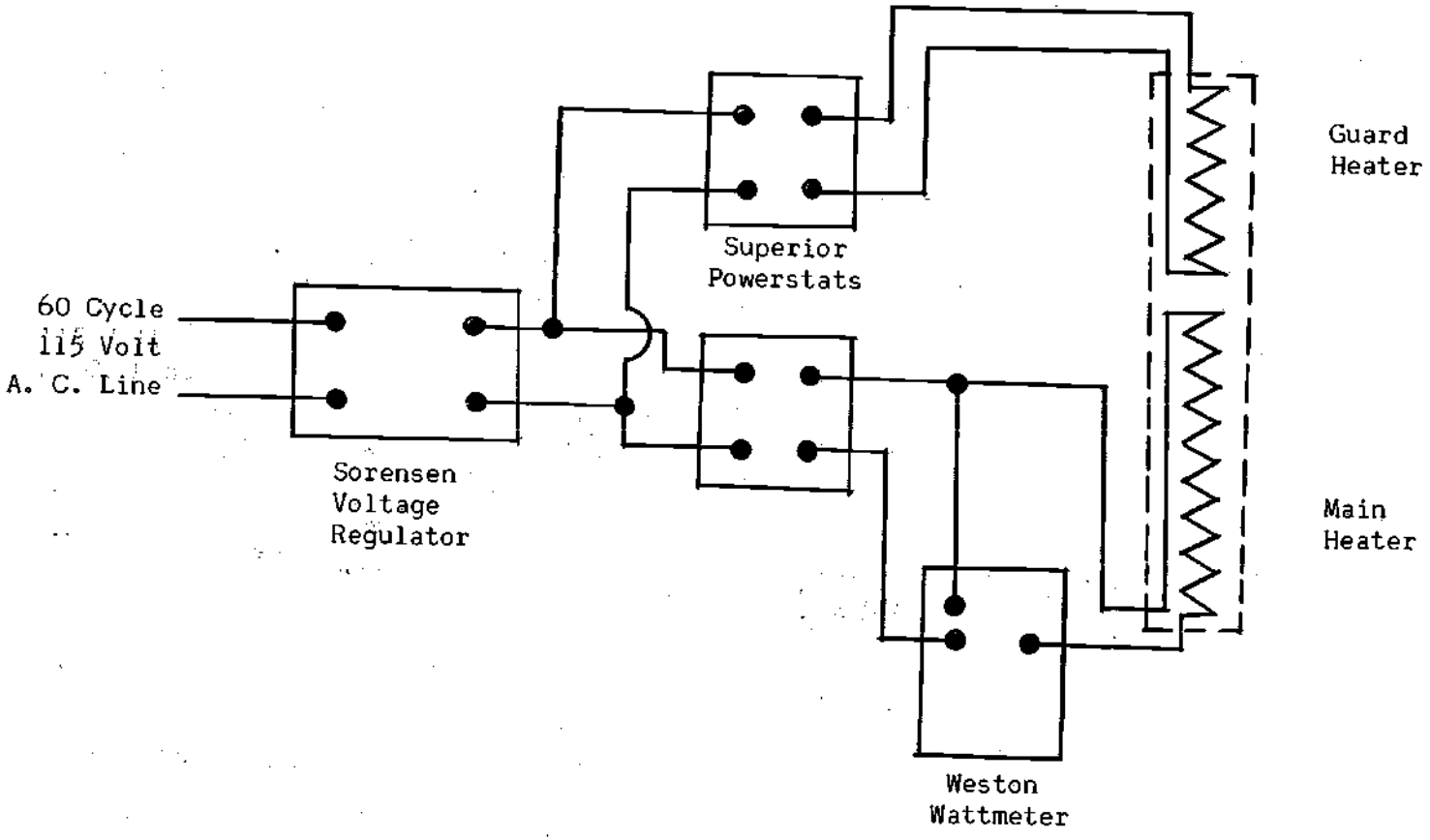

Figure 7. Schematic Diagram of Power and Control Apparatus.

type 310 A. C. wattmeter. It was connected in such a way that the losses in the potential circuit could be determined.

The thermocouples were all from one roll of Leeds and Northrup Copper-Constantan Thermocouple wire No. 24.55.1. This is 24 gauge wire insulated with enamel and glass sleeving. The thermocouple junctions were made by welding the wires together with a thermocouple welder. In each of the tests, there were between two and six thermocouples reading the surface temperature of the test section depending on the length of the section. There was at least one thermocouple for every three inches of length of test section. The thermocouples were placed at three equally-spaced angular positions around the test section. There was one thermocouple which read the guard heater surface temperature. Three thermocouples were used to read the air temperature, and three indicated the wall temperature of the enclosure. Two of the air temperature thermocouples were shielded from radiation from the cylinder by a cylindrical shield, open at the top and bottom. The third thermocouple was unshielded and closer to the cylinder than the first two. No appreciable difference in temperature could be noted among the three thermocouples.

The outputs of the thermocouples were read on a Leeds and Northrup Millivolt Potentiometer No. 8686. A Leeds and Northrup thermocouple switch was used with an ice bath for a common cold junction. All of the thermocouple leads were brought out of the enclosure to a common terminal board which was enclosed so as to keep all of the dissimilar metal junctions (those between the constantan thermocouple leads and the copper thermocouple switch) at the same temperature, thereby cancelling the EMF produced by these junctions.

CHAPTER V

EXPERIMENTAL PROCEDURE AND DATA REDUCTION

Overall heat-transfer coefficients for steady-state free convection from vertical isothermal cylinders of various heights and diameters as described in the previous chapter were experimentally determined.

Experimental Procedure

A given test section was placed in the enclosure and mounted on the adjustable table as described in Chapter IV. The heater and thermocouple wires were attached to their proper terminal positions, and the test section was leveled by adjustment of the legs of the table such that it was vertical as noted by a level placed against the side of the cylinder.

The power was turned on; and when the temperatures appeared to be changing only very slightly, adjustments were made on the guard heater so as to keep the guard heater thermocouple reading within 0.5° F of the top main section thermocouple. This was done manually by adjusting the Powerstat which supplied the guard heater and was continued during the run as needed. When the temperatures seemed to be steady, readings of all the thermocouples and the power input to the main heater section were taken every 10 to 15 minutes for at least an hour.

To measure the losses in the potential circuit, the main heater was momentarily disconnected and the reading on the wattmeter was recorded.

If the variation in surface temperature over the main heater section was more than 12 per cent of the mean temperature difference, the run was discarded as not being isothermal. If the surface temperature varied in one hour more than five per cent of the mean temperature difference, the run was discarded as unsteady.

Reduction of Experimental Data

Computation

From the experimental data, the overall heat-transfer coefficient was calculated and the fluid properties of air were obtained. From these, the standard dimensionless groupings may be obtained. This was done using a computer program for the Burroughs 220 written in Algol language. The actual computer program and explanation of symbols are given in Appendix B, page 100.

Neglecting conduction out the top or bottom of the test section, the total loss from the section by convection and radiation is given by

$$q_{to} = 3.413\ P/A \qquad (109)$$

Where P is the electrical power dissipated in the main heater in watts and A is the surface area of the test section ($\pi d\ell$) and q_{to} is the total heat transferred from the test section per unit area in Btu/hr ft^2.

The assumption of no conduction out the top of the cylinder was substantiated by the fact that the guard section was kept essentially

at the same temperature as the top of the main heater section. It was further assumed that there was negligible heat loss out the wooden starting section because of the low thermal conductivity of the wood and the method of mounting the test section.

The heat loss from the cylinder per unit area by radiation may be approximated by the transfer between two concentric cylinders. For this case, Eckert and Drake (37) give the following relation:

$$q_{ra} = \frac{\bar{\sigma}(T_1^4 - T_2^4)}{1/\varepsilon_1 + A_1/A_2(1/\varepsilon_2 - 1)} \qquad (110)$$

where $\bar{\sigma}$ is the Stefan-Boltzman constant, ε is the emissivity and T the absolute temperature. In this chapter, T represents the absolute temperature. This is true throughout the experimental portion of this thesis. Subscript 1 refers to the inner cylinder and 2 to the outer cylinder. Assuming that the area of the outer enclosure was much greater than that of the cylinder, this becomes:

$$q_{ra} = \varepsilon_s \bar{\sigma}(T_s^4 - T_w^4) \qquad (111)$$

where the subscript s refers to the cylinder surface and subscript w to the enclosure wall. The emissivity of the cylinder surface was taken as 0.045, the value given by McAdams (38) for polished nickel. Duhig (39) measured the emissivity of a piece of copper plated in the same manner in which the test sections were plated. He found that over the

temperature range in this experiment that the emissivity varies less than ten per cent from 0.045.

The convective heat transfer may then be calculated as follows:

$$q_{co} = q_{ro} - q_{ra} \tag{112}$$

and the overall heat-transfer coefficient is by definition:

$$\bar{h} = \frac{q_{co}}{t_s - t_a} \tag{113}$$

All of the fluid properties were evaluated at a film temperature as suggested by McAdams (38) where the film temperature is

$$t_f = \frac{t_s + t_a}{2} \tag{114}$$

The variation of the fluid properties with temperature was expressed in the form of equations as follows:

$$k = 1.313371 \times 10^{-2} + 2.5870573 \times 10^{-5}t - 6.1050061t^2 \tag{115}$$

$$Z \times 10^{-6} = 4.3348727 - 4.210649 \times 10^{-2}t + 2.2256586 \times 10^{-4}t^2 \tag{116}$$
$$- 6.6493277 \times 10^{-7}t^3 + 8.43861 \times 10^{-10}t^4$$

$$\sigma = 0.72040 - 1.69519 \times 10^{-4}t + 1.71468 \times 10^{-7}t^2 \tag{117}$$

Where t has the dimensions degrees F; k, Btu/hr ft °F; Z, $1/ft^3$ °F; and ø is dimensionless. The equations for k and Z were obtained from Purdy (41). The three equations were obtained by taking the data for dry air from National Bureau of Standards Circular 564, Table of Thermal Properties of Gases (40) and fitting the data with least-squares curves for the range of temperature from 8° F to 260° F. The difference between the equations and the tabulated data were no greater than ± 0.05 per cent for k and ø and ± 0.6 per cent for Z. Some error was introduced into the calculations by not considering the effect of the water vapor in the air on these properties. Errors caused by not considering water vapor were estimated to be no greater than 2.5 per cent in the determination of ξ and negligible in the determination of Nu_{r_o}.

The following dimensionless groups can now be calculated:

$$\overline{Nu}_{\ell} = \frac{\bar{h}\ell}{k} \tag{118}$$

$$\overline{Nu}_{r_o} = \frac{\bar{h}r_o}{k} \tag{119}$$

$$Gr_{\ell} = Z(t_s - t_a)\ell^3 \tag{120}$$

$$\xi = \frac{2^{3/2}}{Gr_{\ell}^{1/4}} \frac{\ell}{r_o} \tag{121}$$

$$\text{Ratio} = \frac{\overline{Nu}_{\ell}}{\overline{Nu}_{\ell\ fp}} \tag{122}$$

Where the Nusselt number for the flat plate is obtained from McAdams' equation

$$\overline{Nu}_{\ell\ fp} = 0.590(Gr_{\ell} \cdot \sigma)^{1/4} \qquad (123)$$

Error Estimate

Since the majority of the experimental data was compared to other results in terms of the Nusselt number based on r_o, it is of interest to estimate the maximum experimental error in the determination of Nu_{r_o}.

Errors could have been introduced into the results from the following measurements: cylinder diameter and length; electrical power input; test section, air and enclosure temperatures; thermal conductivity of the air; and the emissivity of the cylinder surface.

The height of each test section was measured with a scale and is estimated to be accurate within ± 1/32 inch. The diameters of the test sections were measured by micrometer and found to deviate a maximum of ± 0.003 inches. The possible error in diameter will be taken as ± 0.005 inches.

The wattmeter manufacturer claims an accuracy of ± 0.25 per cent of the full scale readings. Calculations were made to estimate the conduction from the top and bottom of the test section. Considering this and the accuracy of the wattmeter, the maximum possible error in the power reading was estimated to be ± 0.125 watts.

The thermocouples used in the test section were calibrated at the steam point and were found to be accurate within ± 1.5° F. All thermocouples at room temperature were accurate within 1.0° F. The error introduced by the potentiometer was negligible. The maximum error in each temperature reading was taken at ± 1.5° F.

Values for the thermal conductivity of the air were taken from National Bureau of Standards Circular 564 (40) which claims that they are accurate within ± 2.0 per cent. The errors introduced by the least-squares fit and by not considering the water vapor in the air are both negligible. The maximum error in the thermal conductivity was taken to be ± 2.0 per cent.

The surface emissivity of the bright nickel plate on copper was taken to be ± 10 per cent as measured by Duhig (39).

These estimates were programmed into the computer data reduction program and a maximum per cent error is given with each data point using the standard procedure for computing the accumulation of errors in arithmetic processes. (See Appendix B, page 100.) Points with greater than 15 per cent possible error were discarded.

Preliminary estimates of the error involved in a particular ξ indicated that it was much smaller than that related to the corresponding local Nusselt number.

CHAPTER VI

RESULTS

Analytical Results

Prandtl Number of 0.72

The finite-difference calculations described in Chapter III were carried out for a Prandtl number of 0.72. Near the leading edge (X = 0), the results differed somewhat from those of Sparrow and Gregg (19). Figure 8, page 62, shows both sets of results in this range. At the first grid point, $\xi = 0.0556$, the finite-difference result was approximately 45 per cent higher than Sparrow and Gregg's results which should be accurate at this low value of ξ. By the twentieth grid point, $\xi = 0.1189$, the finite-difference result was within two per cent of the Sparrow and Gregg's result. This was considered the matching point for the two solutions, and it was assumed that Sparrow and Gregg's solution was correct up to this point and the finite-difference solution was assumed valid after this point. An alternate method of determining the starting point of a finite-difference solution and a method to be used if no other analytical results are known is presented in Appendix D, page 114.

Hellums (33) noted a similar trend in the finite-difference solution of the flat plate problem. At low values of X, the predicted heat-transfer coefficient was high, but came progressively closer to the exact value given by Ostrach (4). He attributed this to being near the

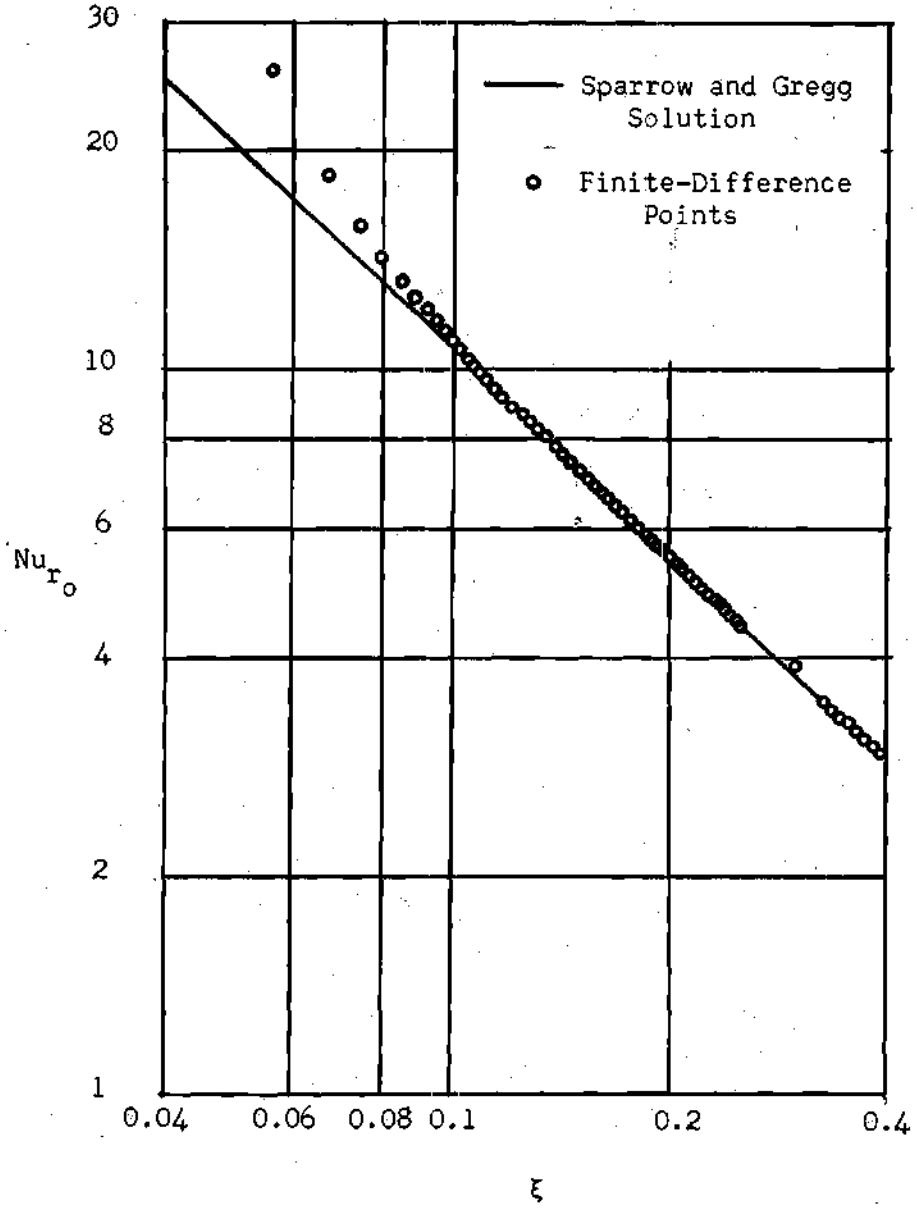

Figure 8. The "Leading Edge" Effect for a Prandtl Number of 0.72.

leading edge where the variables change rapidly with X.

In the present work, this effect was noted not only at the leading edge, but also at any point at which the X increment was increased. In Figure 8, the value of the Nusselt number at $\xi = 0.2990$ was high. The value of X was increased at the point immediately preceding this ($\xi = 0.2490$). At the next point ($\xi = 0.3284$), the Nusselt number was essentially in agreement with Sparrow and Gregg's result. This type of behavior resulted each time that the X increment was increased. The deviation was progressively less as X increased. For a Prandtl number of 0.72, the values at these points which were obviously in error were taken as the interpolated value considering the next higher and lower points, assuming that the Nusselt number based on r_o was a linear function of $1/\xi$ (an exact relation for the flat plate). Actually, the use of these values, which were in error, in computing the average Nusselt number would have produced little error in the average values; and this is what was done for all other Prandtl numbers.

A summary of the results of the finite-difference program are given in Table 2, page 64. Figures 9 and 10, pages 65 and 66, show a comparison between the present theoretical results and those of Sparrow and Gregg (19) and Hama, Recesso and Christiaens (25). In Figure 9, the dependence of the local Nusselt number based on r_o on the distance parameter ξ is shown. The present theory agrees with that of Sparrow and Gregg quite well up to a value of $\xi = 1$. At this point, Sparrow and Gregg's theory begins to deviate and then turns drastically downward. If Sparrow and Gregg had taken more terms in their series, it would be

Table 2. Analytical Heat-Transfer Results for a Prandtl Number of 0.72

ξ	Nu_{r_o}	$\overline{Nu}_{r_o}$	$\frac{Nu_x}{Nu_{x\ fp}}$	$\frac{\overline{Nu}_\ell}{\overline{Nu}_{\ell\ fp}}$
0.2114*	5.2487	6.8562	1.0992	1.0770
0.2514	4.5267	5.8502	1.1274	1.0928
0.4472	2.7766	3.5556	1.2301	1.1815
0.7952	1.7302	2.1830	1.3631	1.2899
1.414	1.1361	1.4017	1.5914	1.4728
2.514	0.78438	0.93713	1.9536	1.7506
4.472	0.57330	0.66907	2.5400	2.2233
7.952	0.43781	0.49970	3.4492	2.9526
14.14	0.34440	0.38894	4.8244	4.0865
25.14	0.28361	0.31113	7.0636	5.8120

*For ξ values less than 0.2114, Sparrow and Gregg's results were used.

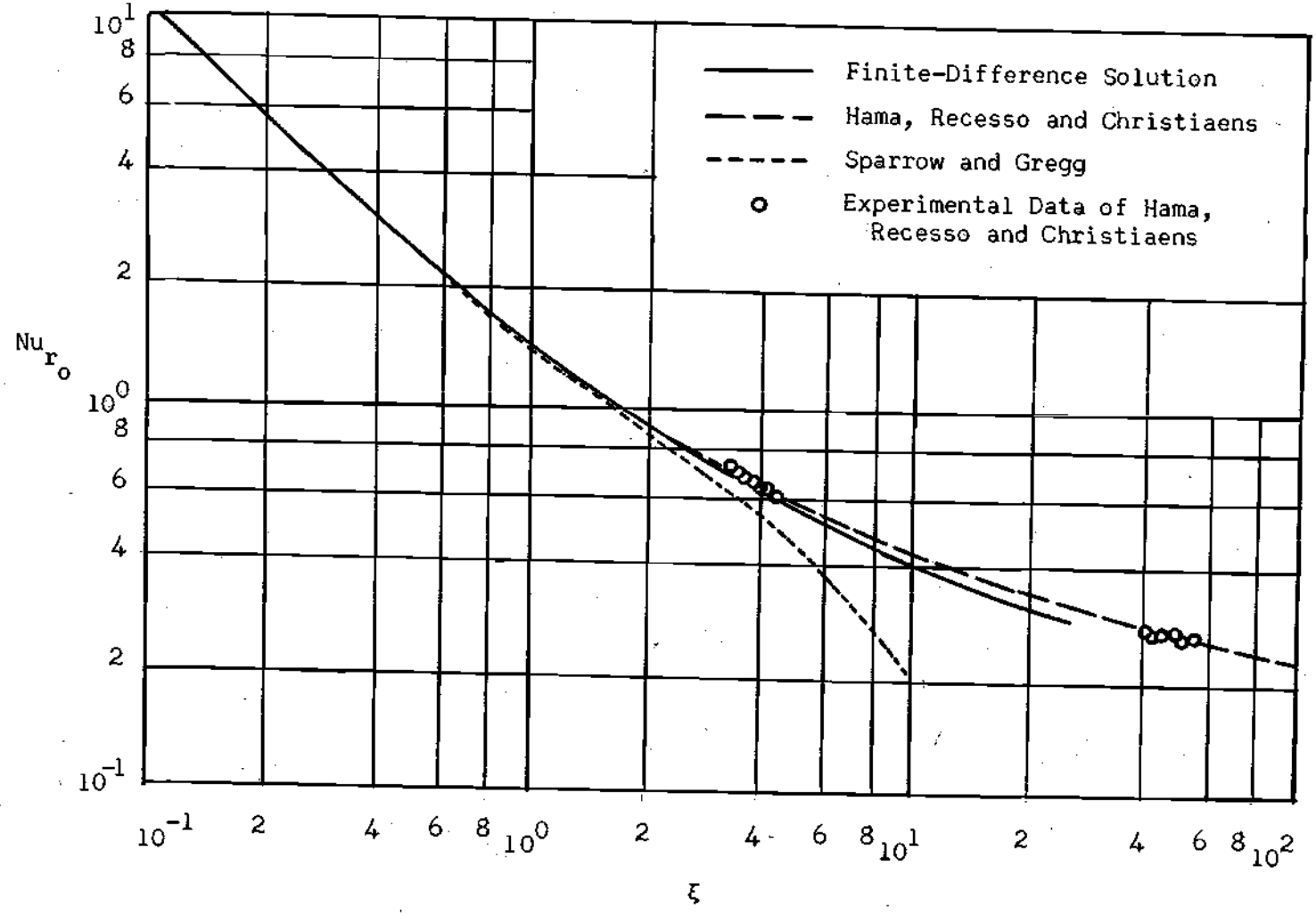

Figure 9. Local Nusselt Numbers for a Prandtl Number of 0.72.

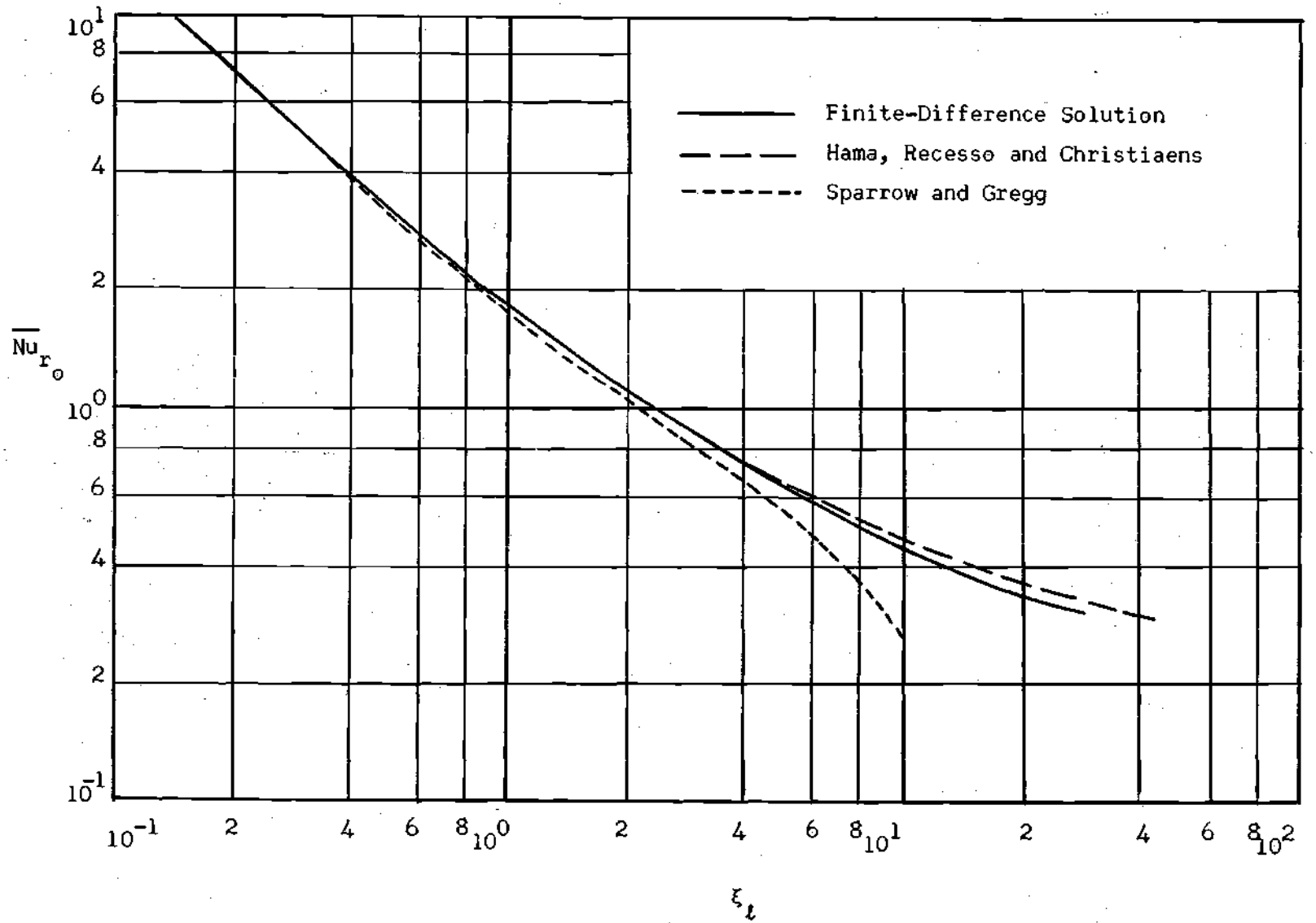

Figure 10. Average Nusselt Numbers for a Prandtl Number of 0.72.

expected that their solution would be accurate at larger values of ξ. The results of Hama, Recesso and Christiaens agree well with the present work. At the last point of the finite-difference solution, $\xi = 25.14$, the difference between the two curves is approximately 8 to 10 per cent. Experimental values obtained by Hama, Recesso and Christiaens are also shown on this plot. The analytical curve for the present work is seen to go slightly below these points. This fact is discussed in the analysis of experimental data.

Figure 10, compares the average Nusselt number predicted by three methods mentioned above. Again, the present results are very close to those of Sparrow and Gregg up to a ξ value of approximately one, at which point the Sparrow and Gregg curve begins to fall away. At this point, the curve for the present solution approaches the values which the present author obtained by numerically integrating the local values quoted by Hama, Recesso and Christiaens. At values of ξ greater than 10, this curve lies somewhat below that of Hama, Recesso and Christiaens. This seems reasonable since Sparrow and Gregg's truncated series should be most accurate at low values of ξ and the Hama, Recesso and Christiaens solution is an asymptotic solution and should be approached at high values of ξ.

An important adjunct to the present method of obtaining the heat-transfer parameters is that the velocity and temperature profiles are obtained also. Temperature profiles can be obtained for the solution of Hama, Recesso and Christiaens, but its form has been assumed. Figures 11 and 12, pages 68 and 69 show typical velocity and temperature profiles

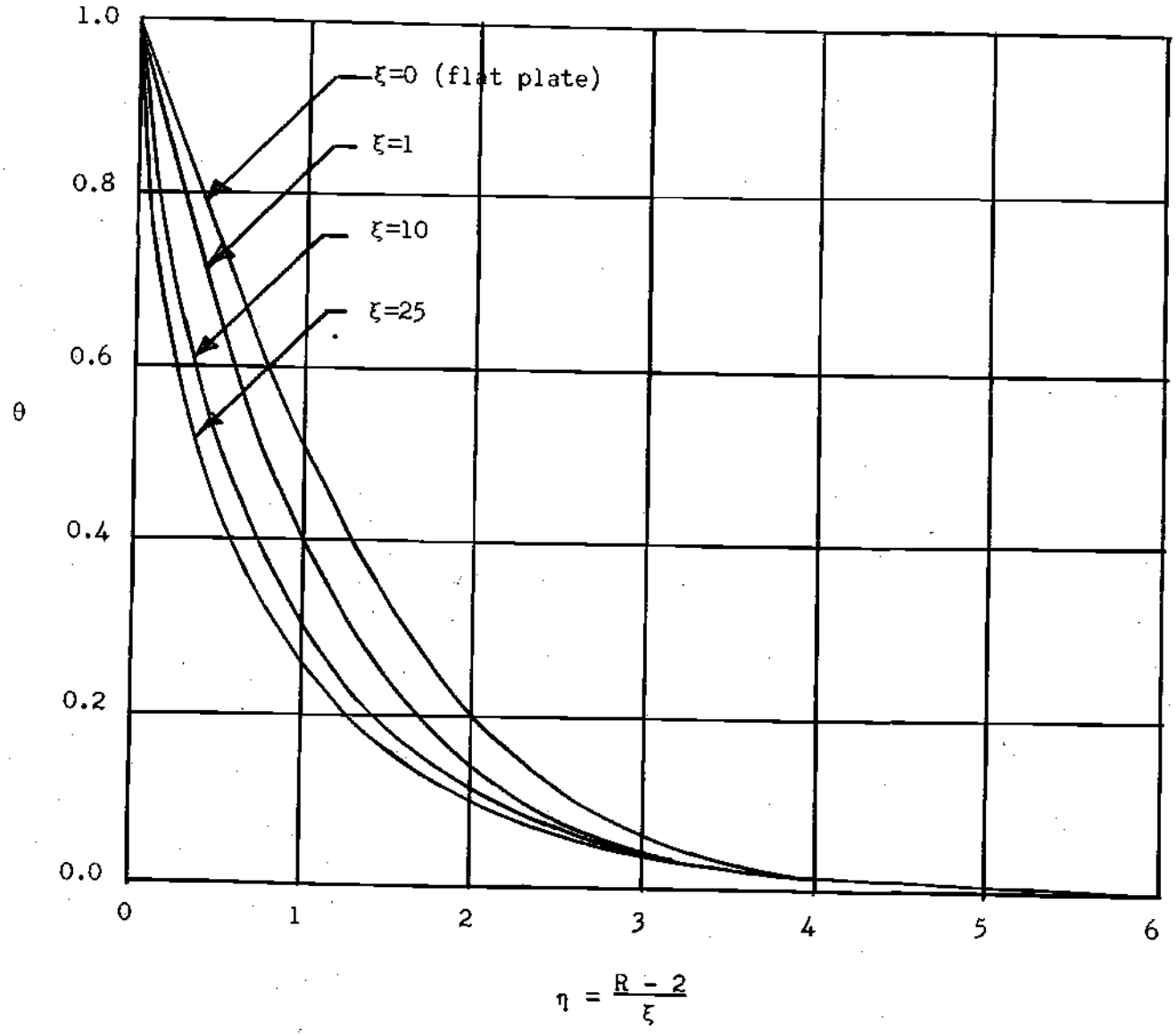

Figure 11. Temperature Profiles for a Prandtl Number of 0.72.

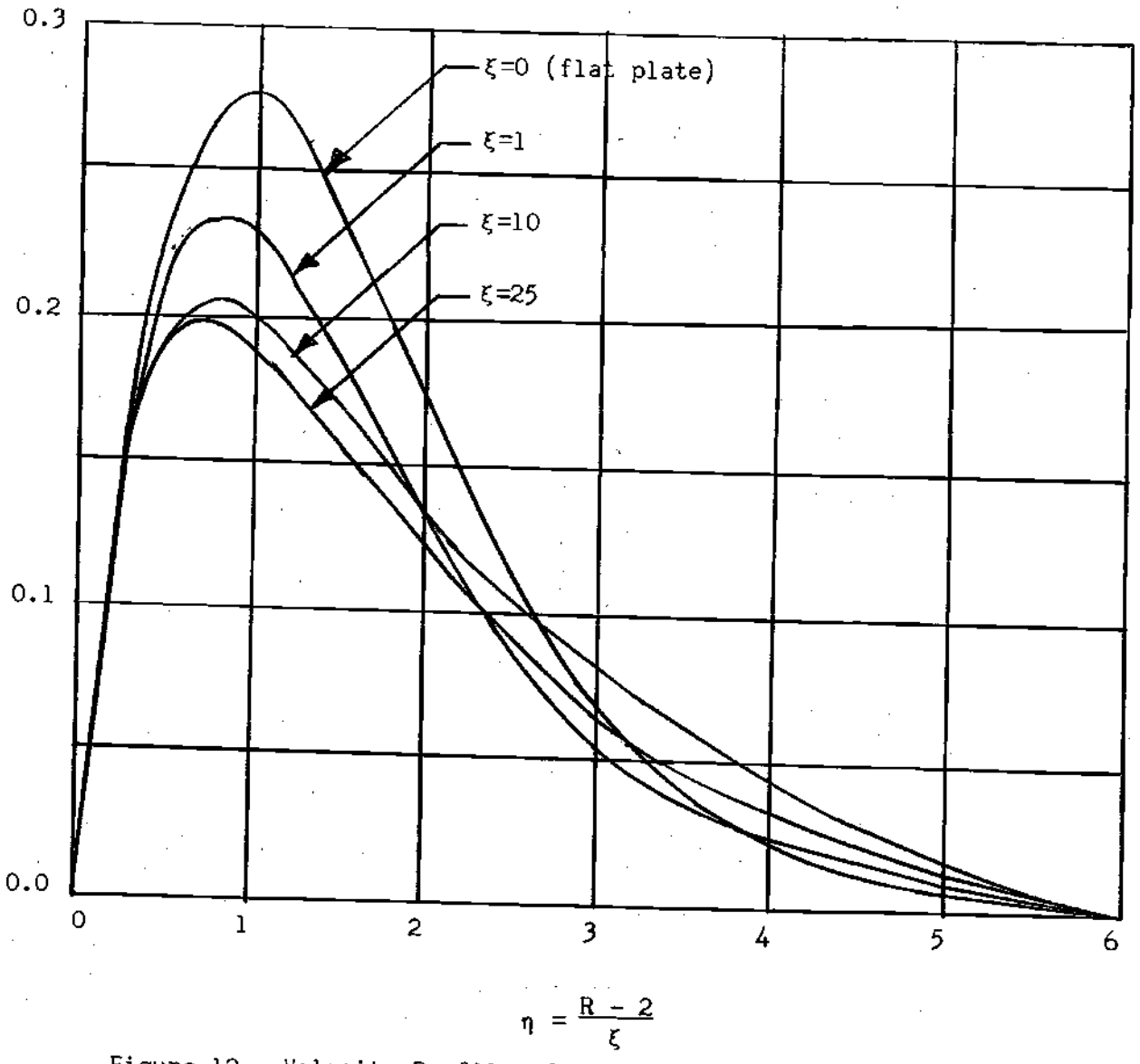

Figure 12. Velocity Profiles for a Prandtl Number of 0.72.

for a Prandtl number of 0.72. Figure 11 gives the non-dimensional temperature, θ, plotted against the similarity parameter, η, of Ostrach for the flat plate. As the value of ξ increases, the effect of curvature becomes more pronounced, and the profiles deviate more from the flat plate profile.

Figure 12 shows the "similar" velocity for the flat plate solution, U/ξ^2 plotted versus the similarity parameter, η. At values of η greater than three, the curves for U/ξ^2 at different ξ values crossed each other. This behavior was not noted in the solutions at the other Prandtl numbers. The reason for this is probably that in the computation for a Prandtl number of 0.72, steady state was not achieved at large distances from the wall. Although the effect on the heat-transfer coefficient as a result of this is very small, the effect on the velocity profiles may be greater. Also, because of the way in which the data are presented, a small error in U is magnified at small values of ξ.

In both Figures 11 and 12, the abscissas do not correspond to the same physical distance from the cylinder surface for different values of ξ. Indeed, it corresponds to ten times the distance at $\xi = 10$ as it does at $\xi = 1$. Therefore, as ξ increases (larger vertical distances), the temperature and velocity fields extend further into the fluid. Also, the ordinate in Figure 12 is the velocity divided by ξ^2, Ostrach's similar velocity. Therefore, again as ξ increases, the maximum velocity increases, but the maximum velocity divided by ξ^2 decreases. The maximum velocity at $\xi = 1$ is approximately 0.24 units while the maximum velocity at $\xi = 10$ is approximately 2.10 units.

Some experimental data are available for the measured temperature profiles. Figure 13, page 73, shows the temperature profiles predicted by the finite-difference method and the experimental results of Hama and Recesso. At values of ξ less than one, the agreement is quite good. At high values of ξ, these results predict higher values than those measured. Again, this might be due to the inability to achieve steady-state values far from the wall as mentioned previously. It might be due in part to experimental errors in measuring the temperatures. A small error in measuring the temperatures would give a greater effect on θ in this range than closer to the wall.

Other Prandtl Numbers

In order to investigate the feasibility of using the finite-difference method and to obtain results at low Prandtl numbers, equations (70), (71), and (72) were solved for a Prandtl number of 0.01. The following incremental increases in ΔX were made: from $X = 0$ to $X = 0.0004$ in steps of $\Delta X = 0.00001$; from $X = 0.0004$ to $X = 0.004$ in steps of $\Delta X = 0.0004$; then, increasing ΔX by a factor of ten, every nine steps to $X = 2.0$. The results were treated in the same manner as those for the Prandtl number of 0.72. Results were obtained for a range of ξ from zero to slightly past one. The results are summarized in Table 3, page 72. The table also shows values predicted from Sparrow and Gregg's "stagnant film" analysis. Figures 14 and 15, pages 74 and 75, show the relationship between the Nusselt number for the cylinder compared with that for the flat plate. Sparrow and Gregg's "stagnant film" solution is not plotted in Figure 15 because it coincides with the finite-difference solution throughout this range.

Table 3. Analytical Heat-Transfer Results for a Prandtl Number of 0.01

ξ	Nu_{r_o}	$\overline{Nu}_{r_o}$	$\frac{Nu_x}{Nu_{x\ fp}}$	$\frac{\overline{Nu}_\ell}{\overline{Nu}_{\ell\ fp}}$	$\overline{Nu}_{r_o}$ (stagnant film)
0.1000*	2.1545	2.6370	1.327	1.218	2.63
0.1203	1.8382	2.2886	1.361	1.272	2.28
0.1326	1.7002	2.1190	1.392	1.292	2.09
0.1414	1.6194	2.0152	1.410	1.317	1.988
0.2114	1.2193	1.4958	1.588	1.454	1.468
0.2514	1.0829	1.3186	1.677	1.525	1.300
0.3760	0.85528	1.0053	1.972	1.742	0.994
0.4472	0.75730	0.90178	2.0851	1.860	0.893
0.6687	0.62379	0.72245	2.568	2.224	0.710
0.7952	0.55608	0.65311	2.723	2.396	0.650
1.189	0.46655	0.53056	3.4160	2.918	0.534

*For ξ values less than 0.1000, the following equations were used (see Appendix D):

$$Nu_{r_o} = \frac{0.1624}{\xi} + 0.4709$$

$$\overline{Nu}_{r_o} = \frac{0.2165}{\xi} + 0.4709$$

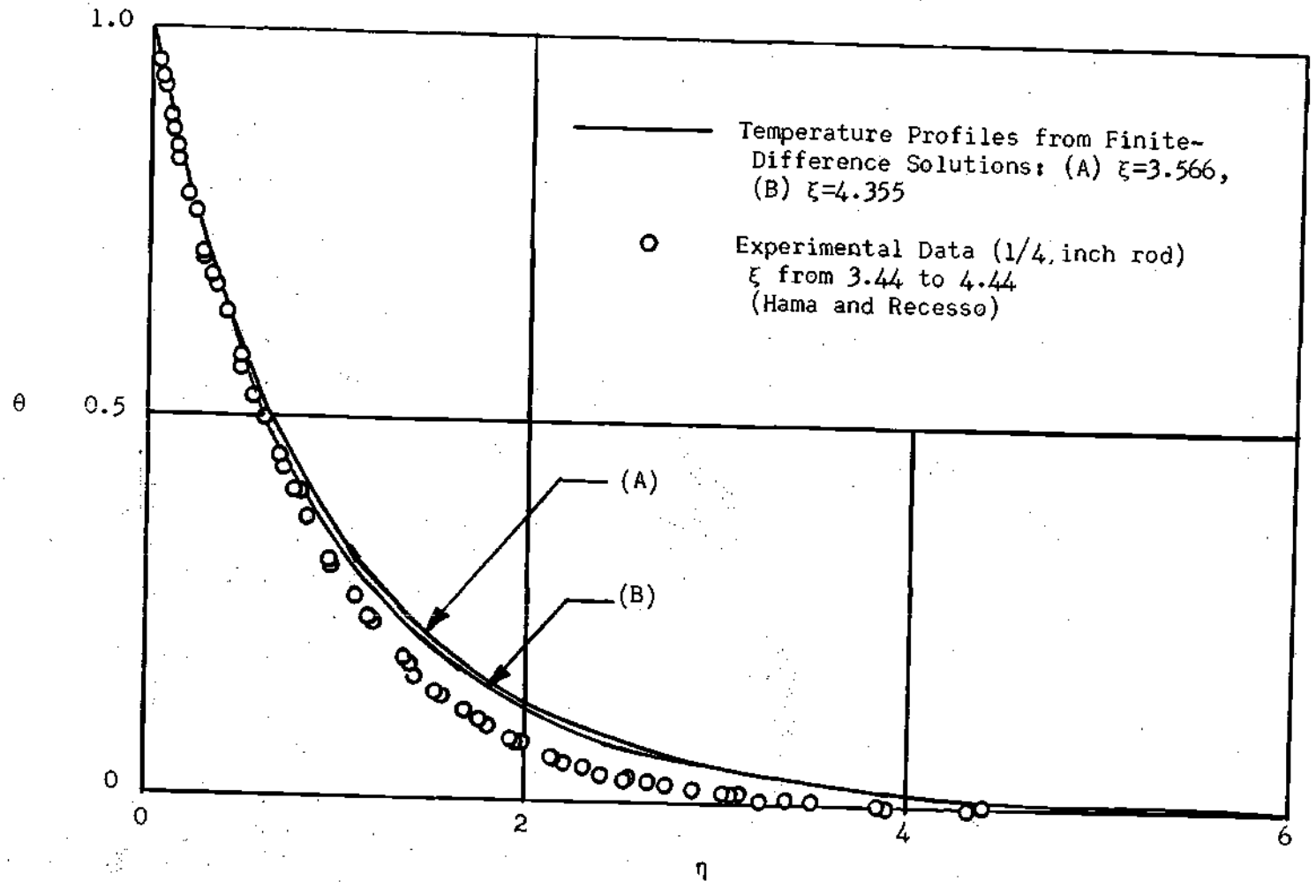

Figure 13. Comparison of Analytical Temperature Profiles with Experimental Data for a Prandtl Number of 0.72.

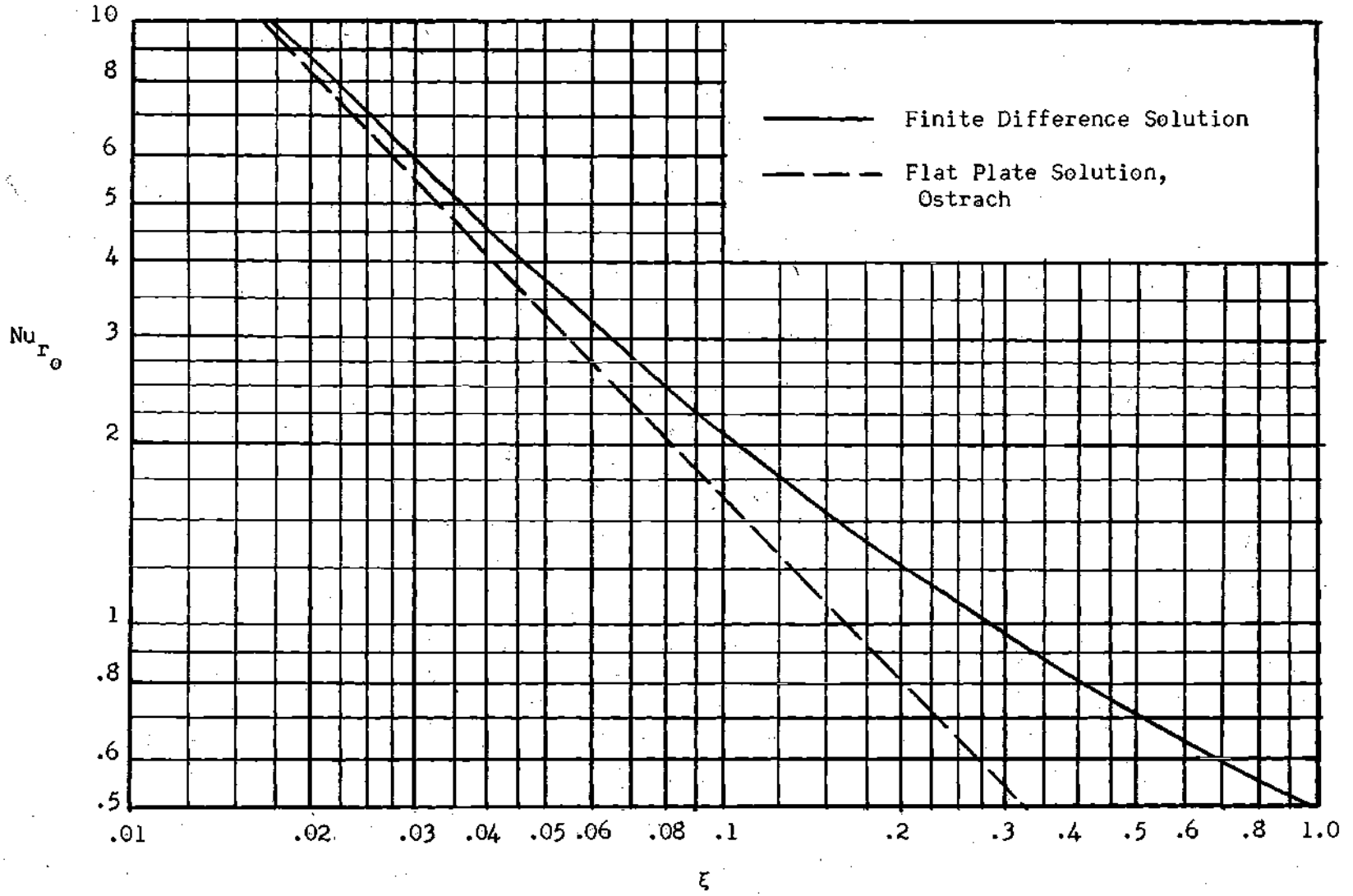

Figure 14. Local Nusselt Numbers for a Prandtl Number of 0.01.

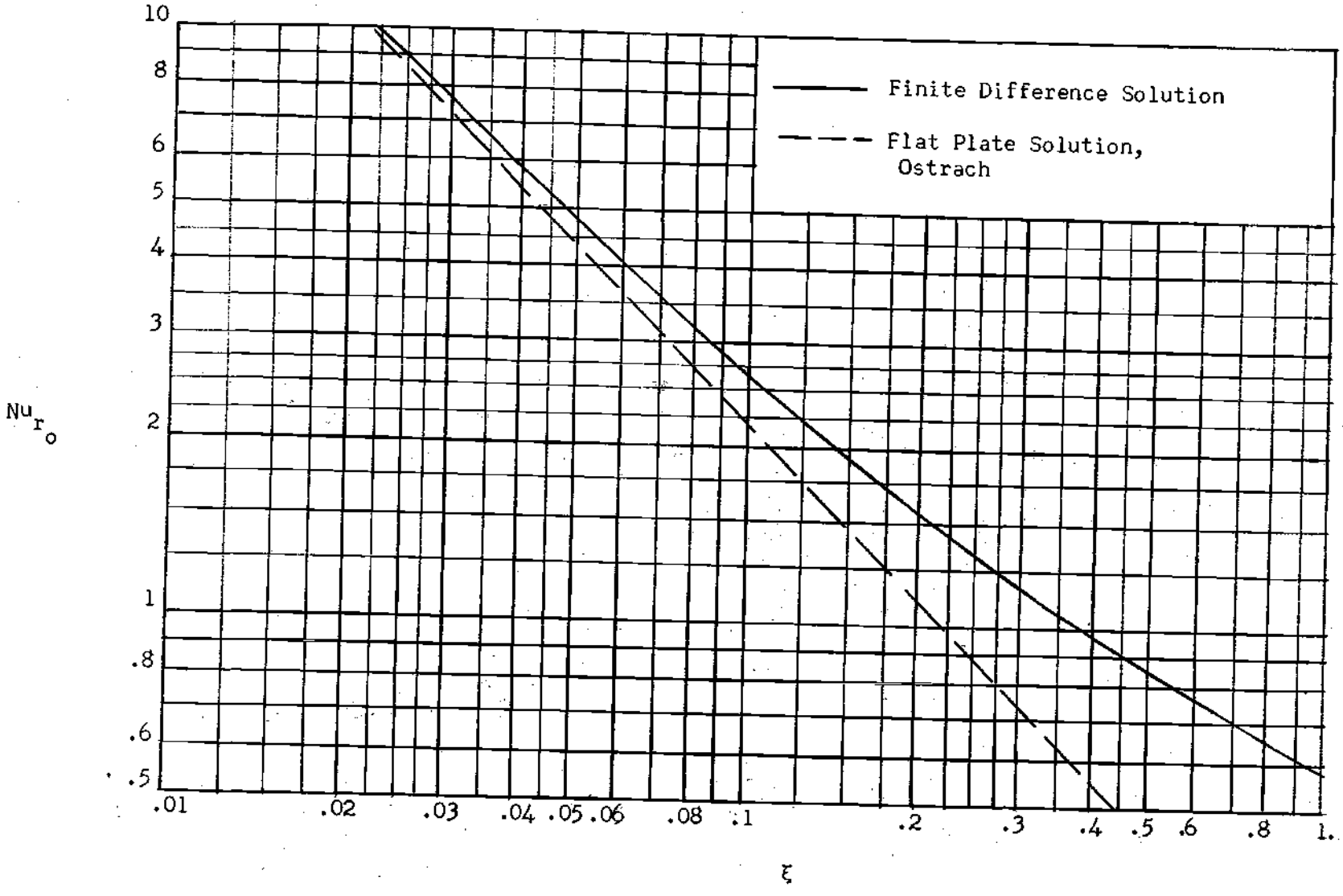

Figure 15. Average Nusselt Numbers for a Prandtl Number of 0.01.

In the range of ξ from 0 to 1, the results were fitted with a three-term series of form similar to the series obtained by Sparrow and Gregg. Since the first term comes from the flat plate solution and the second was found in the starting solution (Appendix D, page 114), this was easy to do. The resulting equation for the local Nusselt number was:

$$Nu_{r_o} = \frac{0.1624}{\xi} + 0.4709 - 0.1496\xi \qquad (124)$$

Upon integration, the average Nusselt number is obtained:

$$\overline{Nu}_{r_o} = \frac{0.2165}{\xi} + 0.4709 - 0.1197\xi \qquad (125)$$

Thus, the local and average Nusselt number ratios are given by:

$$\frac{Nu_x}{Nu_{x\ fp}} = 1.0000 + 2.8996\xi - 0.9211\xi^2 \qquad (126)$$

$$\frac{\overline{Nu}_\ell}{\overline{Nu}_{\ell\ fp}} = 1.0000 + 2.1750\xi - 0.5528\xi^2 \qquad (127)$$

The above results deviate from the finite-difference values less than $\pm$ 2.0 per cent for the range of ξ from 0.0 to 1.0. Figures 16 and 17, pages 77 and 78, show velocity and temperature profiles for a Prandtl

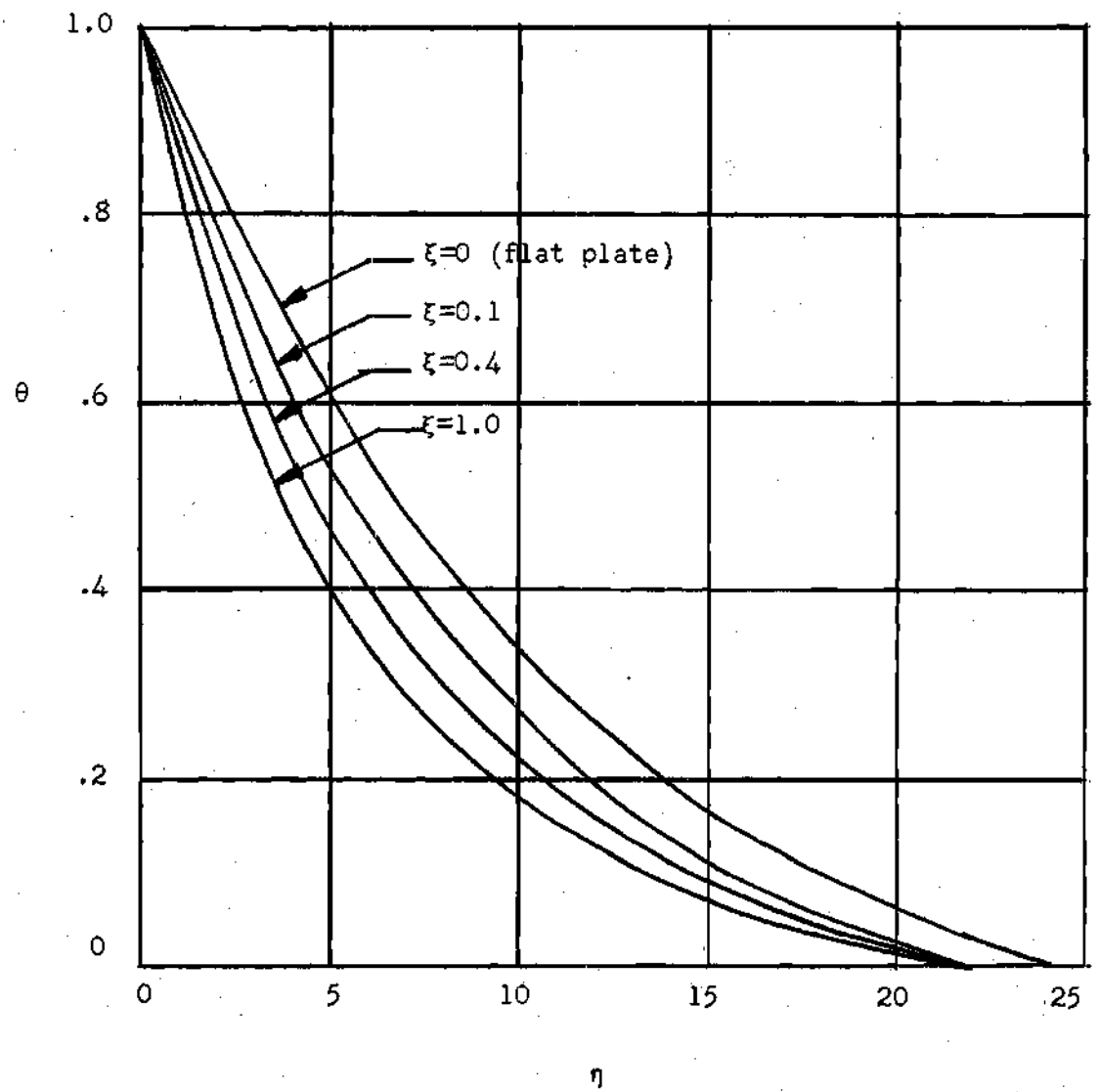

Figure 16. Temperature Profiles for a Prandtl Number of 0.01.

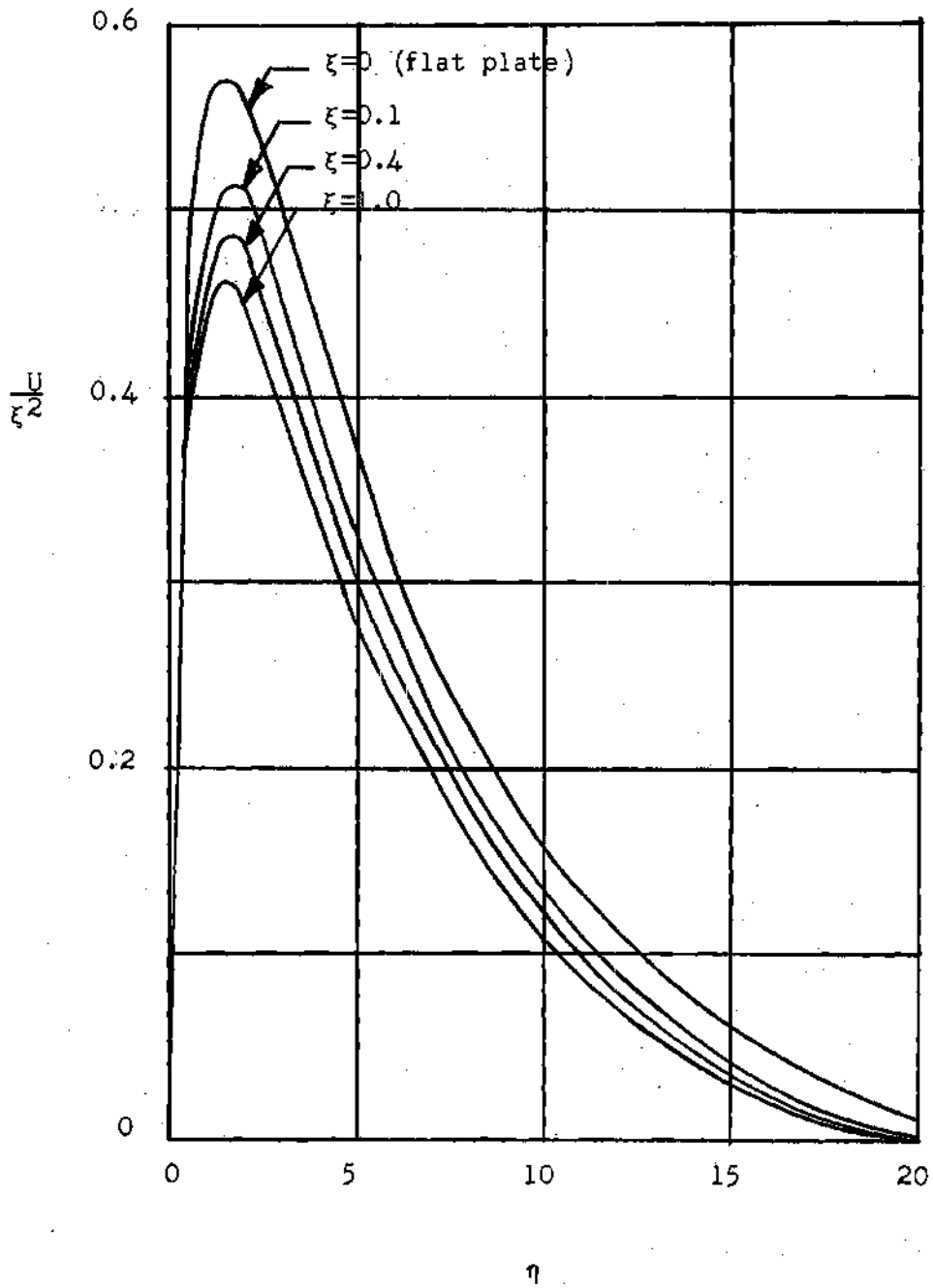

Figure 17. Velocity Profiles for a Prandtl Number of 0.01.

number of 0.01. The same remarks apply to these figures as did to Figures 11 and 12. For these profiles, the curves do not cross each other as they did for the Prandtl number of 0.72.

Equations (70), (71), and (72) were solved for a Prandtl number of 100.0 to determine the feasibility of this approach at high Prandtl numbers and to obtain results for this Prandtl number. The following incremental changes were made: from X = 0.0 to X = 0.004 in steps of $\Delta X = 0.0001$; then to X = 0.040 in steps of $\Delta X = 0.004$; then every nine steps, ΔX was increased by a factor of ten until $X = 4 \times 10^7$ was reached. (This corresponds to a ξ value of 79.52.) The results are summarized in Table 4, page 80. This table also gives values predicted by the "stagnant film" theory. Figures 18 and 19, pages 81 and 82, compare the Nusselt number to that for a flat plate. Experimental data by Cox (30) are shown in Figure 19, page 82, for Prandtl numbers between 100 and 200. The "stagnant film" theory agrees relatively well with the present theory. The results seem somewhat lower than those predicted by this theory. No closed form expression could be obtained because of the wide range of ξ. For ξ less than 1.414, the following are good approximations:

$$Nu_{r_o} = \frac{4.382}{\xi} + 1.250 + 0.232\xi \qquad (128)$$

$$\overline{Nu}_{r_o} = \frac{5.843}{\xi} + 1.250 + 0.186\xi \qquad (129)$$

These results are within ± 2.0 per cent for this range.

Table 4. Analytical Heat-Transfer Results for a Prandtl Number of 100.0

ξ	Nu_{r_o}	$\overline{Nu}_{r_o}$	$\frac{Nu_x}{Nu_{x\ fp}}$	$\frac{\overline{Nu}_\ell}{\overline{Nu}_{\ell\ fp}}$	$\overline{Nu}_{r_o}$ (stagnant film)
0.2514*	18.67	24.65	1.058	1.060	23.60
0.4472	11.14	14.987	1.136	1.142	13.52
0.7952	6.481	8.795	1.172	1.194	7.84
1.414	4.148	5.222	1.338	1.262	4.61
2.514	2.455	3.127	1.404	1.344	2.80
4.472	1.759	1.953	1.792	1.496	1.76
7.952	1.011	1.264	1.825	1.720	1.162
14.14	0.7113	0.8616	2.293	2.081	0.812
25.14	0.5315	0.6268	2.040	2.690	0.600
44.72	0.4263	0.4725	4.345	3.615	0.464
79.52	0.3286	0.3657	5.960	4.971	0.372

*For ξ values less than 0.2514 the following equations were used (see Appendix D):

$$Nu_{r_o} = \frac{4.382}{\xi} + 1.250$$

$$\overline{Nu}_{r_o} = \frac{5.843}{\xi} + 1.250$$

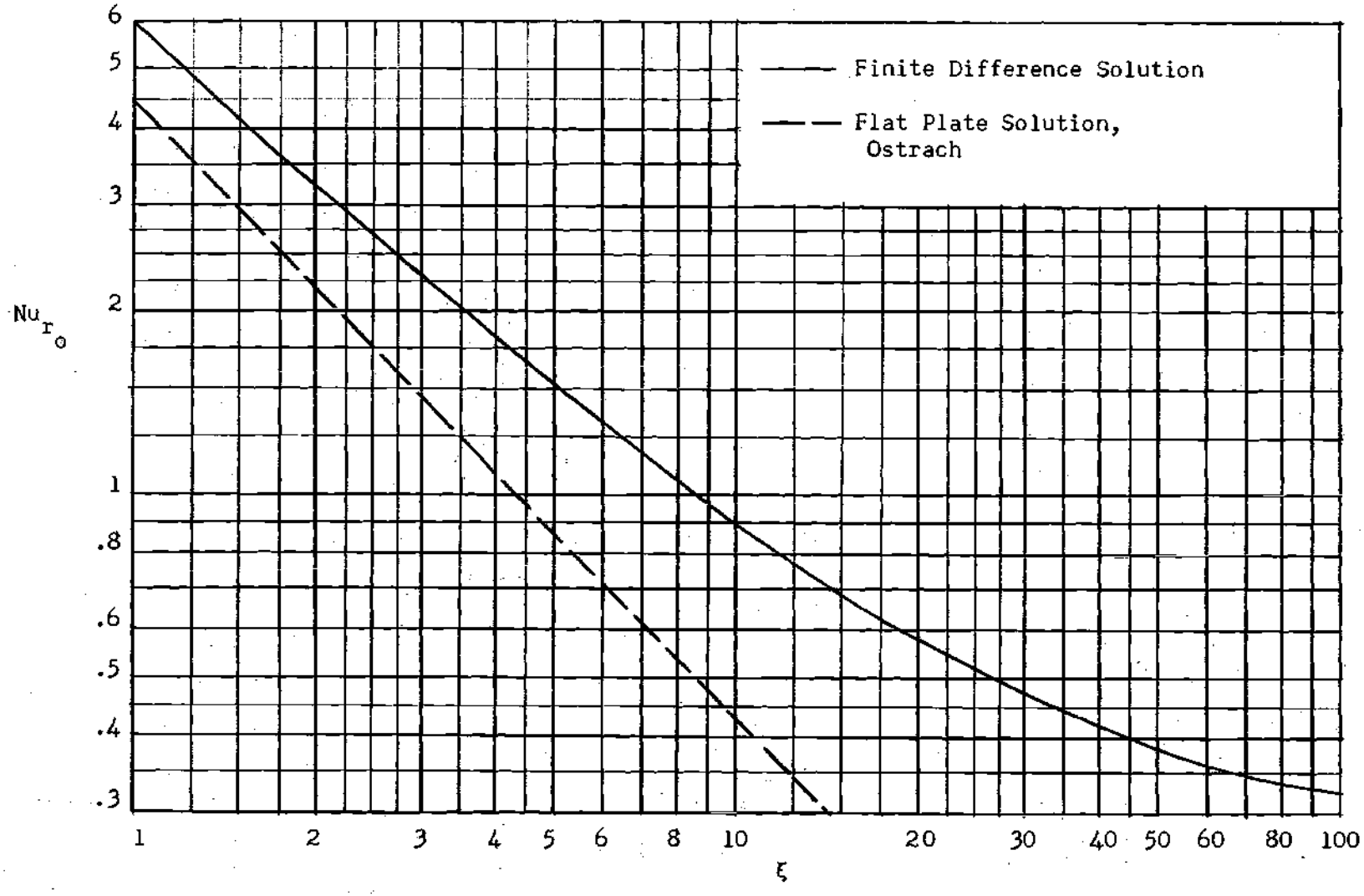

Figure 18. Local Nusselt Numbers for a Prandtl Number of 100.0.

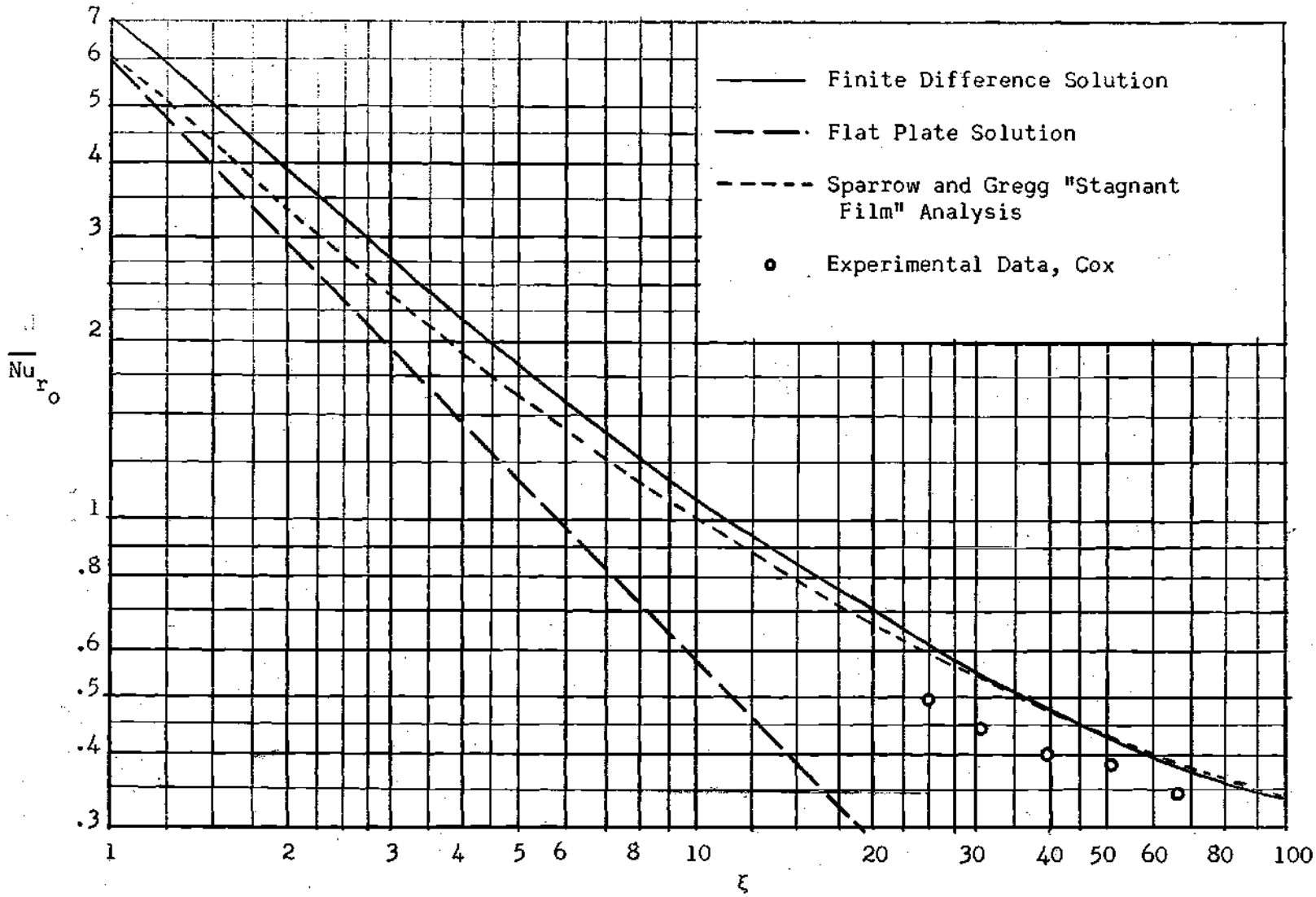

Figure 19. Average Nusselt Numbers for a Prandtl Number of 100.0.

Figures 20 and 21, pages 84 and 85, show the temperature and velocity profiles for a Prandtl number of 100.0. Again, they are plotted in terms of the flat plate similarity parameters so that care must be taken in interpreting them at various ξ positions. The curves do not cross at high values of η as they did for a Prandtl number of 0.72. The velocity profile for $\xi = 1.046$ was forced to go to zero prematurely. The dashed line is probably a better approximation of the real profile. This, however, did not seem to affect the values near the wall and the heat-transfer coefficient.

Figures 22 and 23, pages 86 and 87, compare the effect of curvature for the three Prandtl numbers. It is evident from these figures that at a given value of ξ, the effect of curvature is more pronounced at low Prandtl numbers. This is due to the fact that the thermal boundary layer is thicker at low Prandtl numbers, so the effect of curvature is more noticeable.

Experimental Results for Air

The experimental phase of this thesis involved measuring overall heat-transfer coefficients in air. A summary of the results is given in Figure 24, page 88. It was decided to plot the Nusselt number based on r_o rather than the ratio of the Nusselt number for the cylinder to that of a flat plate of the same height. This was done to avoid choosing a particular experimental correlation for the flat plate. The experimental results are tabulated in Appendix C, page 107.

Along with the experimental data from this work, the data obtained by Carne (16) which was within the laminar range and the data of Battaglia

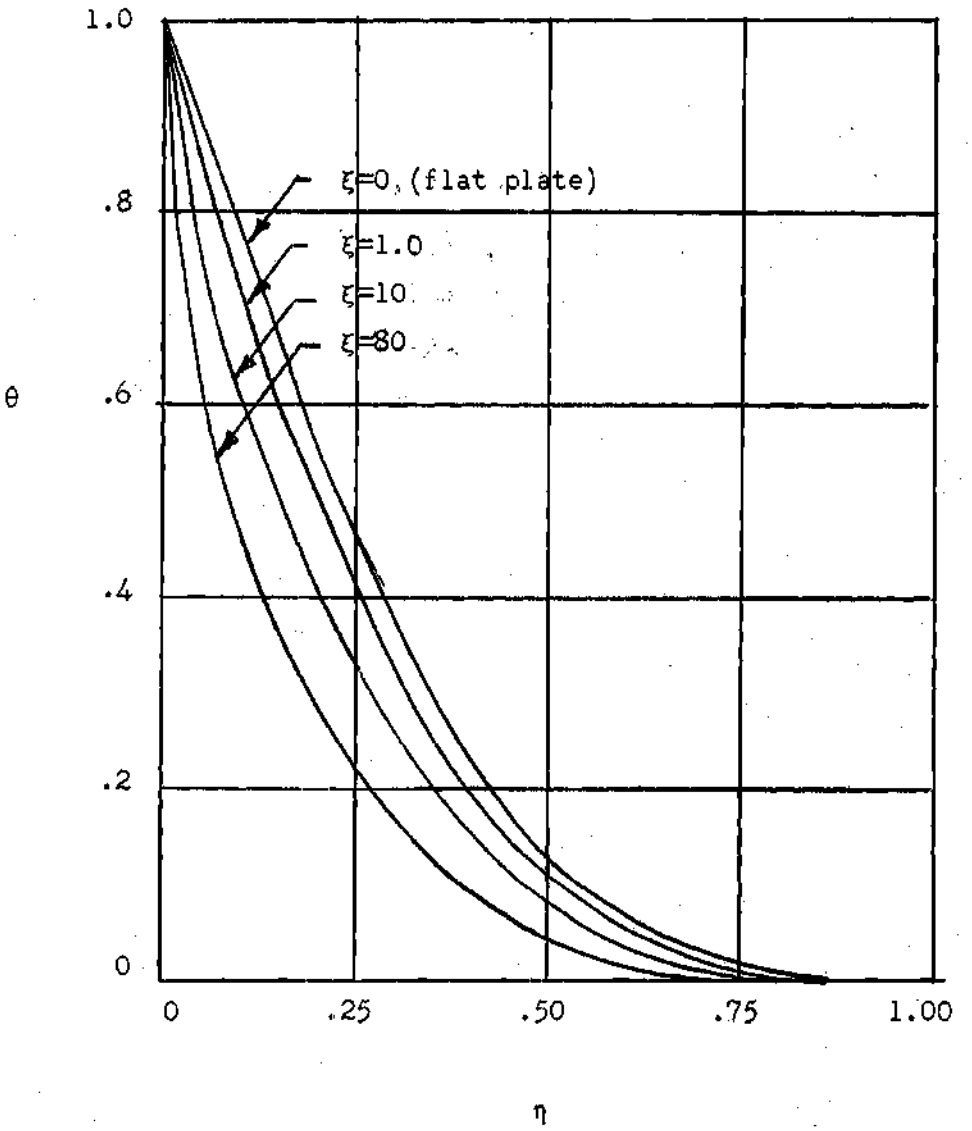

Figure 20. Temperature Profiles for a Prandtl Number of 100.0.

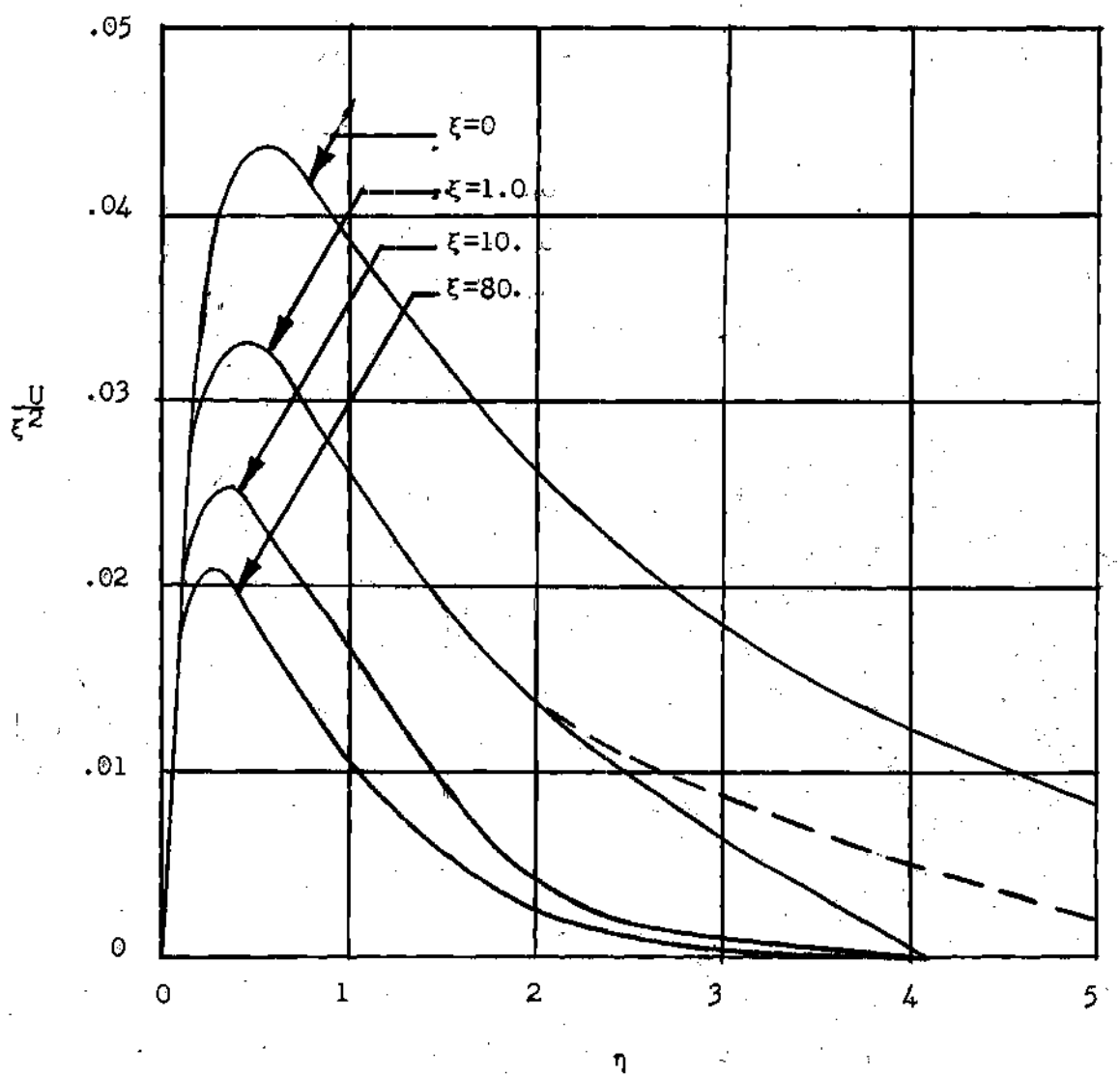

Figure 21. Velocity Profiles for a Prandtl Number of 100.0.

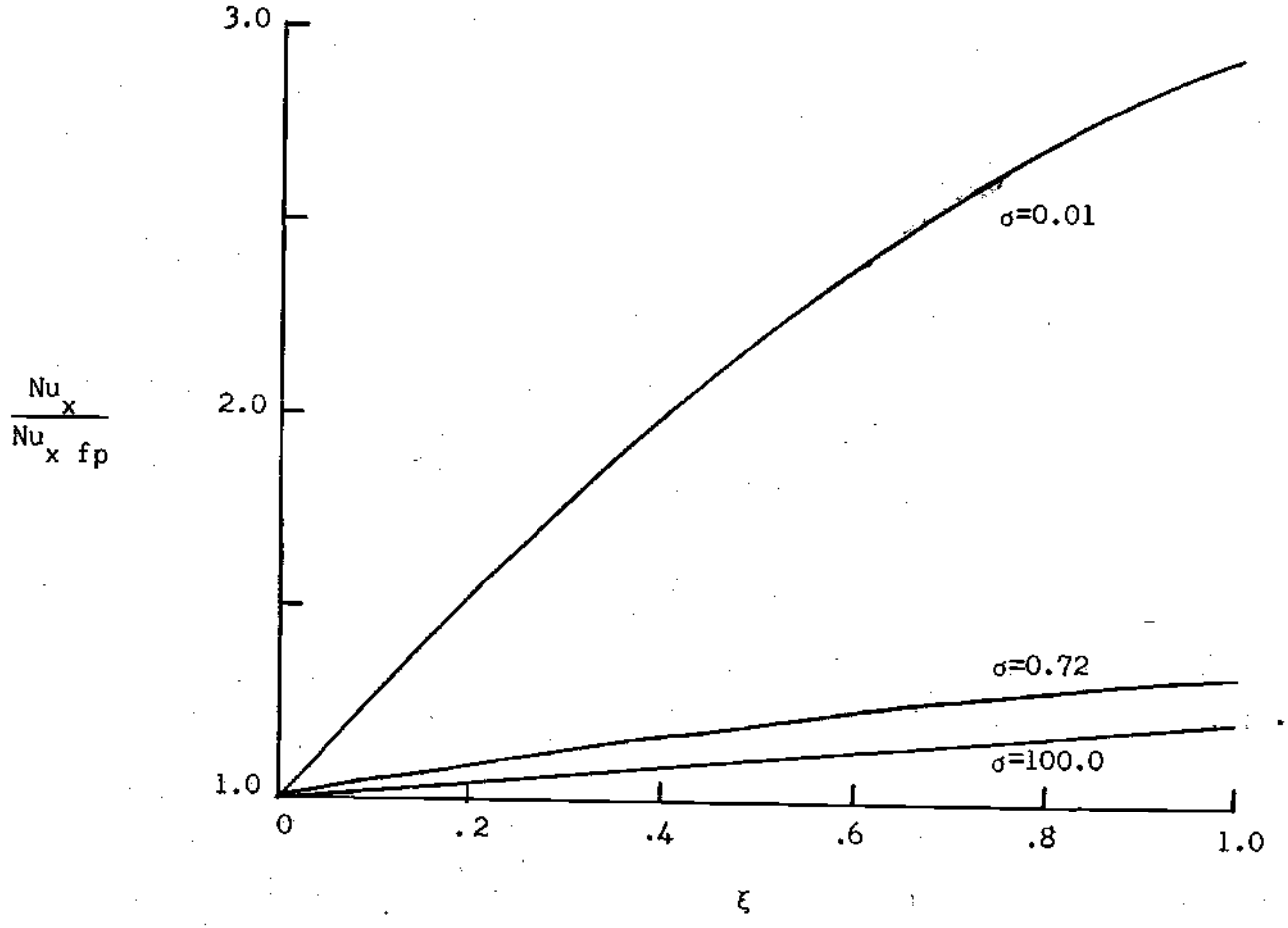

Figure 22. Effect of Curvature on Local Nusselt Numbers.

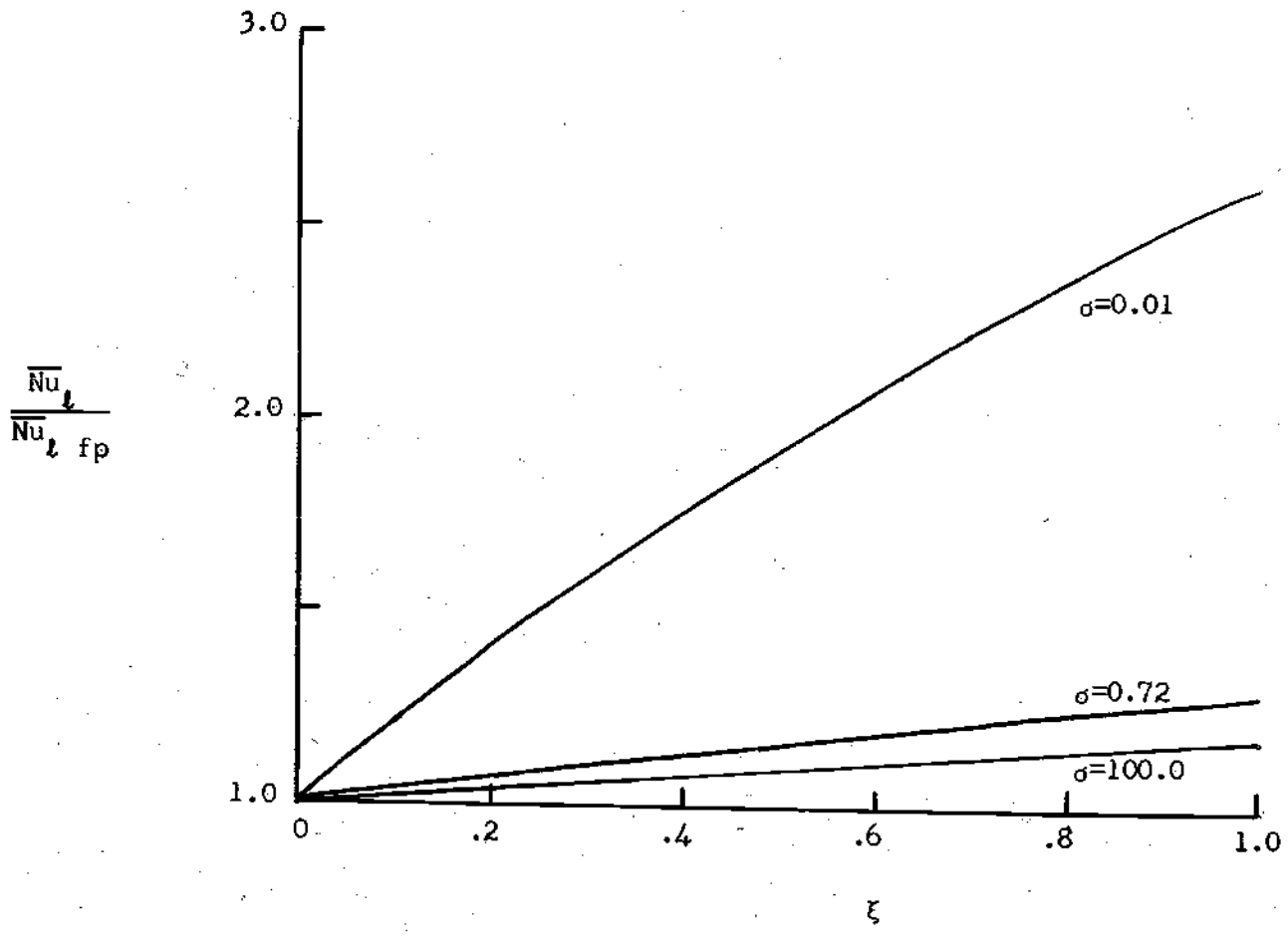

Figure 23. Effect of Curvature on Average Nusselt Numbers.

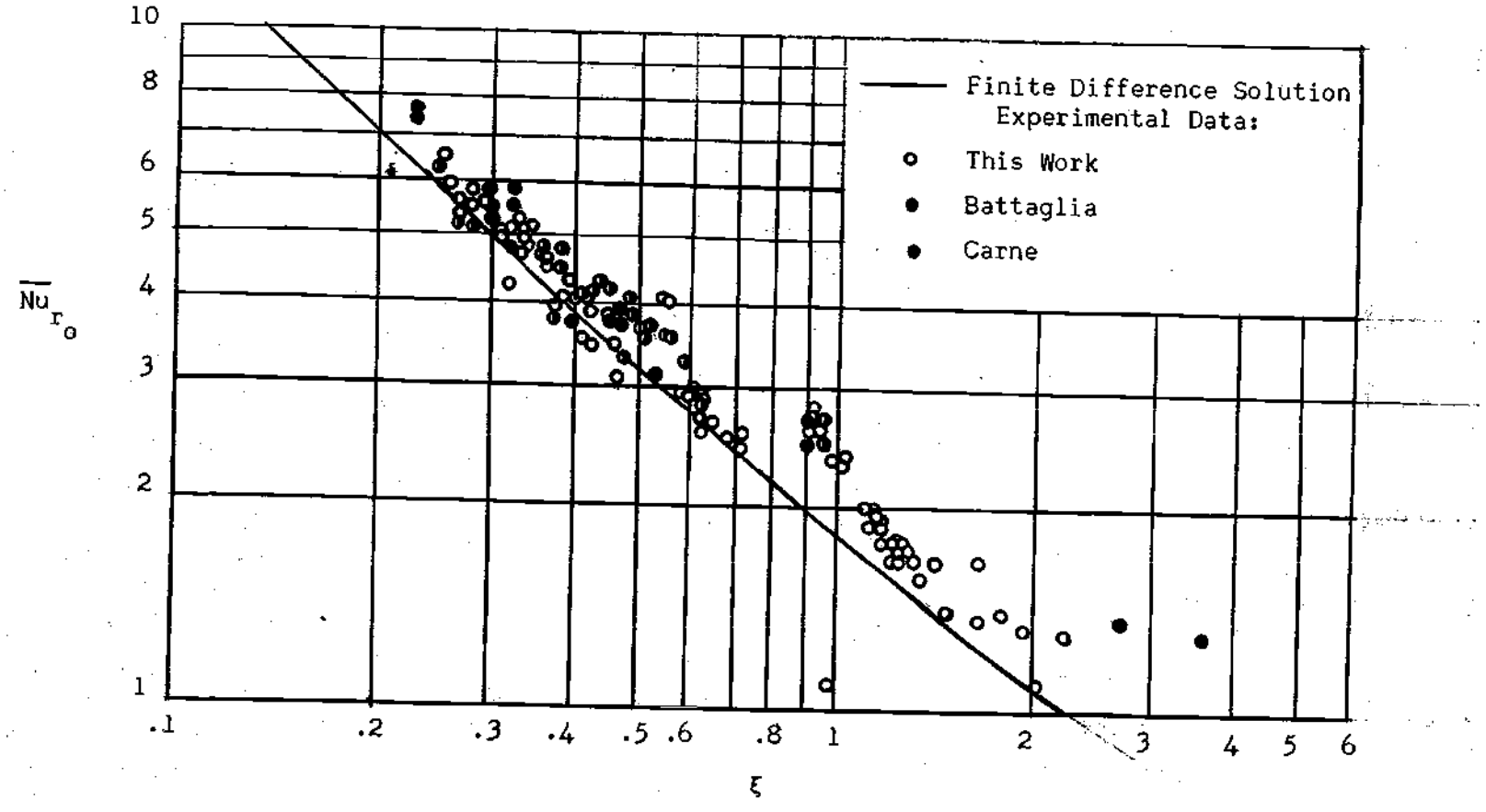

Figure 24. Experimental Results for Air.

(29) are plotted. Although both of the above-mentioned works show unusual trends when plotted by themselves, they both seem to fall within the experimental scatter when taken as a whole. The theoretical curve for a Prandtl number of 0.72 is plotted in Figure 24 also. Considering all of the data plotted, 54 per cent of it lies within ± 10 per cent of the theoretical curve; and 84 per cent within ± 20 percent. The majority of the data is on the high side of the curve. This is probably, at least for the data from this work, due to the method of computing the convective heat transfer. In neglecting the heat conducted out the ends of the cylinders, a slightly high prediction was made of the heat convected from the cylinder; and, therefore, the apparent Nusselt number was high. This may also account for the difference between the experimental data of Carne and Battaglia and the theoretical results.

CHAPTER VII

CONCLUSIONS AND RECOMMENDATIONS

An analytical study of the problem of free-convection heat transfer from a vertical isothermal cylinder by using finite differences was undertaken for Prandtl numbers of 0.72, 0.01 and 100.0. An experimental investigation of this problem was conducted for a Prandtl number of 0.72.

Conclusions

The results of the analytical and experimental solutions presented herein for a Prandtl number of 0.72 agree quite well. The analytical solution agrees well with the solution of Sparrow and Gregg for ξ values less than one, and with that presented by Hama, Recesso and Christiaens for ξ's greater than ten. It has, therefore, been shown that the finite-difference method is applicable to this particular problem, if care is taken to avoid the "leading edge" effect by a method such as that outlined in Appendix D. The amount of computer time required for the solution at a Prandtl number of 0.72 was slightly more than five hours. This is not an unreasonable amount of time.

The results for Prandtl numbers of 0.01 and 100.0 appear to be reasonable when compared with the flat plate solution. They also agree with the "stagnant film" analysis of Sparrow and Gregg. The solution for a Prandtl number of 100.0 agrees well with the experimental data of Cox (30). Thus the analytical method appears to be feasible for both low and high Prandtl numbers.

Recommendations

It is recommended that the finite-difference method be employed to obtain solutions to the isothermal cylinder problem at other Prandtl numbers, especially low Prandtl numbers where the deviation from the flat plate is greatest and there has been the least work done. This would involve a minimum of work, since the computer program as described in Appendix A can be used without modifications.

With only slight modification, the computer program may be used with different boundary conditions. Any arbitrary variation of the cylinder surface temperature could be considered. A free stream velocity could be used to obtain solutions for a combined free and forced convection problem with the same difference equations. A more realistic boundary condition at the leading edge for the free-convection problem might be considered, such as a small axial velocity at $X = 0$. All of these could be done just by changing the boundary conditions, without effecting the differential equations and the difference scheme.

It is further recommended that experimental work be continued at moderate values of ξ (less than ten). This is especially needed at low Prandtl numbers where the author found no experimental data.

APPENDIX A

COMPUTER PROGRAM FOR SOLUTION OF THE FINITE-DIFFERENCE EQUATIONS

The finite-difference equations (70), (71) and (72) subject to the boundary conditions, equations (44) through (50) were solved using the Burroughs 220 digital computer at the Rich Electronic Computer Center at the Georgia Institute of Technology. The program was written in Algol language and is appended to the end of this section. The notation in the program is essentially the same as that in the text, so no additional nomenclature is given.

Figure 25, page 93, is a flow diagram for the computer program. Initially, the following data are read into the computer: DX, the X increment; DR, the R increment; X, the initial boundary value of X; XINC, the value of X1 at which the X increment is increased; XOUT, the final value of X1; PR, the Prandtl number; FPO, a parameter from the flat plate solution relating to the heat transfer. Then, all values of U, V and H (that is θ) are set equal to zero. The value of N, the number of R positions in the grid, is then computed knowing DR and R_∞ as described in Chapter III. If N is greater than some predetermined number (in this case, 35), the R increment is doubled and appropriate changes are made in U, V and H.

EPS is the prescribed allowable change in the function H after ten iterations at the first grid point beyond the wall. It was taken to be such that the change in H would affect the value of the corresponding

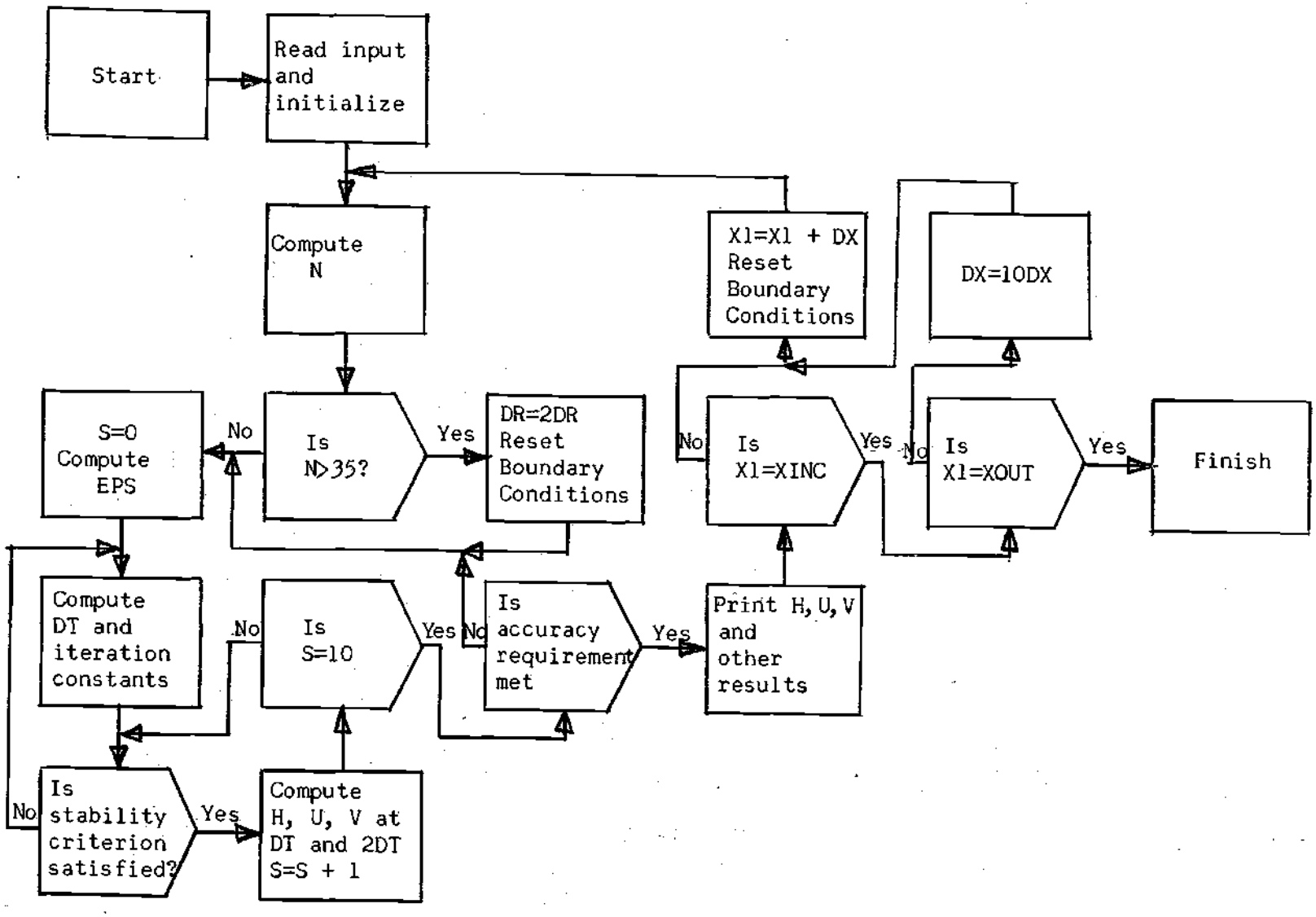

Figure 25. Flow Diagram for Finite-Difference Computer Program.

local flat plate Nusselt number by 1.0 per cent. (The change in the cylinder Nusselt number would be smaller percentage-wise since at a given ξ, the cylinder Nusselt number will be larger than that of the flat plate.)

DT, the time increment, is then computed in such a way that it is 95 per cent of the maximum value which satisfies the stability requirement given in equation (85) for Prandtl numbers less than unity. (The equation for Prandtl numbers greater than one is identical to equation (85) with the exception of the omission of the Prandtl number from the last term in the denominator.) The various constants in the iteration scheme are then computed.

A test for stability is then made. (It will be satisfied automatically for the first iteration.) Then, the values of U, V and H at time $T + \Delta T$ are computed by equations (70), (71) and (72) and the results placed in U1, V1 and H1. Then, the iteration continues to $T + 2\Delta T$ placing the results in U, V and H.

A test is then made to determine if 20 iterations have been completed. If not, the program loops back to the point where DT is tested for stability. When 20 iterations have been completed, the results are tested to see if steady state is reached (if the change in H after 20 iterations is less than EPS.) If it is not satisfied, the program goes through 20 more iterations. When the test is satisfied, the heat-transfer results are computed as outlined in Chapter III, and the results are printed out.

If X1 (the value of X at which the iteration takes place) is less

than XINC, it is increased by DX, and the boundary conditions are set with the previous answers. The program then loops back to the computation of N. If X1 is equal to XINC, but less than XOUT, the increment DX is increased by a factor of ten and then the program loops back to increasing the value of X1 by the new DX. If X1 is equal to XOUT, the program is stopped.

The actual computer program follows.

```
                    BAC-220 STANDARD VERSION  2/1/62

COMMENT CARL BLIEM  EXT 457   PROB NO 912                                    $
COMMENT FINITE DIFFERENCE SOLUTION OF BOUNDARY LAYER EQUATIONS FOR
FREE CONVECTION FROM VERTICAL ISOTHERMAL CYLINDERS                           $
ARRAY   H(2,180), U(2,180), V(180), H1(2,180), U1(2,180), V1(180),
        TS(180), G(180), D(180), F(180), IN(180)                             $
INTEGER  J, L, N, S, S1                                                      $
COMMENT READ INPUT AND INITIALIZE                                            $
TRANS.. READ ($$DATA)                                                        $
        FOR L = (1, 1, 100)                                                  $
BEGIN   H(1,L) = 0.0  $  U(1,L) = 0.0  $  H1(1,L) = 0.0                      $
        U1(1,L) = 0.0 $  H(2,L) = 0.0  $  U(2,L) = 0.0                       $
        V(L) = 0.0 END $ H(2,1) = 1.0  $  H1(2,1) = 1.0                      $
COMMENT COMPUTE N                                                            $
CON..   X1 = X + DX                                                          $
        XI1 = (X1)*0.25                                                      $
        NF = (24.0 (XI1))/DR                                                 $
        N = FIX (NF)                                                         $
        IF N GTR 35                                                          $
BEGIN   DR = 2.0DR  $          N = N/2  $  FOR L = (2,1,N - 1)               $
BEGIN   H(2,L) = H(2,2L - 1)  $  U(2,L) = U(2,2L - 1)     END                $
        FOR L = (N,1,2N)                                                     $
BEGIN   H(2,L) = 0.0  $  U(2,L) = 0.0                     END END            $
        EPS = ((0.000812)DR)/XI1                                             $
        S1 = 0                                                               $
        AB = ((4.0).DR)/DX                                                   $
```

```
        FOR L = (2,1,N - 1)                                          $
BEGIN   G(L) = ((2.0 + (L - 2)DR)/((2.0 + (L - 1)DR)))               $
        V(L) = G(L).V(L - 1) - (AB).(U(2,L) - U(1,L))    END         $
COMMENT COMPUTE DT                                                   $
ST..    S = 0    $    T = H(2,2)                                    $
CALC..  TA = 4.0/DX                                                  $
        TE = 1.0 /((PR)((DR)*2.0))                                   $
        FOR L = (2,1,N - 1)                                          $
        TS(L) = 1.0 /(TA.U(2,L) - (V(L)/DR) + (2.0)TE)               $
        MINTS = TS(2)   $
        FOR L = (3,1,N - 1)   $
        IF MINTS GTR TS(L)   $
        MINTS = TS(L)   $
        DT = 0.95.MINTS   $
COMMENT COMPUTE VALUES OF ITERATION CONSTANTS                        $
        A = (DT).(TA)                                                $
        B = DT/DR    $    C = B/DR    $    E = C/PR                  $
        FOR L = (2,1,N - 1)                                          $
BEGIN   G(L) = (2.0 + (L - 2)DR)/(2.0 + (L - 1)DR)                   $
        D(L) = B/((2.0)(2.0 + (L - 1)DR))    $    F(L) = D(L)/PR  END $
COMMENT TEST STABILITY CRITERION                                     $
STEP..  FOR L = (2,1,N - 1)                                          $
BEGIN   TEST = 1.0 - 2.0E - A.U(2,L) + B.V(L)                        $
        IF TEST LSS 0.0                                              $
        GO TO CALC                                          END      $
COMMENT COMPUTE VALUES OF H, U, AND V AT T AND T + DT                $
```

```
        FOR L = (2,1,N-1)                                                    $
BEGIN   H1(2,L) = (1.0-2.0E-A.U(2,L)+B.V(L) )H(2,L)+A.U(2,L).H(1,L)+(E
+F(L)-B.V(L) )H(2,L+1)+(E-F(L))H(2,L-1)                                       $
        U1(2,L) = (1.0-2.0C-A.U(2,L)+B.V(L) )U(2,L)+A.U(2,L).U(1,L)+(C
+D(L)-B.V(L) )U(2,L+1)+(C-D(L))U(2,L-1)+DT.H1(2,L)                            $
        V1(L) = G(L).V1(L-1)-(A/B)(U1(2,L)-U1(1,L))          END             $

        FOR L = (2,1,N-1)                                                    $
BEGIN   H(2,L) = (1.0-2.0E-A.U1(2,L)+B.V1(L) )H1(2,L)+A.U1(2,L).H1(1,L)
+ (E+F(L)-B.V1(L) )H1(2,L+1)+(E-F(L))H1(2,L-1)                               $
        U(2,L) = (1.0-2.0C-A.U1(2,L)+B.V1(L) )U1(2,L)+A.U1(2,L).U1(1,L)
+(C+D(L)-B.V1(L) )U1(2,L+1)+(C-D(L))U1(2,L-1)+DT.H(2,L)                       $
        V(L) = G(L).V(L-1)-(A/B)(U(2,L)-U(1,L))      END                     $

COMMENT TEST FOR COMPLETION AT GIVEN XI STATION                              $

        S = S + 1   $   IF S LSS 10   $   GO TO STEP                         $
       S1 = S1 + 1                                                           $
        ERR = T-H(2,2)                                                       $
        FINIS = ABS(ERR)                                                     $
        IF FINIS GIR EPS  $
        GO TO ST                                                             $

COMMENT COMPUTE HEAT TRANSFER RESULTS                                        $
        NUR = (1.0-H(2,2))/(LOG(1.0+DR/2.0))                                 $
        RATIO = (DER(X1*0.25))/FPO                                           $
        WRITE($$ANS1,FMT1)                                                   $
        WRITE($$FMT3)                                                        $

        FOR L = (1,1,N)                                                      $
BEGIN   R = 2.0+(L-1)DR                                                      $
        WRITE ($$ ANS3, FMT4)   $

  END   $

        WRITE($$ANS4,FMT6)                                                   $
        CONB = NUR-(0.0812/XI1)    $    WRITE($$ANS2,FMT2)                 $
        IF X1 GEQ XOUT                                                       $
        GO TO TRANS                                                          $
```

```
        IF X1 GEQ XINC                                                    $
BEGIN   DX = 10.0DX   $   XINC = 10.0DX  .              END               $
SHIFT.. X = X1                                  $
        SCA = ((X+DX)/X)*0.5                                              $
        FOR L = (1,1,N)                                                   $
BEGIN   H(1,L) = H(2,L)   $   U(1,L) = U(2,L)                             $
        H1(1,L) = H(1,L)   $   U1(1,L) = U(1,L)                           $
        U(2,L) = SCA.U(2,L)                             END               $
        GO TO CON                                                         $
INPUT   DATA(DX,DR,X,XINC,XOUT,PR,FPO)                                    $
INPUT   DATA2(X1,N,FOR L = (1,1,44)   $   H(2,L),FOR L = (1,1,44)  $
        U(2,L))                                                           $
OUTPUT  ANS1(XI1,S1)                                                      $
OUTPUT  ANS2(CONB)                                                        $
OUTPUT  ANS3(R,H(2,L),U(2,L),V(L))                                        $
OUTPUT  ANS4(NURO,RATIO,NAVG)                                             $
FORMAT  FMT1(B10,*STEADY STATE ANALYTICAL RESULTS FOR XI=*,S5.4,B2,*NO
  ITER*,I4,W3,W2)                                                         $
FORMAT  FMT2(*B=*,F19.8,WO)                                               $
FORMAT  FMT3(*R*,B12,*THETA*,B13,*AXIAL VELOCITY*,B5,*RADIAL VELOCITY*,
  W2)                                                                     $
FORMAT  FMT4(S7.6,3F19.8,WO)                                              $
FORMAT  FMT6(*NUR=*,F14.8,B2,*LOC RATIO=*,F14.8,*NUR AVG*,F14.8,W4)       $
        FINISH                                                            $

COMPILED PROGRAM ENDS AT 1287

PROGRAM VARIABLES BEGIN AT 1461
```

APPENDIX B

COMPUTER PROGRAM FOR REDUCTION OF EXPERIMENTAL DATA

The computer program given below computes the heat-transfer parameters from the experimental data. The input to the program consists of: 1) the diameter and length of the cylinder in inches and the run number of the last data point for that length and diameter, 2) the run number; the surface, ambient air, and enclosure wall temperature; and the power input to the cylinder at these conditions. The output from the program was: the run number, the surface temperature, the air temperature, the power input, the cylinder average Nusselt number based on 1, the ratio of the average Nusselt number for the cylinder to that for a flat plate, the average cylinder Nusselt number based on r_o, the per cent error in the average Nusselt number based on r_o. Figure 26, page 101, shows a flow diagram of the computer program.

Since some of the terminology in the program differs slightly from that given in the List of Symbols and that used in the body of the thesis, the definition of symbols used in the program is given in the following list:

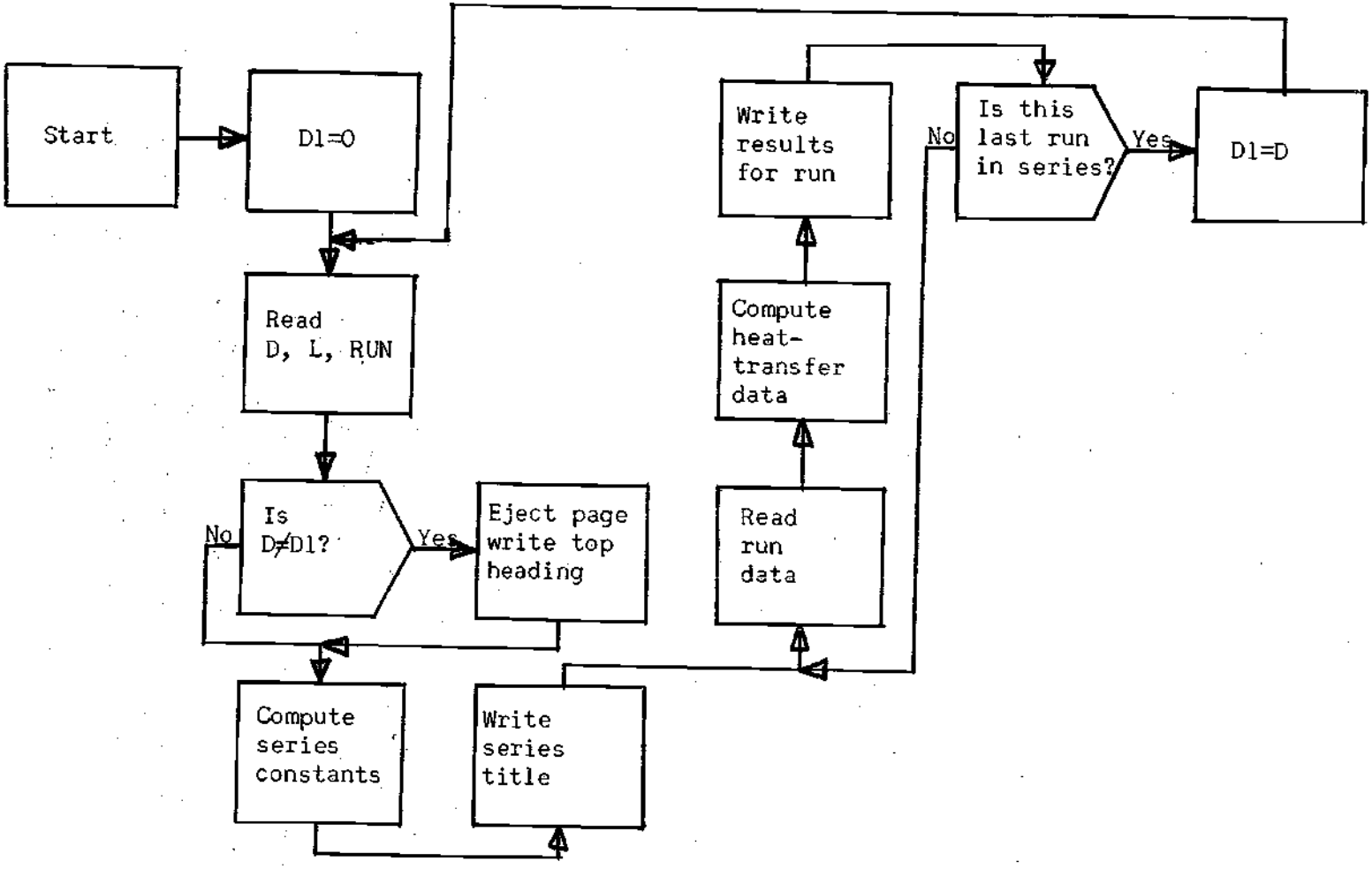

Figure 26. Flow Diagram for Data-Reduction Computer Program.

Computer Symbol	Meaning	Units
A	A	ft^2
D	$D = 2r_o$	in
DT	$t_s - t_a$	°F
E	ϵ	-
GR	Gr_ℓ	-
GRP	$Gr_\ell \cdot Pr$	-
GRPS	$(Gr_\ell \cdot Pr) \times 10^{-8}$	-
GRS	$Gr_\ell \times 10^{-8}$	-
HC	h_ℓ	Btu/hr ft^2 °F
K	k	Btu/hr ft °F
L	ℓ	in, ft
N	Number of last run in a given set of data	-
NUC	$\overline{Nu}_\ell$	-
NUF	$\overline{Nu}_{\ell\ fp}$	-
P	P	watts
PR	σ, the Prandtl number	-
QCO	q_{co}	Btu/hr ft^2
QRA	q_{ra}	Btu/hr ft^2
QTO	q_{to}	Btu/hr ft^2
RATIO	$\overline{Nu}_\ell \sqrt{\overline{Nu}_{\ell fp}}$	Btu/hr ft^2
TA	t_a	°F
TAS	T_s	°R
TAW	T_w	°R

Computer Symbol	Meaning	Units
TF	t_f	°F
TS	t_s	°F
TW	t_w	°F
XI	ξ	-
Z	$Z \times 10^{-6}$	$ft^3/°R$
E __	Error in __ (e.g., EQTO is error in QTO)	
PE __	Per cent error in __ (e.g., PED is per cent error in D)	

BAC-220 STANDARD VERSION 2/1/62

```
COMMENT CARL BLIEM ME RESEARCH PROB NO 912                                    $
COMMENT COMPUTATION OF AVERAGE NUSSELT NUMBER FOR FREE CONVECTION
        FROM OUTSIDE OF VERTICAL ISOTHERMAL CYLINDERS                         $
INTEGER RUN,N                                                                 $
        D1 = 0.0                                                              $
SET..   READ($$DIM)                                                           $
        IF D NEQ D1    $    WRITE($$HEAD)                                    $
        E = 0.045                                                             $
        WRITE($$SKIP)                                                         $
        WRITE($$LEN,TITLE1)                                                   $
        A = (3.14159)D.L/(144.0)                                              $
        WRITE($$TITLE2)                                                       $
TRANS.. READ($$DATA)                                                          $
        TAS = TS + 459.7                                                      $
        TAW = TW + 459.7                                                      $
        QTO = (3.41278)P/A                                                    $
        QRA = (0.174**-8).E.((TAS*4.0)-(TAW*4.0))                             $
        QCO = QTO-QRA                                                         $
        DT = TS-TA                                                            $
        HC = QCO/DT                                                           $
        TF = TA + DT/2.0                                                      $
        K = ((1.313371**-2)+((2.5870573**-5)-(6.1050061**-9)TF)TF)            $
        PR = ((0.72040)+(-(1.69519**-4)+(1.71468**-7)TF)TF)                   $
        Z = ((4.3348727)+(-(4.2120649**-2)+((2.2256586**-4)+
        (-(6.6493277**-7)+(8.43861**-10)TF)TF)TF)TF)                          $
        NUC = (HC.L)/(12.0K)                                                  $
        GR = ((10.0*6)Z.DT)((L/12.0)*3.0)                                     $
        GRP = GR.PR                                                           $
        NUF = 0.590(GRP*0.25)                                                 $
```

```
        RATIO = NUC/NUF                                                    $
        X1 = ((2.0*2.5)L)/((GR*0.25)D)                                     $
        GRS = (10.0*-8)GR                                                  $
        GRPS = (10.0*-8)GRP                                                $
        NUR = (D/2.0L)NUC                                                  $
        PED = 0.005/D   $   PEL = 0.03125/L   $   PEP = 0.125/P            $
        PEDT = 3.0/DT   $   PEK = 0.02        $   PEE = 0.10               $
        PEQTO = PEP+PEL+PED                                                $
        EQTO = PEQTO.QTO                                                   $
        PDTA = 10.1/(TAS*4.0-TAW*4.0)                                      $
        PEQRA = PEE+PDTA                                                   $
        EQRA = PEQRA.QRA                                                   $
        EQCO = EQTO+EQRA                                                   $
        PEQCO = ECCO/QCO                                                   $
        PENUR = (PED+PEQCO+PEK+DEDT)100.0                                  $

        WRITE($$ANS,FMT1)                                                  $

        IF RUN EQL N                                                       $

BEGIN   D1 = D                                                             $

        GO TO SET                                        END               $
        GO TO TRANS                                                        $

INPUT   DIM(D,L,N)                                                         $

INPUT   DATA(RUN,TS,TW,TA,P)                                               $

OUTPUT  LEN(D,L,E)                                                         $

OUTPUT  ANS(RUN,TS,TA,P,XI,NUC,RATIO,NUR,PENUR)                            $

FORMAT  TITLE1(B5,*DIAMETER=*,X6.3,*IN. LENGTH=*,X7.3,
        *IN. EMMISIVITY=*,X6.3,W2)                                         $

FORMAT  TITLE2(*RUN*,B2,*TS*,B5,*TA*,B5,*P*,B6,*XI*,B6,*NUL*,B5,*NUC/NU
        F NUR*,B5,*PCT*,W2)                                                $

FORMAT  FMT1(I3,X7,1,X6.1,X7.2,X8.4,X8.2,X8.4,X8.3,X7.2,WO)                $

FORMAT  HEAD(*EXPERIMENTAL RESULTS FOR OVERALL HEAT TRANSFER FROM
        ISOTHERMAL CYLINDERS*,W3,W2)                                       $
```

```
        FORMAT SKIP(W0)                                    $
                FINISH                                     $
COMPILED PROGRAM ENDS AT 0606
PROGRAM VARIABLES BEGIN AT 4111
```

APPENDIX C

RESULTS OF THE EXPERIMENTAL INVESTIGATION

Table 5 gives the heat-transfer results for all of the experimental runs considered in this work. The following is an explanation of symbols used:

Symbol	Meaning	Units
RUN	Run number	-
TS	t_s	°F
TA	t_a	°F
P	P	watts
XI	ξ	dimensionless
NUL	$\overline{Nu}_{\ell}$	dimensionless
NUC/NUF	$\overline{Nu}_{\ell}/\overline{Nu}_{\ell\ fp}$	dimensionless
NUR	$\overline{Nu}_{r_o}$	dimensionless
PCT	Maximum percentage error in Nu_{r_o}	per cent

Table 5. Experimental Results for Air

Run	TS	TA	P	XI	NUL	NUC/NUF	NUR	PCT
	Diameter = 1.900 in.		Length = 5.984 in.		Emmisivity = .045			
2	262.3	81.9	19.75	.2572	40.84	1.0942	6.484	4.32
3	261.0	74.6	19.30	.2531	38.76	1.0217	6.153	4.37
4	189.0	68.0	9.82	.2623	32.08	.8750	5.093	5.05
5	217.0	72.2	13.88	.2585	37.20	1.0006	5.907	4.59
6	114.0	70.7	2.79	.3160	26.94	.8835	4.277	8.45
7	137.8	73.8	5.71	.2944	36.99	1.1313	5.873	5.84
9	243.3	71.0	17.40	.2532	38.45	1.0137	6.105	4.41
10	303.4	67.2	25.70	.2462	39.69	1.0183	6.302	4.22
11	324.4	68.6	27.87	.2461	39.03	1.0015	6.196	4.22
	Diameter = 1.900 in.		Length = 11.967 in.		Emmisivity = .045			
1	136.5	64.9	9.78	.3370	56.30	.9852	4.469	4.79
2	162.7	68.9	14.07	.3245	60.43	1.0189	4.797	4.37
4	191.0	69.3	19.12	.3125	61.81	1.0042	4.906	4.15
5	215.4	66.1	25.16	.3029	65.32	1.0291	5.185	3.97
6	245.2	65.5	31.08	.2970	65.42	1.0113	5.193	3.91
7	281.1	69.8	38.28	.2957	66.36	1.0224	5.268	3.88
8	272.1	71.7	36.57	.2978	67.33	1.0444	5.345	3.87

(Continued)

Table 5. (Continued) Experimental Results for Air

Run	TS	TA	P	XI	NUL	NUC/NUF	NUR	PCT
	Diameter = 1.900 in.			Length = 18.109 in.		Emmisivity = .045		
2	132.1	61.6	12.78	.3724	74.71	.9543	3.919	4.45
5	171.5	75.2	21.40	.3628	88.20	1.0990	4.627	3.98
14	319.0	67.0	72.00	.3238	101.99	1.1377	5.350	3.65
15	123.0	69.2	10.00	.3978	76.83	1.0483	4.030	4.72
18	292.2	68.2	60.00	.3261	97.20	1.0912	5.099	3.69
19	236.3	74.6	40.00	.3383	93.20	1.0844	4.889	3.76
20	167.0	76.2	20.00	.3670	87.82	1.1070	4.607	4.02
25	336.0	67.3	76.00	.3236	99.36	1.1079	5.212	3.70
26	272.2	77.5	50.00	.3345	93.83	1.0803	4.922	3.74
	Diameter = 1.050 in.			Length = 3.000 in.		Emmisivity = .045		
1	151.0	88.8	1.50	.4642	17.68	.9404	3.094	13.29
2	183.2	80.9	2.80	.4194	19.68	.9463	3.445	9.25
3	205.3	83.2	3.50	.4104	20.22	.9518	3.539	8.33
4	141.2	81.0	1.60	.4600	19.80	1.0433	3.466	12.68
5	161.5	84.2	2.30	.4421	21.86	1.1072	3.825	10.13
6	174.2	81.4	3.00	.4264	23.60	1.1532	4.130	8.80
7	195.4	84.7	3.40	.4174	21.91	1.0489	3.835	8.36
8	198.9	82.6	3.80	.4129	23.36	1.1059	4.088	7.92

(Continued)

Table 5. (Continued) Experimental Results for Air

Run	TS	TA	P	XI	NUL	NUC/NUF	NUR	PCT
	Diameter = 1.050 in.			Length = 6.042 in.		Emmisivity = .045		
1	246.0	73.0	11.45	.4608	45.82	1.2032	3.981	5.14
2	207.0	75.3	8.15	.4771	44.09	1.1977	3.831	5.58
3	139.5	64.0	4.10	.5083	41.14	1.1886	3.575	7.12
4	165.4	66.1	5.90	.4881	44.10	1.2241	3.832	6.14
6	266.0	74.9	13.10	.4585	46.72	1.2211	4.060	5.00
7	308.8	82.3	16.20	.4595	46.90	1.2296	4.075	4.87
	Diameter = 1.050 in.			Length = 18.052 in.		Emmisivity = .045		
1	129.5	70.9	6.60	.7099	84.03	1.1347	2.444	5.79
2	144.3	71.1	8.70	.6816	87.70	1.1374	2.550	5.30
3	151.4	63.4	11.00	.6505	92.52	1.1452	2.690	4.95
4	171.4	65.5	13.10	.6346	89.77	1.0844	2.610	4.79
5	182.5	65.0	15.50	.6246	95.28	1.1333	2.771	4.59
6	199.0	65.5	17.60	.6148	93.60	1.0961	2.722	4.55
7	218.6	72.4	21.15	.6160	101.01	1.1858	2.937	4.39
8	226.5	67.0	23.50	.6041	102.56	1.1809	2.982	4.34
9	248.8	78.5	25.30	.6129	100.51	1.1749	2.923	4.36
10	272.0	84.0	28.10	.6135	98.78	1.1566	2.873	4.35

(Continued)

Table 5. (Continued) Experimental Results for Air

Run	TS	TA	P	XI	NUL	NUC/NUF	NUR	PCT
11	280.5	78.2	31.00	.6038	101.08	1.1648	2.939	4.30
12	303.3	82.0	33.80	.6045	98.59	1.1381	2.867	4.31
13	293.0	77.4	32.85	.6006	99.52	1.1410	2.894	4.31
14	317.6	83.0	36.55	.6038	99.38	1.1461	2.890	4.31
	Diameter = .540 in.		Length = 5.950 in.			Emmisivity = .045		
1	185.6	87.8	1.75	.9874	24.10	.7075	1.093	13.04
2	191.6	81.5	4.50	.9582	57.58	1.6401	2.613	7.64
3	239.6	84.8	6.70	.9225	58.66	1.6103	2.662	6.73
4	278.1	85.6	8.80	.9048	60.21	1.6225	2.732	6.29
5	165.7	88.1	2.85	1.0271	52.43	1.6003	2.379	9.33
6	224.8	88.6	5.65	.9430	56.62	1.5886	2.569	7.10
7	240.7	83.5	6.55	.9187	56.40	1.5421	2.559	6.80
9	310.3	94.6	9.85	.9120	58.29	1.5846	2.645	6.19
10	198.4	85.3	4.45	.9614	54.92	1.5700	2.492	7.71
11	218.4	85.5	5.35	.9407	55.33	1.5483	2.511	7.23
12	246.1	88.0	6.50	.9257	55.23	1.5218	2.506	6.83
13	143.6	80.6	2.20	1.0519	51.06	1.5947	2.317	10.65
14	173.3	84.0	3.25	.9948	51.82	1.5321	2.351	8.77

(Continued)

Table 5. (Continued) Experimental Results for Air

Run	TS	TA	P	XI	NUL	NUC/NUF	NUR	PCT
	Diameter = .540 in.			Length = 15.188 in.		Emmisivity = .045		
1	109.1	86.0	1.20	1.6587	76.22	1.4696	1.355	15.59
2	125.0	86.4	2.10	1.4837	78.81	1.3598	1.401	10.94
3	127.8	84.1	2.80	1.4389	93.26	1.5605	1.657	9.27
4	137.2	78.2	3.60	1.3396	88.42	1.3775	1.571	8.26
5	135.0	74.2	3.90	1.3220	93.76	1.4413	1.666	7.95
6	149.6	75.1	4.95	1.2755	95.82	1.4217	1.703	7.24
7	164.6	78.6	5.70	1.2525	94.10	1.3716	1.672	6.92
8	178.0	80.1	6.55	1.2299	93.80	1.3430	1.667	6.64
9	186.8	76.8	7.75	1.2007	98.43	1.3761	1.749	6.31
10	207.1	86.5	8.70	1.2067	98.42	1.3836	1.749	6.16
11	255.1	90.4	13.00	1.1702	103.69	1.4151	1.843	5.68
12	272.6	80.0	15.50	1.1322	104.98	1.3864	1.866	5.54
13	84.2	78.0	.30	2.2275	72.56	1.8774	1.290	48.68
14	101.6	80.1	1.30	1.6666	90.47	1.7521	1.608	14.59
15	99.1	82.1	.90	1.7651	78.73	1.6148	1.399	19.14
16	96.0	83.6	.60	1.9102	72.62	1.6119	1.291	26.40
17	93.5	83.8	.40	2.0247	61.42	1.4451	1.092	37.58

(Continued)

Table 5. (Concluded) Experimental Results for Air

Run	TS	TA	P	XI	NUL	NUC/NUF	NUR	PCT
18	155.6	81.5	5.00	1.2926	96.34	1.4489	1.712	7.22
19	169.1	83.2	6.00	1.2641	98.67	1.4519	1.754	6.78
20	184.6	83.7	7.15	1.2326	98.77	1.4175	1.755	6.45
21	218.7	84.7	10.40	1.1861	105.40	1.4567	1.873	5.88
22	246.2	88.1	12.70	1.1703	106.51	1.4535	1.893	5.68
23	289.6	87.7	17.00	1.1439	108.13	1.4434	1.922	5.45
24	304.6	83.2	19.50	1.1282	112.32	1.4791	1.996	5.35
25	320.0	85.8	21.00	1.1303	112.88	1.4897	2.006	5.33
26	330.2	87.6	22.00	1.1320	113.14	1.4957	2.011	5.31

APPENDIX D

A METHOD OF OBTAINING A STARTING SOLUTION FROM THE FINITE-DIFFERENCE DATA

Because of the "leading edge" effect mentioned by Hellums (32) and noted in the present work, the finite-difference method does not give accurate results at extremely low values of ξ. Since the local Nusselt number becomes infinite at X = 0, some consideration of the values at small X must be taken in computing the average Nusselt numbers. Also, since the "leading edge" effect is not too well defined, some criterion must be established to determine when the finite-difference data is accurate. The following gives a method for doing both.

The work of Sparrow and Gregg (19) shows that for any Prandtl number, the following relation holds between Nu_{r_o} and ξ.

$$Nu_{r_o} = \frac{A}{\xi} + B + C\xi + D\xi^2 + \ldots$$

where A, B, C, D, ...are constants.

The value of A may be determined from the flat plate solution for it has been shown that

$$Nu_{r_o\ fp} = \frac{A}{\xi}$$

For sufficiently small ξ, the infinite series may be truncated after two terms:

$$Nu_{r_o} \approx \frac{A}{\xi} + B$$

Since A is known, if the flat plate solution exists, B can be determined from the finite-difference data. Let

$$\tilde{B} = Nu_{r_o} - \frac{A}{\xi}$$

Because of the "leading edge" effect, Nu_{r_o} will be high for the first points. As this effect diminishes, it would be expected that $\tilde{B}$ would become approximately constant and then start to rise again as the term C becomes important. (For a Prandtl number of 0.72, Sparrow and Gregg (19) found that C was negative.) The value of B may be chosen then as the minimum value of $\tilde{B}$.

When this was done for a Prandtl number of 0.72, a value of B was taken as 0.4818. Figure 27, page 116, shows $\tilde{B}$ as a function of X. For a Prandtl number of 0.01, C was negative and so the shape of the curve was essentially the same as that for a Prandtl number of 0.72. For a Prandtl number of 100.0, C was found to be positive so B was chosen at the point of inflection instead of at a minimum. No trouble was encountered in this case, however, because the curve was relatively flat where B was chosen. Using this value to determine Nu_{r_o} at $\xi = 0.1189$,

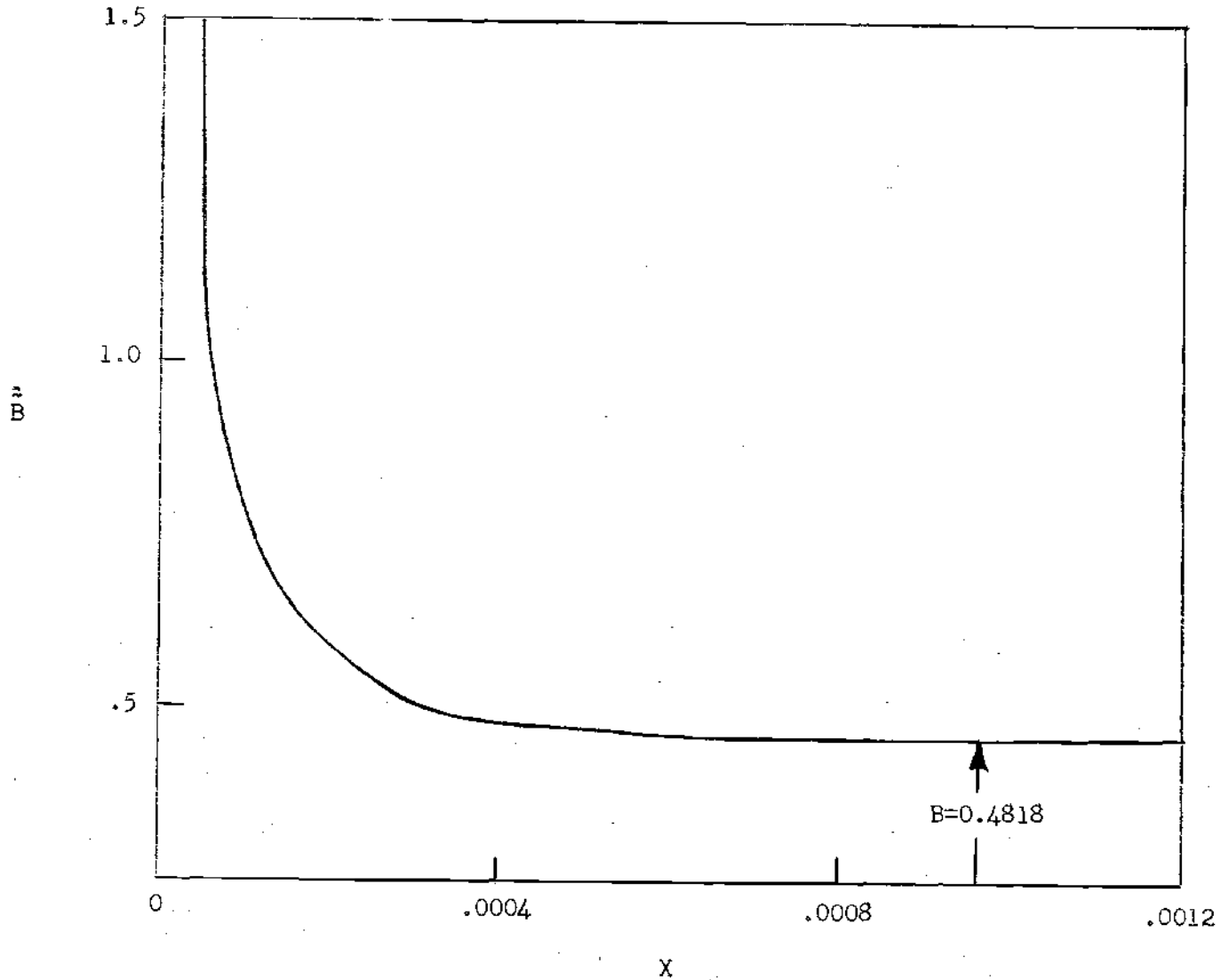

Figure 27. Determination of B for a Prandtl Number of 0.72.

Nu_{r_o} was found to differ from Sparrow and Gregg's value by 0.40 per cent, even though the value of B differed by 15 per cent. Note also that the value of Nu_{r_o} computed at $\xi = 0.1189$ is only 1.62 per cent lower than the finite-difference value and 2.08 per cent lower than the value obtained by Sparrow and Gregg. It was decided to start the numerical integration at this point. This was the method used in starting the solution for the other Prandtl numbers, when no solutions similar to those of Sparrow and Gregg existed.

For the case where the Prandtl number was 0.01, B was found to be 0.471. For a Prandtl number of 100.0, B found by the same method was 1.250.

BIBLIOGRAPHY

1. Lorenz, L., "Über das Wärmeleitvermögen der Metalle für Wärme und Elektrizität," Annalen der Physik und Chemie, 13, 1881, pp. 422-477, 582-606.

2. Nusselt, W., and W. Jürges, "Das Temperaturfeld über einer lolrecht stehenden geheizten Platte," Zeitschrift des Vereines deutscher Ingenieure, 72, 1928, pp. 597-603.

3. Schmidt, E., and W. Beckmann, "Das Temperatur- und Geschwindigkeitsfeld von einer Wärme abgebenden senkrechten Platte bei natürlicher Konvektion," Techniche Mechanik und Thermodynamik, 1, 1930, pp. 341-349, 391-406.

4. Ostrach, S., An Analysis of Laminar Free-Convection Flow and Heat Transfer about a Flat Plate Parallel to the Direction of the Generating Body Force, National Advisory Committee on Aeronautics, Technical Report 1111, 1953.

5. Sparrow, E. M., and J. L. Gregg, Details of Exact Low Prandtl Number Boundary-Layer Solutions for Forced and Free Convection, National Aeronautics and Space Administration, MEMO 2-27-59E, 1959.

6. Goldstein, S., Modern Developments in Fluid Mechanics, Vol. 2, London: Oxford University Press, 1938, pp. 641-643.

7. Saunders, O. A., "Natural Convection in Liquids," Proceedings of the Royal Society, London, Series A, 172, 1939, pp. 55-71.

8. Weise, R., "Wärmeübergang durch freie Konvektion an quadratischen Platten," Forschung auf dem Gebiete des Ingenieurwesens, 6, 1935, pp. 281-292.

9. Eckert, E. R. G., and E. Soehngen, "Interferometric Studies on the Stability and Transition to Turbulence of a Free Convection Boundary Layer," Proceedings of the General Discussion on Heat Transfer, The Institution of Mechanical Engineers, London, 1951, pp. 321-323.

10. Hermann, R., Heat Transfer by Free Convection from Horizontal Cylinders in a Diatomic Gas, National Advisory Committee on Aeronautics, T M 1366.

11. Jodlbauer, K., "The Temperature and Velocity Fields in the Vicinity of a Tube Under Free-Convection Conditions," Forschung auf dem Gebiete des Ingenieurwesens, 4, 1933, pp. 157-172.

12. Seftleben, H., "Die Wärmeabgabe von Körpern Veischiedener Form in Flüssigkeiten und Gasen bei freier Strömung," Zeitschrift anglwandte Physik, 3, 1951, pp. 361-373.

13. King, W. J., "The Basic Laws and Data of Heat Transfer, III - Free Convection," Mechanical Engineering, 54, 1932, pp. 347-353.

14. Merk, H. J., and J. A. Prins, "Thermal Convection in Laminar Boundary Layers, I," Applied Scientific Research, 4A, 1953, p. 22.

15. Griffiths, E., and A. H. Davis, The Transmission of Heat by Radiation and Convection, Special Report No. 9, Food Investigation Board, H. M. Stationery Office, London, 1922.

16. Carne, J. B., "Heat Loss by Natural Convection from Vertical Cylinders," Philosophical Magazine, Journal of Science, Series 7, 24, 1937, pp. 634-653.

17. Elenbaas, W., "The Dissipation of Heat by Free Convection from Vertical and Horizontal Cylinders," Journal of Applied Physics, 19, 1948, pp. 1148-1154.

18. Langmuir, I., "Convection and Conduction of Heat in Gases," Physical Review, 34, 1912, pp. 401-422.

19. Sparrow, E. M., and J. L. Gregg, "Laminar-Free-Convection Heat Transfer from the Outer Surface of a Vertical Circular Cylinder," Transactions of the American Society of Mechanical Engineers, 78, 1956, pp. 1823-1828.

20. Hama, F. R., and J. Christiaens, Experiment on the Axisymmetric Free-Convection Field Along a Vertically-Suspended Wire, University of Maryland, Institute of Fluid Dynamics and Applied Mechanics, TN BN-138, 1958.

21. LeFevre, E. J., and A. J. Ede, "Laminar Free Convection from the Outer Surface of a Vertical Cylinder," Ninth International Congress of Applied Mechanics Proceedings, 4, 1956, pp. 175-183.

22. Yang, K., "Possible Similarity Solutions in Laminar-Free-Convection on Vertical Plates and Cylinders," Transactions of the American Society of Mechanical Engineers, Series E, 82, 1960, pp. 230-236.

23. Millsaps, K., and K. Pohlhousen, "The Laminar Free-Convection Heat Transfer from the Outside Surface of a Vertical Circular Cylinder," Journal of Aeronautical Sciences, 25, 1958, pp. 357-360.

24. Hama, F. R., and J. V. Recesso, The Axisymmetric Free-Convection Temperature Field Along a Vertical Thin Cylinder, University of Maryland, Institute of Fluid Dynamics and Applied Mechanics, TN BN-116, 1958.

25. Hama, F. R., J. V. Recesso, and J. Christiaens, Journal of Aero/Space Sciences, 26, 1959, pp. 335-342.

26. LeFevre, E. J., "Laminar Free Convection from a Vertical Plane Surface," Ninth Congress of Applied Mechanics Proceedings, 4, 1956, pp. 168-174.

27. Glauert, M. B., and M. J. Lighthill, "The Axisymmetric Boundary Layer on a Long Thin Cylinder," Proceedings of the Royal Society, London, Series A, 230, 1955, pp. 188-203.

28. Madden, A. J., and E. L. Piret, "Heat Transfer from Wires to Gases at Sub-Atmospheric Pressures Under Natural Convection Conditions," Proceedings of the General Discussion on Heat Transfer, Institution of Mechanical Engineers, London, 1951, pp. 328-333.

29. Battaglia, A. W. G., An Experimental Investigation of Laminar Free Convection Heat Transfer from the Surface of a Vertical Circular Cylinder, M. S. Thesis, Georgia Institute of Technology, 1960.

30. Cox, J. B., Laminar Free Convection Heat Transfer from Vertical Cylinders, M. S. Thesis, Georgia Institute of Technology, 1962.

31. Crawford, D. W., Measurement of Velocity Profiles with a Hot-Wire Anemometer, M. S. Thesis, Georgia Institute of Technology, 1962.

32. Sparrow, E. M., and J. L. Gregg, "The Variable Fluid-Property Problem in Free Convection," Transactions of the American Society of Mechanical Engineers, 80, 1958, p. 879.

33. Hellums, J. P., Finite Difference Computation of Natural Convection Heat Transfer, Ph. D. Thesis, University of Michigan, 1961.

34. Douglas, J., and D. W. Peaceman, "Numerical Solution of Two Dimensional Heat Flow," American Institute of Chemical Engineers Journal, 1, 1955, p. 505.

35. Richtmyre, R. D., Difference Methods for Initial Value Problems, New York: Interscience Publishers, Inc., 1957.

36. McAdams, W. H., Heat Transmission, New York: McGraw-Hill Book Company, Inc., 1954, p. 172.

37. Eckert, E. R. G., and R. M. Drake, Heat and Mass Transfer, New York: McGraw-Hill Book Company, Inc., 1959, p. 405.

38. McAdams, op. cit., p. 475.

39. Duhig, H. H., A Calorimetric Determination of Thermal Emissivity, M. S. Thesis, Georgia Institute of Technology, 1963.

40. National Bureau of Standards Circular 565, Issued November 1, 1955, pp. 69, 70, 71.

41. Purdy, K. R., Private Communication.

VITA

Carl John Bliem, Jr. was born on June 25, 1934, in Atlanta, Georgia. He attended public schools in Atlanta and was graduated from Henry Grady High School, Atlanta, Georgia, in 1952.

In 1952, he entered the Georgia Institute of Technology and received the degree of Bachelor of Mechanical Engineering in 1956.

Upon graduation, he became a research engineer at the Research Laboratory of the International Business Machines Corporation at Poughkeepsie, New York.

He left this position to return to the Graduate Division of the Georgia Institute of Technology to work toward the degree of Master of Science in Nuclear Engineering, which was awarded in 1959. During this time, he worked as a graduate assistant in Mechanical Engineering and spent one summer with the Union Carbide Nuclear Company in Oak Ridge, Tennessee, as a development engineer.

After receiving his M. S. degree, he became a part-time Instructor in the School of Mechanical Engineering at the Georgia Institute of Technology and began work leading toward a doctorate. In 1962, he became an Assistant Professor of Mechanical Engineering at the University of Tennessee.

He married the former DeLane Clark of Atlanta, Georgia and has two daughters, Cynthia and Caribeth.

He is a member of the American Society of Mechanical Engineers,

the American Society for Engineering Education and the Societies of Phi Eta Sigma, Pi Tau Sigma, Tau Beta Pi and Phi Kappa Phi.